

**SOLVATOCHROMISM AND PROTOTROPISM OF SUBSTITUTED  
FLUORENES ; 2, 7 — DIAMINOFLUORENE AND RELATED  
DIAMINES : ABSORPTION AND FLUORESCENCE PERSPECTIVES**

A Thesis Submitted  
In Partial Fulfilment of the Requirements  
for the Degree of

**DOCTOR OF PHILOSOPHY**

by  
**R. MANOHARAN**

to the

**DEPARTMENT OF CHEMISTRY**

**INDIAN INSTITUTE OF TECHNOLOGY, KANPUR**

**FEBRUARY, 1988**

DEDICATED  
TO  
MY  
APPA AND AMMA

✓CHM-1900-D-MAN-SOL

- 8 NOV 1989

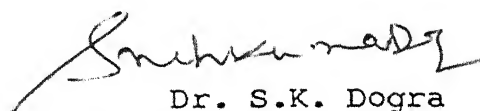
CENTRAL LIBRARY  
1000 1000

106265

CERTIFICATE-I

Certified that the work presented in this thesis entitled, ''SOLVATOCHROMISM AND PROTOTROPISM OF SUBSTITUTED FLUORENES; 2,7-DIAMINOFLUORENE AND RELATED DIAMINES: ABSORPTION AND FLUORESCENCE PERSPECTIVES'' by Mr. R. Manoharan, has been carried out under my supervision and not submitted elsewhere for a degree.

February, 1988



Dr. S.K. Dogra  
Department of Chemistry  
I.I.T., Kanpur-208016



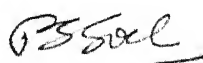
DEPARTMENT OF CHEMISTRY  
INDIAN INSTITUTE OF TECHNOLOGY KANPUR, INDIA

CERTIFICATE OF COURSE WORK

This is to certify that Mr. R. Manoharan has satisfactorily completed all the courses required for the Ph.D. degree programme. These courses include:

Chm 525	Principles of Physical Chemistry
Chm 505	Principles of Organic Chemistry
Chm 545	Principles of Inorganic Chemistry
Chm 524	Modern Physical Methods in Chemistry
Chm 521	Chemical Binding
Chm 634	Symmetry and Molecular Structure
Chm 800	General Seminar
Chm 801	Graduate Seminar
Chm 900	Post-Graduate Research

Mr. R. Manoharan was admitted to the candidacy of the Ph.D. degree programme in September 1985, after he successfully completed the written and oral qualifying examinations.



(Prof. P.S. Goel)  
Head,

Department of Chemistry,  
Indian Institute of Technology,  
Kanpur



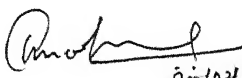
(Dr. S. Sarkar)  
Convener

Departmental Post-  
Graduate Committee,  
Dept. of Chemistry,  
IIT-Kanpur-208 016

STATEMENT

I hereby declare that the work embodied in the thesis entitled, "'SOLVATOCHROMISM AND PROTOTROPISM OF SUBSTITUTED FLUORENES; 2,7-DIAMINOFLUORENE AND RELATED DIAMINES: ABSORPTION AND FLUORESCENCE PERSPECTIVES'" has been carried out by me under the supervision of Dr. S.K. Dogra.

In keeping with scientific tradition, wherever work done by others has been utilized, due acknowledgement has been made.

  
25/02/88  
R. Manoharan

### ACKNOWLEDGEMENTS

It is indeed a great pleasure to record my deep sense of gratitude and heartfelt thanks to Prof. S.K. Dogra for introducing me the exciting world of 'excited states'. His invaluable guidance, constant encouragement and the infectious excitement he brings to every discussion have been very useful for successful completion of this work.

I - am grateful to Dr.Ashok Mishra and Dr.M.Krishnamurthy for their suggestions.

- am thankful to Dr. Hemant Sinha, Ranjit, Joykrishna for their understanding, cooperation and lively companionship in and outside the laboratory.

- remember the short but pleasant association with Phani, Sanjay, Himanshu, Shalini, Debu and Anumita.

- shall treasure the memories of pleasant company of colleagues and friends in general, Moorthy, Ilango, Baskar, Sampath, Govind, Chiddu, Kumaravel, Palaniappan, Dada, Srini, Pratima, Siddharth and Dr. Manoj Kumar in particular.

- deeply appreciate the long association with Sankar, Ramki and Moorthy, my undergraduate class mates.

- acknowledge the authorities of I.I.T. Kanpur for providing the financial assistance in the form of fellowship and infrastructural facilities; Chemical Physics Group, T.I.F.R., Bombay for some lifetime measurements; Anil Johri for immaculate typing of the manuscript and Gowri Singh for neat tracings included in the thesis.

Lastly, I would like to place on record my thanks to my sisters, brothers and uncle for their love and encouragement.

R. MANOHARAN

## SYNOPSIS

Fluorene-9-carboxylic acid derivatives, called MARPHACTINS have long been known as potential plant growth retardants and herbicides. Their effect on Geotropism and Phototropism has been a novel phenomenon. Fluorene derivatives bind to DNA resulting in mutagenity and modification of its protein recognition. A correlation between their carcinogenicity and dissociation constants has also been attempted. Inspite of their important molecular behaviour, these compounds have not been explored at molecular level except in a few cases. It is the aim of the present work to present better insight into the physical and chemical properties of a series of substituted fluorenes and a few structurally related diamines. These molecules have been investigated from different angles such as substituent effect, excited state molecular geometry, solvent effect, effect of acid concentration and proton-induced fluorescence quenching. The thesis entitled "'SOLVATOCHROMISM AND PROTOTROPISM OF SUBSTITUTED FLUORENES; 2,7-DIAMINOFLUORENE AND RELATED DIAMINES: ABSORPTION AND FLUORESENCE PERSPECTIVES'" embodies the detailed discussion resulting in the above investigations.

The thesis contains four chapters. Chapter I gives a brief introduction with a critical overview of some of the ground and excited state phenomena. This chapter also outlines the status-quo report on substituted fluorenes as well as the underlying interest in carrying out the present study.

Chapter II describes briefly the Instrumentation and the preparation of model compounds. It also presents the methodologies for data analysis in both absorption and fluorescence spectral measurements.

In chapter III, the effects of solvent and acid concentration on the absorption and fluorescence spectra of fluorene derivatives are illustrated in detail. The substituents chosen are  $-\text{CH}_3$ ,  $-\text{CH}_2\text{OH}$  and  $-\text{C} \begin{smallmatrix} \nearrow \text{O} \\ \searrow \text{R} \end{smallmatrix}$  ( $\text{R} = \text{H}, \text{CH}_3, \text{Ph}, \text{OH}, \text{OCH}_3, \text{NH}_2$ ) which are appended in different positions of fluorene ring. The following are the important results obtained.

(i) Fluorene and methyl substituted fluorenes undergo proton-induced fluorescence quenching. The excited state equilibrium between the monocation and neutral species of these molecules is not established because of the slow rate of ring protonation.

(ii) The apparent lack of fluorescence of 2-fluorenaldehyde, 2-acetylfluorene and 2-benzoylfluorene in all the solvents except water, constitute the best argument for an  $S_1$  state of  $\pi\pi^*$  type.

(iii) The substituents  $-\text{C} \begin{smallmatrix} \nearrow \text{O} \\ \searrow \text{R} \end{smallmatrix}$  ( $\text{R} = \text{OH}, \text{OCH}_3, \text{NH}_2$ ) at 1- and 4-positions are coplanar with the fluorene ring in both  $S_0$  and  $S_1$  states, so that  $\pi$ -electronic interaction between them is nearly maximal. As a consequence, the long wavelength absorption band is composed of long and short axes polarised transitions. The same substituents at 2-position are non-planar in both  $S_0$  and  $S_1$  states in non-polar solvents, but on excitation become nearly planar in polar and hydroxylic solvents.

(iv) 9-Substituted fluorenes display spectral phenomenology which is remarkably different from that of other substituted fluorenes. In this case, the  $\pi$ -electronic interaction between the substituent, attached to an  $sp^3$  hybridized carbon and the ring is negligibly small so long 9-methylene group is not deprotonated.

(v) Unlike other molecules, the Hammett's acidity function ( $H_0$ ) fails to describe the prototropic behaviour of fluorenamides and 2-carbonyl substituted fluorenes. Amide acidity function ( $H_A$ ) has been used for the protonation of amides and Benzophenone Hammett's scale for the latter compounds.  $H_0$  and  $H_A$  acidity functions have been related with the difference in the hydration requirement of the prototropic reaction of amides and the indicators used to establish  $H_0$  function.

(vi) The site of protonation on  $-CONH_2$  group (whether O-protonation or N-protonation) is controversial, however we speculate it to be at the carbonyl oxygen. The two processes involved in the protonation of amides and 2-carbonyl substituted fluorenes correspond to O-protonation and medium effect on the protonated molecule.

(vii) The trend observed in the dissociation constants is in general agreement with that appear in the literature i.e.  $-C \begin{smallmatrix} \nearrow O \\ \searrow R \end{smallmatrix}$  become more basic upon excitation.

Chapter IV presents the similar study as described above, on 2,7-diaminofluorene. Studies on three isomeric phenylenediamines, 2,3-diaminonaphthalene and 9,10-diaminophenanthrene are also presented

to corroborate the above results. The common features observed for all the diamines are:

(i) In  $S_0$  state, all the diamines behave as proton donors in aprotic polar solvents and proton acceptors in hydroxylic solvents but act as proton donors in all the solvents upon excitation. Diamines become more acidic in  $S_1$  state.

(ii) Fluorimetric titrations for monocation-neutral equilibrium give the ground state  $pK_a$  values. Proton-induced fluorescence quenching is observed for the monocations prior to the formation of dications.

The differing features are:

(i) The red shift observed in the fluorescence of monocation as compared to that of neutral species of 2,7-diaminofluorene is due to a greater solvent relaxation of the former species. But in the case of 2,3-diaminonaphthalene (DAN), it could be due to more coplanarity of the amino group of monocation as compared to those of the neutral species in which both of the amino groups are twisted with respect to the naphthalene ring. Lifetime measurements infer that the rate of protonation of DAN ( $\sim 10^6 - 10^7 \text{ M}^{-1} \text{ s}^{-1}$ ) is slow compared to that of fluorescence ( $2 \times 10^8 \text{ s}^{-1}$ ) such that prototropic equilibrium is not established in  $S_1$  state. The pH independent lifetime of the monocation of DAN demonstrates that static mechanism is operative for proton-induced fluorescence quenching.

(ii) The results obtained for *o*- and *p*-phenylenediamines are rationalized in terms of non-planarity of the amino groups.

(iii) Dual fluorescence is observed for 9,10-diaminophenanthrene. The abnormally large Stokes shifted fluorescence is from a more polar  $^1L_a$  state and the normal fluorescence is from a relatively less polar  $^1L_b$  state.

The conclusions drawn and the possible extension of the work are given at the end of the thesis.



## LIST OF FIGURES

<u>Fig.</u>	<u>page no.</u>
1.1 Jablonski diagram showing fates of polyatomic molecules upon photoexcitation.	2
1.2 Schematic representation of equilibrium and Franck-Condon (F-C) electronic states.	7
2.1 Block diagram of the spectrofluorimeter.	39
2.2 Diagram of low temperature set up for fluorescence and phosphorescence.	40
2.3 Relative intensity distribution of excitation source.	44
2.4 Emission calibration curves: I 300 nm blaze grating, II 500 nm blaze grating.	44
2.5 Corrected fluorescence spectrum of anthrance ( $1 \times 10^{-5}$ M in ethanol).	45
2.6 Corrected fluorescence spectrum of quinine sulphate ( $1 \times 10^{-5}$ M in 0.1N $H_2SO_4$ ).	45
2.7 Block diagram of picosecond spectrofluorometer.	47
3.1 Absorption and fluorescence spectra of neutral and monocation species of fluorene.	50
3.2 Absorption and fluorescence spectra of neutral and monocation species of 1-methylfluorene.	50
3.3 Absorption and fluorescence spectra of neutral and monocation species of 9-fluorenemethanol.	51
3.4 Fluorimetric titration curves for the various prototropic species of fluorene, 1-methylfluorene and 9-fluorenemethanol.	51

3.5	Stern-Volmer plot for proton-induced fluorescence quenching of fluorene, 1-methylfluorene and 9-fluorene-methanol.	57
3.6	Absorption and fluorescence spectra of 1-fluorene-carboxylic acid in different solvents.	60
3.7	Absorption and fluorescence spectra of 4-fluorene-carboxylic acid in different solvents.	61
3.8	Absorption and fluorescence spectra of 2-fluorene-carboxylic acid in different solvents.	62
3.9	Absorption and fluorescence spectra of 9-fluorene-carboxylic acid in different solvents.	63
3.10	Absorption and fluorescence spectra of different prototropic species of 1-fluorene-carboxylic acid.	73
3.11	Absorption and fluorescence spectra of different prototropic species of 4-fluorene-carboxylic acid.	74
3.12	Absorption and fluorescence spectra of different prototropic species of 2-fluorene-carboxylic acid.	75
3.13	Absorption and fluorescence spectra of different prototropic species of 9-fluorene-carboxylic acids.	76
3.14	Fluorimetric titration curves for different prototropic species of fluorene -1-, -2-, and -4- carboxylic acids.	86
3.15	Absorption and fluorescence spectra of 1-, 2-, and 4-fluorenamides in different solvents.	90
3.16	Absorption and fluorescence spectra of different prototropic species of 1-, 2-, and 4-fluorenamides.	98
3.17	Absorption spectra of 2-fluorenamide in different %(w/w) sulfuric acid.	99
3.18	Fluorimetric titration curves for different prototropic species of 1-, 2-, and 4-fluorenamides.	105

3.19	Absorption and fluorescence spectra of different prototropic species of 2-fluorenaldehyde.	114
3.20	Absorption and fluorescence spectra of different prototropic species of 2-acetylfluorene.	115
3.21	Absorption and fluorescence spectra of different prototropic species of 2-benzoylfluorene.	116
3.22	Plot of $(\epsilon_i - \epsilon_u) \times 10^{-3}$ Vs $H_0$ for p-methoxy-acetophenone, p-phenylacetophenone and 2-acetylfluorene.	119
3.23	Fluorimetric titration curves for the prototropic species of 2-fluorenaldehyde, 2-acetylfluorene and 2-benzoylfluorene.	122
4.1	Absorption and fluorescence spectra of 2,7-diaminofluorene in different solvents.	127
4.2	Absorption and fluorescence spectra of different prototropic species of 2,7-diaminofluorene.	131
4.3	Fluorimetric titration curves for different prototropic species of 2,7-diaminofluorene.	138
4.4	Stern-Volmer plot for proton-induced fluorescence quenching of the monocation species of 2,7-diaminofluorene.	140
4.5	Absorption and fluorescence spectra of 2,3-diaminonaphthalene in different solvents.	142
4.6	Absorption and fluorescence spectra of neutral species of 2,3-diaminonaphthalene and 2-aminonaphthalene.	143
4.7	Absorption and fluorescence spectra of different prototropic species of 2,3-diaminonaphthalene.	148

4.8	Fluorimetric titration curves for the different prototropic species of 2,3-diaminonaphthalene.	154
4.9	Fluorescence decay of the monocation of 2,3-diaminonaphthalene. The residuals and autocorrelation function were determined for a single exponential decay of 17.4 ns ( $x^2 = 0.14$ ).	156
4.10	Stern-Volmer plot for proton-induced fluorescence quenching of the monocation of 2,3-diaminonaphthalene.	158
4.11	Fluorescence spectra of o-phenylenediamine in different solvents and at various acid concentration.	161
4.12	Fluorescence spectra of m-phenylenediamine in different solvents and at various acid concentration.	161
4.13	Fluorescence spectra of p-phenylenediamine in different solvents and at various acid concentration.	162
4.14	Fluorimetric titration curves for the different prototropic species of o-, m-, and p-phenylenediamines.	162
4.15	Stern-Volmer plots for proton-induced fluorescence quenching of the monocation species of o-, m-, and p-phenylenediamines.	171
4.16	Absorption and fluorescence spectra of 9,10-diaminophenanthrene in different solvents.	173
4.17	Excitation spectra of 9,10-diaminophenanthrene in ether and acetonitrile.	179
4.18	Absorption and fluorescence spectra of different prototropic species of 9,10-diaminophenanthrene.	182
4.19	Fluorimetric titration curves for different prototropic species of 9,10-diaminophenanthrene.	184
4.20	Stern-Volmer plot for proton-induced fluorescence quenching of monocation species of 9,10-diaminophenanthrene.	187

## LIST OF TABLES

<u>Table</u>	<u>page no.</u>
3.1 Absorption spectral data of fluorene, 1-methylfluorene and 9-fluorenemethanol in different solvents and at various acid concentration.	52
3.2 Fluorescence spectral data of fluorene, 1-methylfluorene and 9-fluorenemethanol in different solvents and at various acid concentration.	54
3.3 Acidity constants of fluorene, 1-methylfluorene and 9-fluorenemethanol.	54
3.4 Proton-induced fluorescence quenching kinetic data for neutral species of fluorene, 1-methylfluorene and 9-fluorenemethanol.	57
3.5 Absorption spectral data of fluorene -1-, -4-, -2-, and -9- carboxylic acids and esters in different solvents.	64
3.6 Fluorescence spectral data of fluorene -1-, -4-, -2-, and -9- carboxylic acids and esters in different solvents.	66
3.7 Stokes shift observed for fluorene -1-, -4-, -2-, and -9- carboxylic acids in different solvents and at various pHs.	70
3.8 Absorption and fluorescence spectral data of different prototropic species of fluorene -1-, -4-, -2-, and -9- carboxylic acids and esters.	77
3.9 Acidity constants of fluorenenecarboxylic acids and esters in their ground and excited singlet states.	87

3.10	Absorption and fluorescence spectral data of 1-, 2- and 4- fluorenamides in different solvents.	91
3.11	Stokes shift observed for 1-, 2-, and 4- fluorenamides in different solvents and at various acid concentrations.	94
3.12	Ground state $pK_a$ of monocation-neutral equilibria of amides: using different acidity scales.	103
3.13	Acidity constants of fluorenamides in the ground and first excited singlet states.	106
3.14	Absorption and fluorescence spectral data of 2-fluorenaldehyde, 2-acetylfluorene and 2-benzoylfluorene in different solvents and at various acid concentration.	110
3.15	Ground state acidity constants of monocation-neutral equilibrium of 2-fluorenaldehyde, 2-acetylfluorene and 2-benzoylfluorene using different acidity scales.	123
3.16	Acidity constants of 2-fluorenaldehyde, 2-acetylfluorene and 2-benzoylfluorene: Determined by absorptiometric and fluorimetric titrations.	123
4.1	Absorption and fluorescence spectral data of 2,7-diaminofluorene in different solvents and at various and concentration.	128
4.2	Acidity constants of 2,7-diaminofluorene in the ground and first excited singlet state.	134
4.3	Spectral data for different prototropic species of 2,7-diaminofluorene in cyclohexane.	134

4.4	Absorption and fluorescence spectral data of 2,3-diaminonaphthalene in different solvents and at various acid concentration.	144
4.5	Acidity constants of 2,3-diaminonaphthalene in the ground and first excited singlet state.	152
4.6	Lifetime of the monocation of 2,3-diaminonaphthalene at different pH.	152
4.7	Absorption and fluorescence spectral data of o-, m-, and p-phenylenediamines in different solvents at various acid concentration.	163
4.8	Stokes shifts ( $\text{cm}^{-1}$ ) observed for phenylenediamines in different solvents and at various acid concentration.	165
4.9	Acidity constants of phenylenediamines in the ground and first excited singlet state.	165
4.10	Proton transfer kinetic data for monocation of phenylenediamines.	171
4.11	Absorption and fluorescence spectral data of 9,10-diaminophenanthrene in different solvents and at various acid concentration.	174
4.12	Absorption and fluorescence spectral data of 9,10-diaminophenanthrene in cyclohexane + TFA medium.	181
4.13	Acidity constants of 9,10-diaminophenanthrene in the ground and first excited singlet state.	185

## CONTENTS

		<u>page no.</u>
CERTIFICATE-I	... ..	i
CERTIFICATE OF COURSE WORK	... ..	ii
STATEMENT	... ..	iii
ACKNOWLEDGEMENTS	... ..	iv
SYNOPSIS	... ..	v
LIST OF FIGURES	... ..	x
LIST OF TABLES	... ..	xiv
CHAPTER-I : INTRODUCTION		
1.1 Substituent effect	... ..	3
1.2 Excited state molecular geometry	... ..	5
1.3 Solvatochromism	... ..	6
1.4 Prototropic reactions	... ..	12
1.5 Proton-induced fluorescence quenching	... ..	14
1.6 Applications	... ..	16
1.7 Scope of the present work	... ..	18
CHAPTER-II: MATERIALS, METHODS AND INSTRUMENTATION		
2.1.1 Synthesis	... ..	25
2.1.2 Solvents	... ..	27
2.1.3 Purity of the materials	... ..	27
2.2.1 Preparation of solutions	... ..	28
2.2.2 Determination of dissociation constants	... ..	29



2.2.3	Quantum yield calculation	...	...	35
2.2.4	Lifetime and quenching constant estimation	...	...	35
2.3.1	Spectrofluorimeter	...	...	38
2.3.2	Experimental procedure	...	...	42
2.3.3	Correction factor determination	...	...	42
2.3.4	Other instruments	...	...	46
CHAPTER-III: SOLVENT AND pH EFFECTS ON THE ELECTRONIC SPECTRA OF METHYL, CARBOXYL, AMIDE AND CARBONYL SUBSTITUTED FLUORENES				
3.1	Fluorene and methyl substituted fluorenes	...	...	48
3.2	Carboxylic acids	...	...	59
3.3	Carboxamides	...	...	88
3.4	Aldehyde and ketones	...	...	108
CHAPTER-IV : EFFECTS OF SOLVENTS AND pH ON THE ELECTRONIC SPECTRA OF 2,7-DIAMINOFLUORENE AND RELATED DIAMINES				
4.1	2,7-Diaminofluorene	...	...	125
4.2	2,3-Diaminonaphthalene	...	...	141
4.3	Isomeric phenylenediamines	...	...	160
4.4	9,10-Diaminophenanthrene	...	...	172
CONCLUSIONS				189
FUTURE PROSPECTS				193
REFERENCES				194
VITAE				xvii
LIST OF PUBLICATIONS				xviii

## CHAPTER-I

### INTRODUCTION

The absorption of light by a molecule leaves it in one of a number of possible vibrational levels of one of its electronically excited states, called Franck-Condon excited (FCE) state. The fate of the molecule in the FCE state, in otherwords, the number of ways by which it loses its energy and returns to the ground state can nicely be illustrated by Jablonski diagram<sup>1</sup> (Fig. 1.1). A complete discussion of the various processes involved in the excited state deactivation has been documented by Gouterman and Seybold,<sup>2</sup> and Lower and El Sayed.<sup>3</sup>

A molecule in its electronically excited state has different electronic charge distribution at the various atomic centres in comparison to that of the ground state, consequently its physical and chemical properties differ from those in the ground state. For example, geometry of the molecule, dipole moment, acid-base properties to name a few.

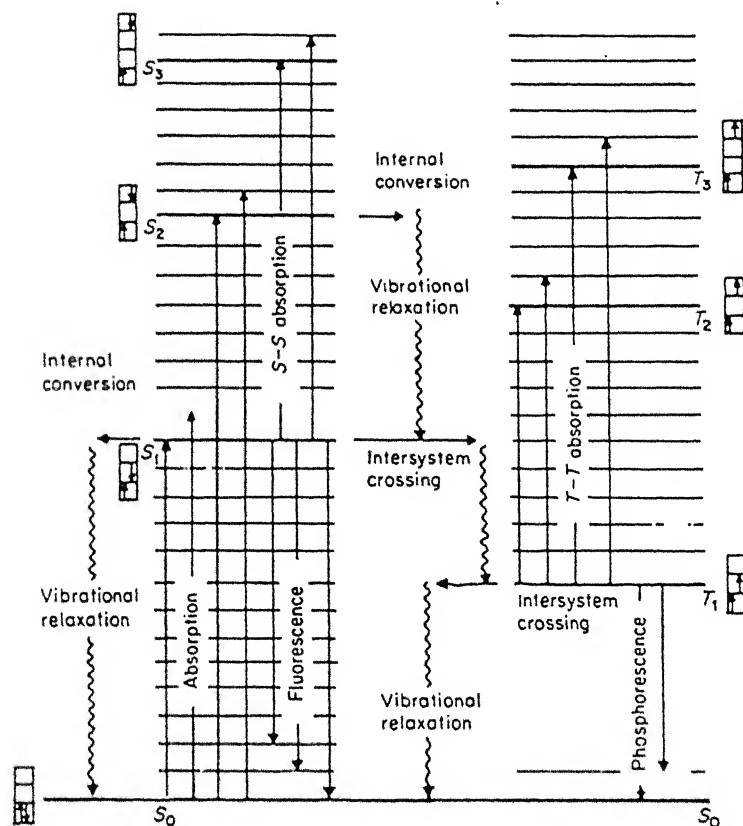


Fig. 1.1 Jablonskii diagram showing fates of polyatomic molecules upon photoexcitation.

In the following sections, a brief description of the effects of substituents and geometry of the substituents with respect to the parent molecule on the absorption and fluorescence spectra will be given. A survey of Solvatochromism, Prototropism and Proton-induced fluorescence quenching followed by a description of application and scope of the present work will be discussed.

### 1.1 SUBSTITUENT EFFECT

Functional groups can exert definite and predictable effect on the electronic transitions of the parent molecule provided we know its geometry with respect to the parent moiety. A comprehensive account of the influence of molecular structure on the electronic spectra have been nicely discussed by Jaffe and Orchin,<sup>4</sup> Suzuki,<sup>5</sup> and Murrill.<sup>6</sup>

For aromatic molecules, in general, three  $\pi \rightarrow \pi^*$  transitions are prominent. The weak, long wavelength absorption band is classified as  $\alpha$ -band, the stronger middle band is para band and the third short wavelength band which is strongest of all is  $\beta$ -band. According to the Platt's notation<sup>7</sup>,  $\alpha$ -band is long axis polarised, para band is short axis polarised and the  $\beta$ -band is either a mixture of both long and short axes polarised transitions or one of them. These transitions are denoted as  $^1A \rightarrow ^1L_b$ ,  $^1A \rightarrow ^1L_a$  and  $^1A \rightarrow ^1B_a$  ( $^1A \rightarrow ^1B_b$ ) respectively. If the molecule is substituted with a basic group, these transitions are red shifted. Further, in the condensed aromatic systems, the substituents present on the longer axis of the molecule affect

the long axis polarised transitions and those at shorter axis affect short axis polarised transitions. It has generally been observed that the para bands are more polar and prone to the presence of substituents. So it is immediately clear that substitution studies are of much useful in qualitatively predicting the nature of a transition.

According to Kasha's rule, fluorescence is generally observed if  $\pi\pi^*$  is the lowest energy transition and phosphorescence if  $n\pi^*$  is the lowest energy transition. Fluorescence quantum yield depends on the rate of fluorescence deactivation in comparison to the rate of radiationless processes. Less the rotational and vibrational freedom the molecule has in its part, greater the probability the molecule deactivates by fluorescence. Appended groups usually diminish the quantum yield by behaving like, as Lewis and Calvin<sup>8</sup> said, "loose bolts in some moving part of a machine". At low temperature, the restricted rotational and vibrational motions of the substituents reduce the degree of internal conversion and thus increase the fluorescence quantum yield.

Alkyl substitution has little effect on the fluorescence spectra of the parent molecule whereas, strongly interacting groups e.g.  $-\text{NH}_2$ ,  $-\text{COOH}$  etc., impart substantial changes. Halogen substitution decreases the fluorescence quantum yield by heavy atom effect. Wehry<sup>9</sup> pointed out that "though there is a considerable evidence of the operation of heavy atom effect in some systems, the effect can not be considered a panacea". In bifunctional molecules possessing both electron donating and electron withdrawing groups, the geometry and steric factors play a major role in determining the resultant resonance and inductive

effects on the absorption and fluorescence spectra. For example, if  $\pi$ -electronic cloud or the lone pair cloud of the substituent is not coplanar with the  $\pi$  cloud of the parent moiety, the spectral features are not altered very much. Although these predictions are generally valid, often the strong interaction between the solute and solvent prevents the separation of the structural effect from the environmental effect on the spectral behaviour.

## 1.2 EXCITED STATE MOLECULAR GEOMETRY

Geometry of the substituted molecules in the ground and excited states assume great significance in the understanding of photophysical and photochemical profiles. The information about the ground state geometry can be obtained by diffraction, dipole moment and spectroscopic techniques.<sup>10</sup> Absorption spectral data such as position, shape and intensity of the band also reasonably infer the topology of the chromophores in  $S_0$  state.<sup>4,6,11-15</sup> Although theoretical work has provided some information about the equilibrium conformation, as such there is no experimental technique which directly predicts the excited state molecular geometry. Nevertheless, differences in absorption and fluorescence spectral parameters have been correlated to the differences in the  $S_0$  and  $S_1$  geometries. Anomalous Stokes shifts observed for the substituted molecules have been attributed to the geometry change upon excitation.<sup>16-22</sup> Werner's<sup>23</sup> extensive work is the important contribution toward the understanding of the relative geometries and solvent cages of  $S_0$  and  $S_1$  states. Gustav et al.<sup>24</sup> have carried out theoretical studies on  $S_0$  and  $S_1$  state geometries

and compared their results with the experimental parameter, Stokes loss (vide infra).

Berlman<sup>25</sup> pointed out that spectroscopic data can be used as a 'straight edge' to provide qualitative evidence concerning the planarity of the molecules. On the basis of this, he classified the chromophores into five different groups. Recently, realising the importance of conformational changes along the torsional coordinates in photophysics and photochemistry new experimental techniques have been developed. Laser induced fluorescence spectroscopy of jet cooled molecules sheds more light on their excited state geometry.<sup>26</sup> A new class of compounds called Twisted Intramolecular Charge Transfer (TICT) compounds display dual fluorescence originating from both normal and TICT states. The main feature of these molecules is, a twisting of the functional groups is induced and assisted by the polarity of the solvents. These compounds are presently being explored in view of their important role in the development of new laser sources and in the primary processes of vision and photosynthesis.<sup>27</sup>

### 1.3 SOLVATOCHROMISM

Theoretical treatments of spectral transitions provide information only about an isolated molecule. Experimentally these predictions regarding spectral transitions can be approximated by carrying out the studies in low pressure gas phase or to a fair approximation in very dilute solution in hydrocarbon solvents. Since our studies are carried out in solution, it is necessary to look at different possible interactions, the solute and solvent may have in solution.

The molecule in the Franck-Condon excited (FCE) state relaxes vibrationally within the time frame of  $10^{-12}$  sec. In this state, the molecule is surrounded by ground state solvent cage. As a result of the change in charge distribution and thus the dipole moment upon excitation, the solvent cage reorganizes accordingly in the new environment. This process, called solvent relaxation, (which involves bond breaking and bond formation) is contemporaneous to vibrational relaxation. The combined effect of vibrational, solvent and geometry relaxations is termed as thermal relaxation. The emission originates from thermally relaxed excited state (TRE) and terminates in one of the manifold of vibrational states of the ground electronic state (FCG state). Because of the rapidity ( $10^{-15}$  sec) of the electronic transition, the molecule in FCG state is still in the excited state equilibrium solvent cage. Rapid solvent relaxation followed by vibrational relaxation then occurs and the solute molecule eventually returns to the thermally equilibrated ground state (as represented in Fig. 1.2). Since the thermally relaxed excited state is lower in energy than FCE

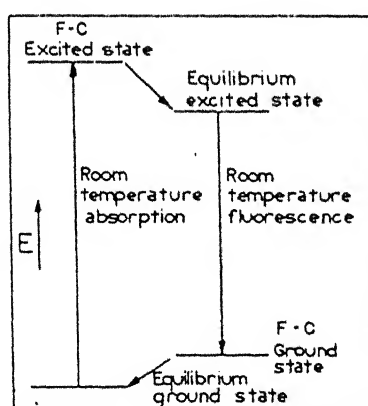


Fig.1.2 Schematic representation of equilibrium and Franck-Condon (F-C) electronic states.



state, and the FCG is higher in energy than the thermally relaxed ground state, fluorescence occurs at longer wavelength than absorption. The loss in energy between the absorption and emission of light is known as Stokes shift and is defined as  $[\bar{\nu}_{\text{abs}}(\text{max}) - \bar{\nu}_{\text{flu}}(\text{max})]$ .

Electronic spectral shifts in different solvents result from dispersive as well as specific interactions of the solvent with the solute. The dispersive interaction, often called general solvent effect includes induced dipole-induced dipole, dipole-induced dipole, dipole-dipole interactions. If the dipole moment of the molecule increases upon excitation (in the case of  $\pi \rightarrow \pi^*$  transition), general solvent effect causes red shift in the electronic spectrum on increasing the polarity of the solvents, whereas a blue shift is noticed when the dipole moment of the molecule decreases (in the case of  $n \rightarrow \pi^*$  transition).

Specific effects can be due to hydrogen bonding, complexation with solvent molecules, acid-base chemistry or charge transfer interaction to name a few. These effects on molecular spectra are often viewed as selective spectroscopic analysis because these impart substantial changes in the electronic spectra. Hydrogen bonding interactions can either be of hydrogen-bond donor or hydrogen-bond acceptor type. In hydrogen-bond donor interaction, there is an electrostatic interaction of a positively polarised hydrogen atom of the solvent with the lone pair electrons of a basic atom in the solute and this results in lowering of energy. If in an electronic excitation process, there is a charge migration towards this basic centre, hydrogen bond donor interaction will stabilize the electronic state and this results

in red shift in the spectrum with increasing hydrogen bond donor capacity of the solvents. Conversely, if during excitation the electron density migrates away from the basic centre, a blue shift is expected.

Hydrogen bond acceptor interaction is also an electrostatic interaction but between the lone pair electrons of the solvent and the positively polarised hydrogen atom of the solute molecule. If the charge density migrates away from this basic centre, progressive red shift is noticed with an increase in the proton acceptor nature of the solvents. On the other hand, a blue shift is observed if the charge density migrates into the basic centre. Normally the trends observed in shifts of absorption and fluorescence band maxima with solvent polarity are the same as long as the electronic states involved and the sites of interaction between the solute and solvent are the same.

When a solute is placed in a solvent, one observes the combined effects of general and specific interactions. The separation of these is often difficult, however, by ingenious and judicious selection of solvents one can qualitatively achieve it to get the information concerning the nature of the transition, dipole moment and distribution of charge density upon excitation.

First thorough and systematic investigations regarding the effect of solvents on the spectra were carried out by Burawoy,<sup>28</sup> and Byliss and McRae.<sup>29</sup> Kasha<sup>30</sup> and McConnel<sup>31</sup> formulated certain rules to identify  $\pi\pi^*$  and  $n\pi^*$  transitions, i.e. bathochromic shift for  $\pi\pi^*$  and hypsochromic shift for  $n\pi^*$  transitions are observed if one goes from hydrocarbon to hydroxylic solvents. The extent of this blue

shift observed in the  $n\pi$  transitions has been correlated with hydrogen bond strength.<sup>29,32,33</sup> A very consolidated and comprehensive account of electronic absorption spectroscopy is given in books written by Jaffe and Orchin,<sup>4</sup> Suzuki,<sup>5</sup> Murrill,<sup>6</sup> and Mataga and Kubota.<sup>54d</sup>

The works of Pringsheim<sup>34</sup> and Förster<sup>35</sup> are the first systematic study on the environmental effects on fluorescence spectra. In 1963, Van Duuren<sup>36</sup> reviewed the subject giving a detailed account of the solvent effect on the fluorescence spectra of various types of aromatic molecules. Pimental,<sup>37</sup> and Mataga et al.<sup>38,39</sup> have emphasized the significance of hydrogen bonding interactions. Weller's<sup>40</sup> article outlines a method to calculate the rate constant for the hydrogen bond formation from the decrease of fluorescence intensity by hydrogen bonding. Recent investigations<sup>41-43</sup> by various groups have established that the main cause of decrease of the fluorescence quantum yield on hydrogen bonding is the enhancement of the rate of internal conversion within the singlet manifold, and various mechanisms have been proposed for this process.<sup>44-48</sup>

A number of theoretical equations have been formulated to relate the spectral shifts with polarity of the solvents.<sup>49-55</sup> As recent as in 1987, Sutin et al.<sup>56</sup> have derived accurate expressions, and these equations can be reduced to equations previously derived by Ooshika<sup>51</sup>, McRae<sup>53</sup>, Mataga<sup>54</sup> and others<sup>55</sup> when same approximations were applied. Since the general solute-solvent interaction is predominantly of electrostatic in nature, and charge redistribution occurs upon excitation, the possibility of relating Stokes shift with the dipolemoment was probed. Infact, equations which relate the solvent polarity parameter and the Stokes shift with the change in dipolemoment of the

molecules have been derived by many workers.<sup>49-58</sup> In none of these treatments specific interactions could be accounted for. Kamlet<sup>59</sup> claims that every property involving a solvent and solute is correlated in his equation. Taft and Co-workers<sup>60,61</sup> have developed a methodology to separate the relative contributions of the general and specific interactions.

Specific interactions such as complex formation impart substantial changes in the electronic spectra. The fluorescence quenching by solvents like  $\text{CCl}_4$  and  $\text{CHCl}_3$  has been explained in terms of an exciplex formation.<sup>62,63</sup> Similarly an 1:1 complex formation between alcohols and 7-azaindole,<sup>64</sup> 1-azacarbazole<sup>65</sup> has been reported to be responsible for the dual emission.

There have been several studies to rationalize intramolecular phototautomerism,<sup>66,67</sup> nature of the hydrogen bonding<sup>68</sup> and chemical structure<sup>69,70</sup> in the  $S_0$  and  $S_1$  states on the basis of solvent effects on the absorption and fluorescence spectra.

With the advent of picosecond spectroscopy it has become possible to monitor the dynamics of the solvent relaxation.<sup>71</sup> Anthon and Clark<sup>72</sup> have carried out a picosecond experiment on the excited state solvation dynamics of 9,9'-bianthryl in alcoholic solutions. A time dependent solute-solvent interaction has been investigated to draw potential information about the physical properties of macromolecules.<sup>73,74</sup> Lakowicz has given a nice description of time dependent solvent relaxation in his book on fluorescence spectroscopy.<sup>75</sup>

#### 1.4 PROTOTROPIC REACTIONS

The acidity or basicity of a molecule is directly related to its electronic structure. Since the electronic transitions, in general, are accompanied by reorganization of the electronic charge density at various atomic centres of the molecule, the acidity and basicity of such molecules vary significantly from one electronic state to another. It is generally observed that aromatic amines and phenols become stronger acids whereas aromatic carboxylic acids, carbonyls and heterocyclics containing tertiary nitrogen atom become more basic upon excitation.<sup>76</sup>

The basis for the measurement of acidity constants is, use of a technique which quantitatively discriminates acidic and basic forms of the molecule. Electronic absorption spectroscopy is one such technique which provides an accurate estimation of ground state  $pK_a$  values. Similarly, fluorescence spectroscopy is an excellent technique for the determination of excited state acidity constants. This is widely used because of its favourable time scale within which most of the prototropic reactions are complete. The different methodologies to calculate  $pK_a$  and  $pK_a^*$  values are outlined in Section 2.2.2.

For the first time, in 1931, Weber<sup>77</sup> noticed that the shift of an acid-base equilibrium occurred at a different pH, depending on whether the shift was observed by absorption and fluorescence spectroscopy. This observation was correctly interpreted by Förster<sup>78,79</sup> as a change in the excited state  $pK_a$ . A detailed study and considerable amount of data were then accumulated by Weller.<sup>80</sup> Since this pioneering work, the subject of acid-base chemistry in the excited state was

explored in many laboratories.<sup>81-88</sup> An excellent review by Ireland and Wyatt<sup>89</sup> contains extensive references of experimental results available in the literature till 1974. Schulman<sup>76,88e</sup> has also reviewed the subject giving due importance to the  $pK_a$  values of compounds of analytical and biological interests.

The proton transfer reactions of the molecules containing bi-functional groups (i.e. electron-donating and electron-withdrawing) in  $S_0$  state are generally the same as observed in  $S_1$  state. But there are certain cases where the decrease in the charge density at the electron donating group and increase in the charge density at the electron attracting group are so large, that the order of prototropic reactions are reversed upon excitation. Under such situation a proton is transferred from one group to another without changing the number of protons. This phenomenon is called phototautomerism. If the proton migration takes place across an intramolecular hydrogen bond between the functional groups, it is called monoprotonic phototautomerism, and it does not depend on the environments. On the other hand, if it takes place between groups which are widely separated, then it depends on the environment and is termed as biprotonic phototautomerism.

The observation of dual fluorescence for bifunctional molecules has been attributed to a rapid intramolecular proton transfer, thus leading to different isomers.<sup>90-98</sup> Double proton transfer has been found to occur in dimers like those of 7-azaindole,<sup>99-101</sup> 2H-indazole<sup>102</sup> and 1-azacarbazole.<sup>103</sup> The role of solvent molecules in the proton transfer has been recognised recently. Cluster of 1-naphthol and ammonia generated through a supersonic jet suggested that four ammonia

molecules are needed to form an ammonium ion.<sup>104</sup> An elegant experiment by Robinson et al.<sup>105</sup> using picosecond technique proved that excited state proton transfer of 2-naphthol is effected by water ( $4 \pm 1$  molecules) cluster.

In recent years, considerable effort has been made to study the proton transfer reactions in micellar dispersions,<sup>106,107</sup> and in model biological systems.<sup>108</sup> Theoretical treatment of proton transfer has also been attempted by several authors.<sup>109-111</sup>

### 1.5 PROTON-INDUCED FLUORESCENCE QUENCHING

Studies of fluorescence quenching have received much impetus because of their wide range of application in analytical and biochemistry. A variety of processes result in fluorescence quenching and these include excited state reactions, energy transfer, complex formation, and collisional quenching.

Two distinct mechanisms of quenching have been recognised. In the first (termed static mechanism), association occurs between the ground state fluorophore and quencher resulting in the formation of a non-fluorescent or weak fluorescent complex. In the second case (termed dynamic mechanism), excited fluorophores undergo collision with quencher during the excited lifetime of the molecule resulting in the non radiational process. These mechanisms can be distinguished in the following manner: (i) If the lifetime of the fluorophore is independent of quencher concentration, static mechanism is operative. For dynamic one, lifetimes are dependent on quencher concentration. (ii) When the quenching mechanism is static, the Stern-Volmer quenching constant will be equal to the association constant. The first

point is the reliable observation to confirm a particular quenching mechanism. The criterion to distinguish the mechanism as well as the mathematical relations describing the fluorescence quenching have been reviewed by many workers.<sup>112-116</sup>

Proton-induced fluorescence quenching was first noticed by Weller<sup>117</sup> as a cause for the lack of correspondence between the fluorimetric titration curves of the conjugate acid-base pair of 2-naphthylamine involved in the prototropic equilibrium. Since then large number of molecules have been reported to undergo these quenching.<sup>118-125</sup> Many theories<sup>126,127</sup> have been proposed to explain the mechanism of quenching and the well acclaimed one is that proposed by Shizuka et al.<sup>128</sup> In their carefully executed experiments it was demonstrated that the quenching mechanism involves protonation at one of the carbon atoms of the aromatic ring. These conclusions are arrived on the basis of following observations: (i) there is relatively little correlation between the rate constant for proton-induced fluorescence quenching ( $k_q$ ) and ionisation potential of the fluorophore ( $I_p^*$ ). This shows that quenching mechanism by proton is different from that by inorganic anions where it is an electron transfer (or charge transfer) process. (ii) The quenching process leads to proton (or isotope) exchange and the value of  $k_q$  is almost equal to the rate constant for an electrophilic protonation. (iii) Fluorophores having an intramolecular charge transfer (CT) structure in the fluorescent state are quenched appreciably by protons than those having no CT character. (iv) The quenching rate of substituted 2-methoxynaphthalenes is about a factor of  $10^2$  slower than that of



1-methoxy isomer. It is possible to explain only on the basis of ring protonation, because MO calculations of excited states reveal that the increase in the electron density in the ring is greater for the 1-isomer than 2-isomer.<sup>129</sup> (v) Proton-induced fluorescence quenching rate constant for aromatic hydrocarbon is less than that for aromatic hydrocarbon containing basic substituents.

Proton-induced fluorescence quenching generally occurs prior to the protonation of the fluorophore, except in few cases.<sup>98b,130</sup> This has been attributed to the short lifetime of the conjugate acid-base pair involved in the equilibrium.

Photochemical reactions result from excited state protonations are generally monitored by the quenching of the substrate fluorescence.<sup>131-133</sup> Recently Pincock and Co-workers<sup>129</sup> have proposed an acidity constant  $[H^+]^{hv}$  to be included in the Stern-Volmer treatments. They have defined  $[H^+]^{hv}$  as the kinetic protonating ability of the medium and explained a method to determine these values. However, the generalization is limited until its validity is tested.

## 1.6 APPLICATIONS

Because of its sensitivity and specificity fluorescence spectroscopy is widely used as an analytical tool for the qualitative and quantitative analysis.<sup>134</sup> Solvent study and excited state prototropism of organic molecules have received wide attention of photochemists, because of their increasing importance in the interpretation of mechanism and yield of photochemical reactions.<sup>135</sup> For example, the product distribution in photoisomerization reactions of 3-styrylpyridines<sup>135b</sup>

and the photoreduction of hydrazine<sup>135c</sup> are related to the acid-base equilibria in  $S_0$  and  $S_1$  states. Wan and Turro have studied photocleavage of benzyl alcohols and the Yates group has examined the photohydration of alkenes and alkynes.<sup>131a,b</sup> In these cases, reaction resulting from excited state protonation, was monitored by quenching of substrate fluorescence. Mac Diarmid<sup>136</sup> et al and Travers et al.<sup>137</sup> have reported that the electrical conductivity increases dramatically by 11 orders of magnitude when polyaniline is protonated. This novel protonation induced insulator-to-conductor transition, called protonic acid doping may have applications in molecular electronic devices.

Molecules which exhibit excited state intramolecular prototropy are exceptionally photostable and are widely used as UV stabilizers to diminish photodegradation of polymers. The dynamic processes of intramolecularly hydrogen bonded aromatic molecules which involve four level energy scheme are important in view of the possibility of making a four level proton transfer laser and designing an information storage device at molecular level.<sup>138</sup>

Fluorescence spectroscopy, because of its favourable time scale, provides a powerful methodology for investigating the dynamic processes of biological molecules.<sup>75</sup> Since coiled chains of proteins are known to uncurl because of ionic repulsion when ionization occurs, Reid<sup>139</sup> suggested that excited state dissociation acts as a trigger in rapid biological process.

## 1.7 SCOPE OF THE PRESENT WORK

Derivatives of fluorene-9-carboxylic acid, called MARPHACTINS have long been known as potential plant growth retardants, herbicides, regulators and senescence inhibitors of detached plant parts.<sup>140</sup> So the effect of these compounds on geotropism and phototropism of plants has been considered as a novel phenomenon. Fluorene derivatives are carcinogenic, and these bind to DNA, resulting in mutagenity and modification of its protein recognition.<sup>141,142</sup> A correlation between the carcinogenicity and dissociation constants has also been attempted.<sup>143</sup> Theoretical studies on the interaction of fluorene derivatives with nucleic acids have recently been reviewed.<sup>144</sup> Some of the diamines are used as analytical reagents for the determination of vanadium and aluminium.<sup>145</sup> In spite of their paramount importance in physiology, biochemistry and analytical chemistry, to our knowledge, the spectral characteristics of these molecules have not been explored systematically and extensively except in a few cases.<sup>143,146-153</sup> It is the aim of this work to draw better insight into the chemical and physical properties of fluorene derivatives in the ground and excited singlet states. The quantum of information on the absorption and fluorescence characteristics of these systems available till now, is summarized as follows.

(i) As fluorene is a first member of the series of O-O' bridged biphenyls, the electronic spectrum of fluorene can be best understood from the spectrum of biphenyl. Unlike biphenyl, the absorption spectrum of fluorene is vibrationally well resolved, and

red shifted presumably because of the strained nearly planar geometry of the molecule. The spectrum comprises of three band systems.<sup>146</sup> The moderately intense and strong transitions observed at 300 nm and 260 nm are polarised along the long axis of the molecule whereas the weak transition at 287 nm is short axis polarised. The long wavelength absorption band of fluorene comprises of very complex vibrational structure. It has been shown that this electronic band consists of three vibrational frequencies with values  $800\text{ cm}^{-1}$ ,  $500\text{ cm}^{-1}$  and  $1420\text{ cm}^{-1}$ .

The fluorescence spectrum of fluorene is also structured (300 nm, 331 nm) and essentially holds a mirror image relationship with the long wavelength absorption band.<sup>147</sup> The band position and intensity of the absorption and fluorescence spectra are nearly insensitive to the solvent environment.

(ii) Fluorene and methoxyfluorenes form excimer at low temperature.<sup>148</sup> A theoretical model for excimers has been proposed by Minn et al.<sup>149</sup>

(iii) The ground state  $\text{pK}_a$  values, reveal that the behaviour of 9-substituted fluorene is different from that of other substituted compounds.<sup>143</sup> For example, 9-fluorenamine in which amino group is attached at the saturated 9-methylene carbon is considerably more basic than its purely aromatic congeners. This essentially behaves like an aliphatic amine.

It is speculated from the difference in  $\text{pK}_a$  values, that there is an intramolecular hydrogen bonding between the carboxylic group at

1-position and hydrogen atoms at 9-positions of fluorene molecule.

(iv) 9-Aminofluorene exhibits unusual dual emission. The solvent dependent long wavelength fluorescence was attributed to TICT conformer in the  $S_1$  state.<sup>150</sup>

(v) Transfer of triplet energy from 2-acetylfluorene to lanthanide ions have shown that the  $^3\pi\pi^*$  state is of lower energy than that of  $^3n\pi^*$  state.

Since the information available on the absorption characteristics of fluorene systems is fragmentary and that on fluorescence is scarce, we pursued the systematic study on the effects of substitution, solvent and pH on the absorption and fluorescence characteristics of substituted fluorenes. The study on bifunctional molecules would be more fascinating because they form basis for the understanding of steric hindrance, resultant resonance and inductive effect, geometry and dipole moment. To carry out the investigation, a series of seventeen substituted fluorenes and six structurally related diamines have been selected. These are divided into three groups such as methyl substitution, carbonyl substitution and diamines. The selection of these molecules can be rationalized as follows.

(i) It has been shown that molecules other than arylamines also undergo proton-induced fluorescence quenching.<sup>128,129</sup> This stimulated the interest to see whether simple substituted fluorenes (fluorene, 1-methylfluorene and 9-fluorenomethanol) would also undergo the proton induced fluorescence quenching or not. The advantage of these molecules is that these have simple groups which are devoid

of other prototropic equilibrium. The protonation aspect can also be studied in the light of the experimental and theoretical results which predict that aromatic hydrocarbons become more basic upon excitation.<sup>154</sup> Moreover, it is believed that understanding of the basic molecule is a kind of prerequisite for the understanding of similar reactions of the substituted compounds.

(ii) The second group i.e. carbonyl systems include acids, esters, amides, aldehyde and ketones..

(a) The effect of  $\text{-COOH}$  and  $\text{-COO}^-$  groups on the spectral changes of condensed ring systems have revealed that  $\text{-COOH}$  (with few exceptions) and  $\text{-COO}^-$  are nonplanar in the  $S_0$  state but become coplanar with the aromatic system in the  $S_1$  state. The degree of planarity is more for  $\text{-COOH}$  group than that of  $\text{-COO}^-$  group.<sup>23,155</sup> This aspect of studies on fluorene systems would give interesting information about the geometry of the substituents with respect to the fluorene moiety. To see the effects of these substituents on the spectral transitions, substitution is carried out at different positions of fluorene. In fluorene-1- and -4-carboxylic acids,  $\text{-COOH}$  is along short axis of the molecule and hence are expected to impart nearly identical effects. In fluorene-2-carboxylic acid  $\text{-COOH}$  group is along long axis. In fluorene-9-carboxylic acid it is attached to an aliphatic carbon. The acidity and basicity of these compounds are expected to be different.

(b) Protonation reaction of amides has received great attention<sup>156-172</sup> because of the controversial protonation site, inapplicability of Hammett's acidity scale and the medium effect. On the

same lines, fluorenamides can also be investigated to locate the site of protonation and evaluate actual  $pK_a$  values. If the Hammett's acidity scale is not valid for these also, hydration requirement can be invoked to relate  $H_o$  and  $H_A$  scales.

(c) The study of carbonyls would be interesting owing to the fluorescence activation by hydroxylic solvents i.e. reversal of excited states may take place.<sup>173,174</sup> Keeping this phenomenon in mind, three carbonyls such as 2-fluorenaldehyde, 2-acetylfluorene and 2-benzoylfluorene were prepared. The spectral shifts and basicities can be correlated with electron withdrawing ability of the substituents.

(iii) Bifunctional molecules having electron donating and electron withdrawing groups have been studied extensively.<sup>175-178</sup> But similar systematic study on molecules having both electron donating groups is less.<sup>179-183</sup> One such study<sup>179</sup> on 9,10-phenanthroline, which contains two nitrogen atoms at symmetrical positions, reveals interesting features. That is, while protonation on both of the nitrogen atoms leads to red shift in the absorption spectrum, first protonation results red shift and second, a blue shift in the fluorescence spectrum. This anomalous behaviour of bifunctional molecule stimulated our interest in diamines with substituents at symmetrical positions. 2,7-diaminofluorene is selected because the symmetrical amino groups are placed at positions where the exchange of electron density is possible.

The other diamines which are expected to have similar behaviour are o-phenylenediamine (oPA), p-phenylenediamine (pPA), m-phenylenediamine (mPA), 2,3-diaminonaphthalene (DAN) and 9,10-diaminophenanthrene (DAP).

The added advantage of these compounds is that the detailed studies on their corresponding monoamines are available. So the present investigation can be carried out in the light of following results.

(a) Generally monoamines undergo proton-induced fluorescence quenching with few exceptions.<sup>184</sup>

(b) In some of the monoamines, prototropic equilibrium between the monocation and neutral species is not established in the excited state.

(c) The basicity and spectral shifts can be used to get the knowledge of geometry of the molecules.

For all these compounds, solvent study can be carried out to comment on the nature of the spectral transitions and solute-solvent interactions. The pH dependence can be studied to identify different prototropic species and to calculate  $pK_a$  and  $pK_a^*$  values.

Low temperature (77 K) fluorescence studies, wherever required have been made. Freezing 'locks' the fluorophore in the ground state configuration and prevents solvent cage relaxation and functional group reorganization subsequent to excitation. Thus a comparison of absorption and fluorescence spectra taken in frozen solutions with those taken in fluid media permits distinction between the solvent and conformational effects arising from the ground and excited state molecules. Since the low temperature studies in this work are made whenever a particular prototropic species is non-fluorescent at room temperature, glass forming solvents have not been used. Instead,



measurements have been done in a medium in which the species exist. Due to this some times scattering is observed with fluorescence. In order to get the fluorescence spectrum of any prototropic species, comparison is made with the solutions with and without the solute.

## CHAPTER-II

### MATERIALS, METHODS AND INSTRUMENTATION

#### 2.1 MATERIALS

The compounds such as fluorene (F), 1-methylfluorene (1MF), 9-fluorenemethanol (9FM), fluorene-1- and -9-carboxylic acids (1FA, 9FA), 2-fluorenaldehyde (2FAl), 2-acetylfluorene (2AcF), 2,7-diaminofluorene (DAF), o-and p-phenylenediamines (oPA, pPA), 2,3-diaminonaphthalene (DAN) and 9,10-diaminophenanthrene (DAP) were procured from Aldrich Chemical Co. Fluorene, 9FM, 1MF, 2FAl, 2AcF and DAN were repeatedly recrystallized from ethanol. 9FA and 1FA were recrystallized from methanol, DAF from benzene, pPA from ether and oPA from water. DAP was vacuum sublimed and repeatedly recrystallized from benzene.

##### 2.1.1 Synthesis

Starting materials for the preparation were obtained from Aldrich Chemical Co. The purity of these compounds varied from 98-99% and were used as such for the preparation.

Methylester of 1FA (1FE) was prepared by refluxing the acid and methanol in the presence of catalytic amount of conc.  $\text{H}_2\text{SO}_4$ .<sup>185</sup> 9-Fluorene-carboxylic ester (9FE) was prepared by employing the procedure given in the literature.<sup>186</sup> Both 1FE and 9FE were recrystallized twice from methanol (1FE, 86–87°C; 9FE, 65°C).

Fluorene-2- and -4-carboxylic acids (2FA, 4FA) were prepared by Clemmenson reduction of 9-fluorene-2- and -4- carboxylic acids respectively.<sup>187</sup> 2FA was recrystallized from methanol and 4FA from ethanol (2FA, white flakes, mpt 275–277°C; 4FA, colourless crystalline substance, mpt 195°C).

Ester of 2FA was synthesized by the procedure as used for 1FE. 2FE was recrystallized in methanol (mpt 185–187°C).

2-Benzoylfluorene (2BeF) was synthesized in two steps. 2-Fluorenaldehyde was made to undergo Grignard reaction with bromobenzene to give a pale yellow substance. The major product, a white compound was separated by column chromatography and identified as carbinol. This was oxidized by the following method. Pyridine (50 mM) dissolved in dichloromethane (20 ml) taken in a flask was stirred for 15 minutes, at constant temperature (15°C). To this,  $\text{CrO}_3$  was added portionwise. After the addition of celite, the mixture was stirred further for 20 minutes at 25°C. To this, the carbinol (20 mM) in dichloromethane was added dropwise and stirring was continued for 25 minutes. The reaction mixture was diluted with ether and filtered. After the removal of solvent and pyridine, the compound was recrystallized from ethanol to get white crystalline solid.

To prepare the amides (fluorene-1-, -2- and -4- amides), the following procedure was used. First the acid chlorides of 1FA, 2FA and 4FA were prepared by thionyl chloride method.<sup>188</sup> After the purification, the acid chlorides were dissolved in  $\text{CH}_2\text{Cl}_2$  and reacted with cold  $\text{NH}_3$ . The pasty mass obtained was washed several times, dried and recrystallized from ethanol (1Fam,  $247^\circ\text{C}$ ; 2Fam,  $228^\circ\text{C}$ ; 4Fam,  $137^\circ\text{C}$ ).

m-Phenylenediamine was prepared by the reduction of m-nitroaniline using Sn/conc. HCl. It was recrystallized from benzene.<sup>189</sup>

### 2.1.2 Solvents

A set of five representative solvents were employed for the solvent study. These solvents are cyclohexane and water, the extreme solvents in polarity scale, ether/dioxane, hydrogen bond acceptor or dispersive solvent, acetonitrile, a dispersive solvent and methanol/ethanol hydrogen bond donor solvents. Spectroscopic grade methanol (BDH) was used without further purification. Ether (Alembic), dioxane (Sarabai), acetonitrile (E. Merck), cyclohexane (IDPL), ethanol (BDH) were further purified as described in the literature.<sup>190</sup>

### 2.1.3 Purity of the Materials

Purity of the compounds prepared was checked by Thin layer chromatography, UV, IR, NMR spectral data, melting point and by using fluorescence technique i.e. by getting same spectral profile when excited with different wavelengths. The purity and transparency of the solvents were checked by UV spectra recorded using triply distilled

water as the reference. Solvents were also tested for spurious fluorescence emission.

## 2.2 METHODS

### 2.2.1 Preparation of Solutions

pH of solutions within the range 3-11 was adjusted by the addition of phosphate buffers ( $10^{-3}$  M) as this amount of buffer do not quench fluorescence of the sample and also do not alter the prototropic equilibrium under study.<sup>191</sup> The total analytical concentration of buffers i.e.  $[\text{H}_2\text{PO}_4^-] + [\text{HPO}_4^{2-}]$  was maintained constant for each pH solution by adding appropriate amount of sodium hydroxide and phosphoric acid.

Modified Hammett's acidity scale ( $\text{H}_\text{O}$ )<sup>192</sup> was used for the solutions below pH 1. The  $\text{H}_\text{O}$  function serves specifically as a measure of the tendency for the solution in question to transfer a proton to an uncharged or charged basic molecule, increasingly negative value corresponding to higher acidity. Benzophenone Hammett's scale<sup>193</sup> was used for the prototropic reactions of aldehyde and ketones and  $\text{H}_\text{A}$  acidity scale<sup>194</sup> for the amides. For 20% ethanolic acid solutions of 2FA and 2BeF, a scale proposed by Dolman and Stewart<sup>195</sup> was used. Acid solutions were prepared with sulphuric acid and basic solutions with either sodium hydroxide or potassium hydroxide.

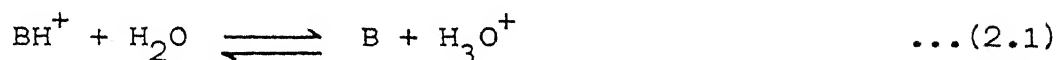
The concentration of a particular compound in all the test solution ( $\text{H}_\text{O}/\text{pH}/\text{H}_\text{A}$ ) was the same. With the help of an Oxford P-7000 Micropipette system, an accurately measured amount (0.1 or 0.2 ml) of aliquots of stock solution of the compound was delivered into a

standardized volumetric flask (10 ml) containing  $H_0/pH/H_-$  solutions. The concentration of the proper solute in the test solution was in the order of  $10^{-5}M$  and for phenylenediamines it was near  $10^{-4}M$ .

Due to the poor solubility of the compounds, test solutions contained either 0.5% or 1% methanol. The absorption and fluorescence spectra of the samples contained in  $1\text{ cm}^2$  cuvette were scanned immediately after preparing the solutions. All the diamines were purged with oxygen free nitrogen for 15 to 20 minutes before the measurements were made.

### 2.2.2 Determination of Dissociation Constants

Ground State : The dissociation of an acid can be represented as,



and the ground state dissociation constant ( $pK_a$ ) in dilute solution can be given by the relation,

$$pH = pK_a - \log I \quad \dots(2.2)$$

where  $I = [BH^+]/[B]$ , ratio of the concentration of conjugate acid to that of the base.

For the dissociation of acids in strong sulphuric acid, activity is invoked instead of concentration to give the following Hammett's equation,

$$H_0 = -\log(a_{H^+} \cdot f_B/f_{BH^+}) = pK_a - \log I \quad \dots(2.3)$$

where 'f' is the activity coefficient of respective species and 'a' the

activity of  $H^+$ . The equations (2.2) and (2.3) demand unit slope for the plot  $H_0/pH/H_-$  Vs  $-\log I$ . This condition may not be obeyed in cases where the prototropic species involve the structural and medium effects.<sup>163,164,195</sup> For example, in the cases of primary amides and benzophenones, the large deviation from the unit slope requirement could not be explained by medium effect alone. So it was explained by Yates et al.<sup>194</sup> that the validity of Hammett's cancellation assumption (i.e. the activity coefficient behaviour of a set of indicators is reasonably independent of changes in the structure) on which the construction of Hammett's scale is based, is not correct. Based on this, a numerous acidity scales have been proposed and are documented in the review by Cox and Yates.<sup>197</sup>

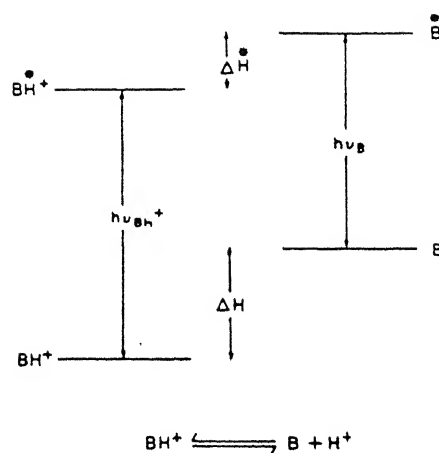
The value of  $I$  in the above equations is given<sup>198</sup> as,

$$I = [BH^+]/[B] = (\epsilon - \epsilon_B)/(\epsilon_{BH^+} - \epsilon) = (A - A_B)/(A_{BH^+} - A)$$

where  $\epsilon$  and  $A$  are molecular extinction coefficient and absorbance.  $pK_a$  was thus calculated as intercept of the plot  $H_0/pH/H_-$  Vs  $\log I$ .

Excited State : The excited state dissociation constants ( $pK_a^*$ ) were obtained by using two methods.

(i) The first one is Förster cycle method<sup>79</sup>, which is based on a thermodynamic cycle (shown in scheme 1) involving acidic and basic forms of the molecule in  $S_0$  and  $S_1$  states.



Scheme 2.1 Förster's relationship of enthalpy changes to electronic transitions.

The energy involved in this cycle is balanced as,

$$\Delta E + \Delta H^* = \Delta E' + \Delta H \quad \dots (2.4)$$

where  $\Delta E$  and  $\Delta E'$  are the energies of the O-O transition of acid and its conjugate base.  $\Delta H^*$  and  $\Delta H$  are the dissociation energies of the acid in  $S_1$  and  $S_0$  states respectively. Using the relation,

$\Delta H = \Delta G + T\Delta S$ , the above equation can be written as,

$$\Delta E + \Delta G^* + T\Delta S^* = \Delta E' + \Delta G + T\Delta S$$

$$\text{i.e. } \Delta E - \Delta E' = (\Delta G - \Delta G^*) + T(\Delta S - \Delta S^*) \quad \dots (2.5)$$

Assuming that the entropy of dissociation in  $S_0$  and  $S_1$  states is the same and using,



$\Delta G = -RT \ln K = 2.3 RT \text{ pK}_a$ , Equation (2.5) can be modified as,

$$\Delta E - \Delta E' = 2.3 RT (\text{pK}_a - \text{pK}_a^*) \quad \text{or}$$

$$\text{pK}_a - \text{pK}_a^* = (\Delta E - \Delta E') / 2.3 RT$$

This can be written as,

$$\text{pK}_a^* - \text{pK}_a = (h\bar{\nu}_B - h\bar{\nu}_{BH^+})c / 2.3 RT \quad \dots (2.6)$$

where  $\bar{\nu}_{BH^+}$  and  $\bar{\nu}_B$  are wavenumbers corresponding to O-O transition of the acidic and basic forms of the molecule respectively. The O-O transition can be obtained either from absorption spectrum, fluorescence spectrum or from the average of absorption and fluorescence band maxima. The accuracy with which  $\text{pK}_a$  can be calculated is limited by the following assumptions employed in deriving the above relation.

- (a) The entropy change of the prototropic reaction in  $S_0$  and  $S_1$  states is equal.
- (b) The electronic states involved in the absorption and fluorescence spectra of  $BH^+$  and B should be the same.
- (c) Prototropic equilibrium, solvent and geometrical relaxations should be the same in  $S_0$  and  $S_1$  states.
- (d) The vibrational energy spacing of  $S_0$  and  $S_1$  states of the given acid as well as the conjugate base should be identical.

If any of these assumptions does not hold in a particular case, one would end up in erroneous results. Schulman et al.<sup>88b</sup> have proposed a modified Förster cycle which includes vibrational, solvent and

geometrical relaxations in both the states.

(ii) The second method is by fluorimetric titration<sup>199</sup> and is widely used to calculate the  $pK_a^*$  values, because none of the previously mentioned assumptions are involved in the determination of  $pK_a^*$  values. In this method, the sample is excited at the isosbestic point and the relative fluorescence intensity ( $I/I_0$ ) is plotted against acid concentrations. If both of the species involved in the equilibrium are fluorescent, the above plot gives a sigmoid curve, for both acidic and basic species whose point of inflection is the same for both forms. If the excited state lifetimes of the species are greater than the rate of proton transfer, the point of inflection is the  $pK_a^*$  value. If the rate of the excited state proton transfer is too slow to complete with the fluorescence deactivation rate, the fluorescence intensity of an emitting species reflects the ground state concentration, which in turn, depends on the ground state  $pK_a$  value. This situation generally occurs if the  $pK_a^*$  values fall in the mid pH regions where there is insufficient amount of protons to establish the equilibrium in the  $S_1$  state. On the other hand, if the excited state proton transfer rate is comparable with fluorescence decay rate, a stretched fluorimetric titration curve is obtained giving rise to both  $pK_a$  and  $pK_a^*$  values.

The estimation of  $I/I_0$  is very simple if the fluorescence band maxima of the prototropic species involved in the equilibrium are well separated. But more often, the fluorescence spectra of conjugate acid-base pair overlap each other. In these cases, the overlapping factors can be introduced as described by Ireland and Wyatt.<sup>89</sup> The actual

intensities are given as,

$$\phi = (F - k'F')/(1 - kk') \quad \dots (2.7)$$

$$\phi' = (F' - kF)/(1 - kk') \quad \dots (2.8)$$

where  $F$  and  $F'$  are the fluorescence intensities,  $k$  and  $k'$  are the overlap ratios of the  $BH^+$  and  $B$  forms respectively. The value of  $k$  is obtained from solutions showing only the characteristic fluorescence of  $BH^+$  form and is the ratio of the fluorescence intensity of  $BH^+$  (measured at analytical wavelength for  $B$ ) to the intensity at the wavelength where  $BH^+$  emission is measured. Similarly,  $k'$  is obtained from the measurements in a solution having  $B$  as the only fluorescent species.

(iii) Though the third method, a time dependent fluorescence technique, has not been utilised in this work, for the sake of completion, it is presented here. This technique uses the following relation,<sup>89,200</sup>

$$pH = pK_a^* - \log \tau_o / \tau_o' \quad \dots 2.9$$

where  $pH$  reflects the acid concentration at which relative intensity curves show an inflection,  $\tau_o$  and  $\tau_o'$  are the fluorescence lifetimes of acidic and conjugate basic species respectively. Alternatively, by calculating the rate of forward and backward proton transfer processes, the value of  $pK_a^*$  can be obtained. So to calculate the accurate  $pK_a^*$  value it is necessary to use time dependent techniques. However steady state fluorescence spectroscopy continues to be at the

helm in all practical purposes because it is less expensive and relatively simple to apply.

### 2.2.3 Quantum Yield Calculation

The fluorescence quantum yields ( $\phi_f$ ) of the compounds were calculated using the solutions with absorbance (at excitation wavelength) less than 0.1. It is because to reduce the self absorption and other quenching phenomena. The fluorescence spectrum recorded in this case was corrected by the procedure mentioned in section 2.3.3. Quinine sulphate in 0.1N  $H_2SO_4$  ( $\phi_f$  0.55,  $\lambda_{ex}$  313,  $\lambda_{em}$  440) and in some cases anthracene in ethanol ( $\phi_f$  0.31,  $\lambda_{ex}$  366 nm) were used as the standards.<sup>201</sup>

The relation used for the quantum yield calculation is as follows,

$$\phi_{\text{unknown}} = \phi_{\text{standard}} \times \frac{F_{\text{unknown}}}{F_{\text{standard}}} \times \frac{q_{\text{standard}}}{q_{\text{unknown}}} \times \frac{A_{\text{standard}}}{A_{\text{unknown}}}$$

where F is the area under the corrected fluorescence spectrum, q the photon out put of the source at the excitation wavelength taken from the curve (Fig. 2.3), A absorbance.

### 2.2.4 Lifetime and Quenching Constant Estimation

Lifetimes of the species which exhibit proton induced fluorescence quenching were calculated from the following relation connecting lifetime ( $\tau_{FM}$ ) and the quantum yield.

$$\tau_1 = \tau_{FM} \cdot \phi_f \quad \dots (2.10)$$

$\tau_{FM}$  was estimated from the intensity of the appropriate absorption envelope using Strickler-Berg relation<sup>202</sup> i.e.

$$\tau_{FM}^{-1} = 2.88 \times 10^{-9} n^2 \langle \bar{\nu}_f^3 \rangle_{av} \frac{g_l}{g_u} \int e^{d \ln \bar{\nu}} \quad \dots (2.11)$$

where  $n$  is refractive index,  $g$  multiplicity weighing factor and

$$\langle \bar{\nu}_f^3 \rangle_{av} = \int F(\bar{\nu}) d\bar{\nu} / \int \frac{F(\bar{\nu}) d\bar{\nu}}{\bar{\nu}^3}$$

where  $F$  is the relative fluorescence intensity at the wave number  $\bar{\nu}$ . This equation predicts reasonably good values for the lifetime for the molecules where S-S transition is strongly allowed and when there are small displacements from equilibrium nuclear configuration upon excitation. In other words, potential energy surfaces of both the states have the same shape, i.e. mirror image symmetry is retained between the absorption and fluorescence profiles.

The lifetimes of neutral and monocation species of 2,3-diaminonaphthalene were measured by picosecond time correlated single photon counting technique. The true fluorescence function can be extracted from two experimental time profiles, one that of the scattered excitation function distorted by the measuring system. Under certain conditions the observed fluorescence decay  $R(t)$  is a convolution of the true decay  $F(t)$  and the measured excitation function<sup>203,204</sup>  $L(t')$  i.e.

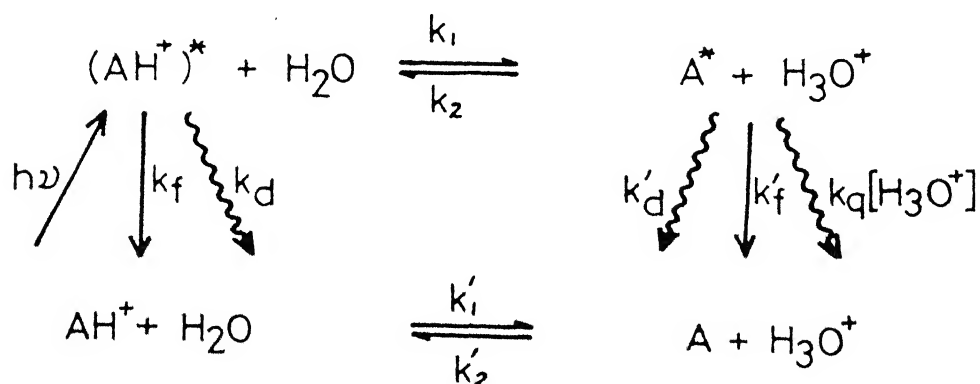
$$R(t) = \int_0^t L(t') F(t-t') dt' \quad \dots (2.12)$$

If the correction factor for the wavelength dependent response of PMT called time shift ( $\mu$ ), is incorporated, the above equation takes a convenient form,

$$R(t) = \int L(t-\mu) F(\mu) d\mu \quad \dots (2.13)$$

when  $R(t)$  and  $L(t)$  are known,  $F(t)$  can be determined by variety of techniques.<sup>205</sup> We have used least squares method.<sup>206</sup>

Proton-induced fluorescence quenching kinetic analysis is done by considering the following reaction scheme,<sup>122d</sup>



$k_1$  and  $k_2$  are the dissociation and association constants of acid and base respectively for  $S_1$  state. The 'prime' stands for ground state.  $k_f$ ,  $k_d$  are the fluorescence decay and radiationless decay constant for the acid and the same with 'prime' stands for the conjugate base. The

$k'_q$  is the proton-induced fluorescence quenching constant for the base.

Using the steady state approximation, one can write,

$$\frac{I^0}{I} = 1 + \frac{1}{k_1 \tau_{AH^+}} + \frac{[k_2 + k'_q(1 + k_1 \tau_{AH^+}^0)] \tau_A^0}{k_1 \tau_{AH^+}^0} [H_3O^+] \quad \dots (2.14)$$

If the value of  $\tau_{AH^+}$  is large,  $k_1 > k_2[H_2O^+]$  at  $[H_3O^+] < 0.5M$ , the following equations should hold

$$k_1 \tau_{AH^+} \gg 1; k_2/k_1 \tau_{AH^+}^0 \ll k'_q$$

The above equation (2.14) simplifies to

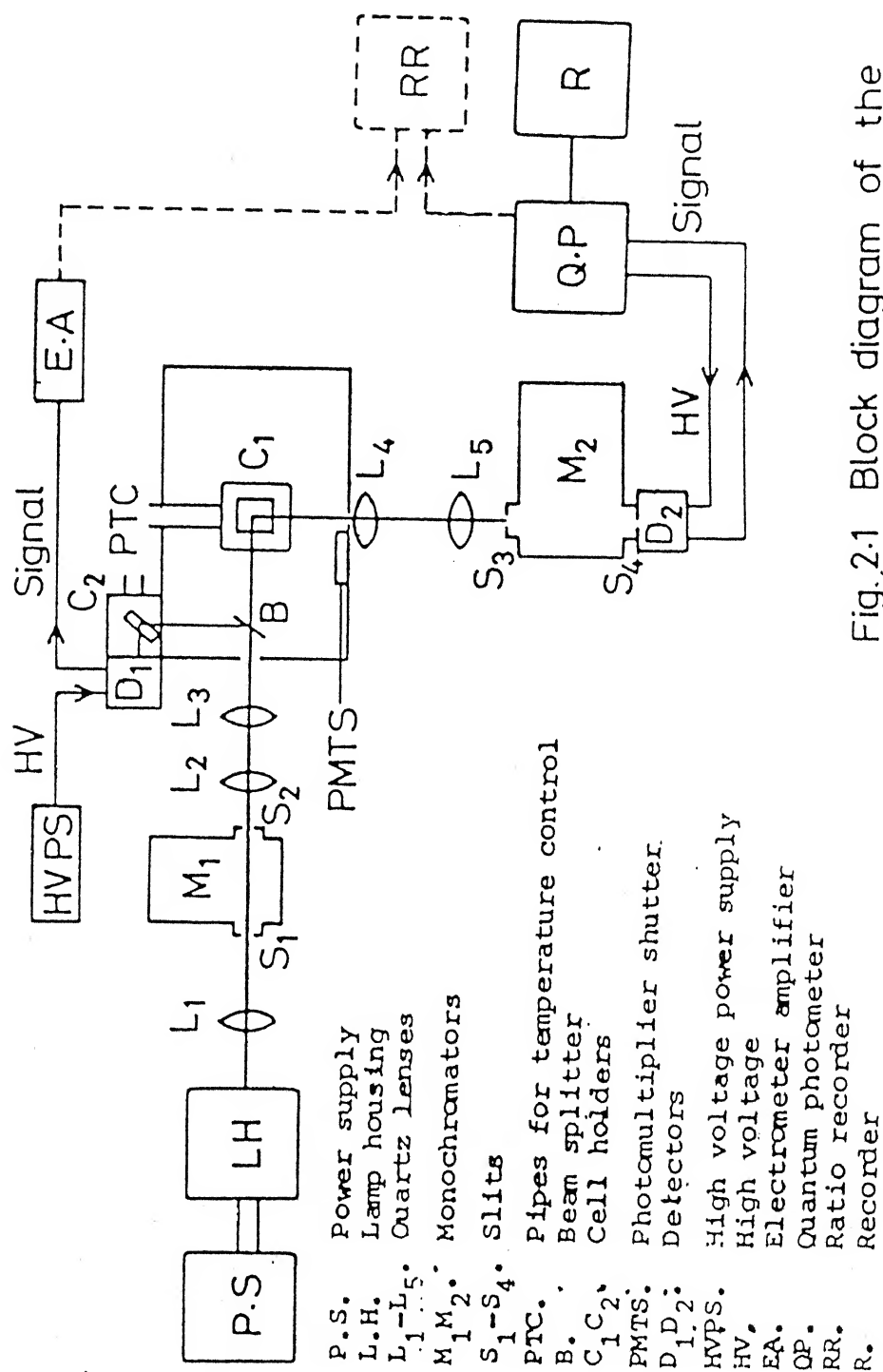
$$\frac{I^0}{I} = 1 + k'_q \tau_A^0 [H^+] \quad \dots (2.15)$$

where  $I$  and  $I^0$  are the fluorescence intensities of A with and without quencher respectively. From the slope of this equation and with the knowledge of  $\tau$ , the proton-induced fluorescence quenching rate constant can be calculated. In order to satisfy the above criteria, measurements were done at low acid concentration.

## 2.3 INSTRUMENTATION

### 2.3.1 Spectrofluorimeter

The scanning spectrofluorimeter was fabricated in our laboratory. The block diagram and the arrangement to take spectra at low temperature are shown in Fig. 2.1 and 2.2 respectively. A brief introduction of various parts is given below.





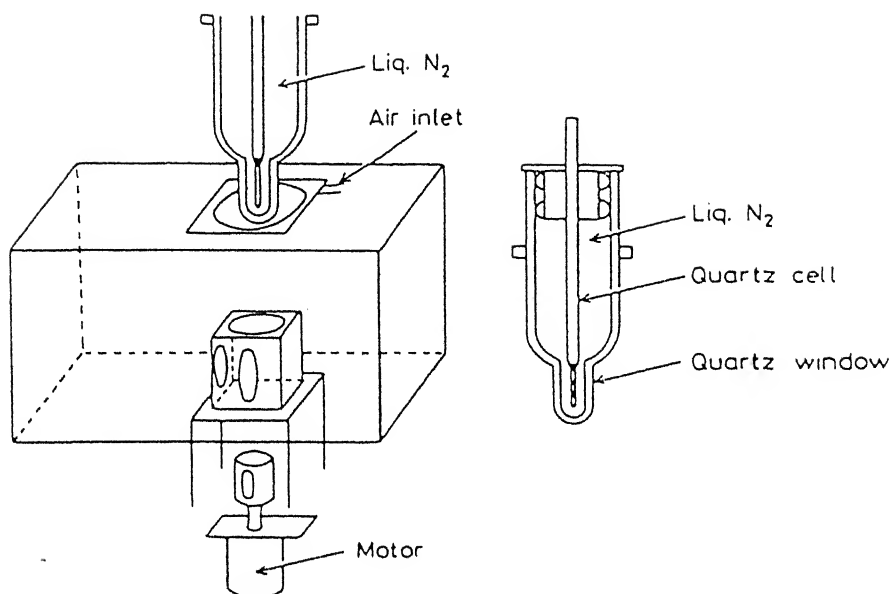


Fig. 2-2 Diagram of low temperature set up for fluorescence and phosphorescence.

A power supply (PS) unit for the lamp (LPS, 251 HR) and the lamp housing (LH 150) were procured from Schoeffel Instruments. The lamp housing can accommodate 150W Xe lamp, 200W Xe-Hg lamp and 200W Hg lamp. The total energy output from the lamp could be monitored and kept constant by the power supply.

Two Jarrell-Ash (0.25 m and f/3.5) Ebert grating monochromators (82-410 and 82-415) were used. The monochromator ( $M_1$ ) with a grating blazed at 300 nm (1180 grooves/mm) with a reciprocal linear dispersion (RDA) of 3.3 nm/mm was used for selecting the excitation wavelength. The monochromator ( $M_2$ ) with two gratings one blazed at 300 nm

(2360 grooves/mm) with RDA of 1.65 nm/mm and the other blazed at 500 nm (1180 grooves/mm) with RDA of 3.3 nm/mm were used for recording the emission spectra. The focal length of quartz lenses ( $L_1$ - $L_5$ ) were chosen to suit the aperture to focal length ratios of monochromators and to have a maximum collection of the exciting as well as emitting light.

A cell compartment which is anodized to minimize light scattering was used and this set up is accessible for temperature variations. For low temperature measurements (77 K), Aminco Bowman's low temperature fluorescence and phosphorescence accessories could be fitted in the cell compartment by replacing the normal cell holders  $C_1$  (Fig. 2.1). There is a provision to pass dry air to remove the condensed moisture from the walls of Dewar flask used for the low temperature measurements. If necessary a beam splitter could be fitted in the cell compartment which enables the calibration of light source.

Princeton Applied Research Quantum Photometer Console (model 1140 A) was used for detection and amplification of emission. It consists of a detector assembly, an amplifier/discriminator (1140 B), electrometer, a highly stabilized voltage supply for photomultiplier tube (PMT) and two rate meters, one with log scale and the other with a linear scale. The detector assembly with IP28 PMT (Hamamatsu, Japan) was fixed at exit slit of  $M_2$ . Very weak signals could be detected on the photon counting mode of the quantum photometer. The amplified signal was read from the rate meter on the front panel. A multirange and multispeed digital recorder (Fisher Recorder Series 5000) was used to record the signal output from the quantum photometer. The emission

monochromator  $M_2$  was scanned by a digital drive system, specifically made for Jarrell Ash monochromators (Jarrell Ash Omnidrive 82-462) which is coupled to the recorder. From time to time both of the monochromators were calibrated with low pressure mercury lamp. The band width of the excitation source is 8 nm.

### 2.3.2 Experimental Procedure

The sample in 1 cm<sup>2</sup> quartz cuvette is excited by a monochromatic radiation selected by  $M_1$  and the emission is collected at right angle. After the dispersion by  $M_2$ , the emission signal is picked up by PMT and is read in the quantum photometer. The complete emission spectrum is recorded by scanning  $M_2$ .

For the low temperature spectra, the cell compartment is fitted with low temperature accessory. The sample in quartz tube is placed in liquid nitrogen, kept in a quartz Dewar flask. Then the Dewar flask with the sample is placed in the cell compartment.

Fluorescence excitation spectra can be obtained by setting  $M_2$  at the fluorescence maximum and scanning  $M_1$ .

### 2.3.3 Correction Factor Determination

In a spectrofluorimeter, the intensity of the lamp, efficiency of the monochromators and the response of PMT are wavelength dependent. So all spectrofluorimeters record only an 'apparent emission or excitation spectrum' in the absence of an automatic correction accessory.

Such uncorrected spectra are grossly distorted version of the true spectra. Several methods have been described to obtain the true spectra using correction factors.<sup>207</sup> The principles of Melhuish's<sup>207d</sup> method for the calculation of correction factor,  $\phi(\lambda)$  for the light source (150 W, Xe lamp) - excitation monochromator combination were followed in this study. This correction factor is the relative intensity distribution of the light source emerging from  $M_1$  at different wavelengths. The intensity profile of the lamp obtained by this method is shown in Fig. 2.3. The correction factor for emission monochromator - IP28 PMT combination,  $R(\lambda)$  was determined by using the procedure described by Chen.<sup>207e</sup> This correction factor is the relative response of  $M_2$ -PMT combination and is divided by  $\phi(\lambda)$  to give  $S(\lambda)$ , the emission correction factor at different wavelengths. A plot of  $S(\lambda)$  Vs  $\lambda$  gives the emission spectral sensitivity curve or the correction curve, as shown in Fig. 2.4 for low blaze and high blaze gratings.

These correction factors were used to correct the fluorescence spectrum of anthracene ( $1 \times 10^{-5}$  M in ethanol) recorded using the low blaze grating and quinine sulphate ( $1 \times 10^{-5}$  M in 0.1N  $H_2SO_4$ ) recorded using the high blaze grating. The corrected spectra obtained are shown in Figs. 2.5 and 2.6 respectively. These fluorescence spectra match exactly in their profile with the spectra reported in the literature.

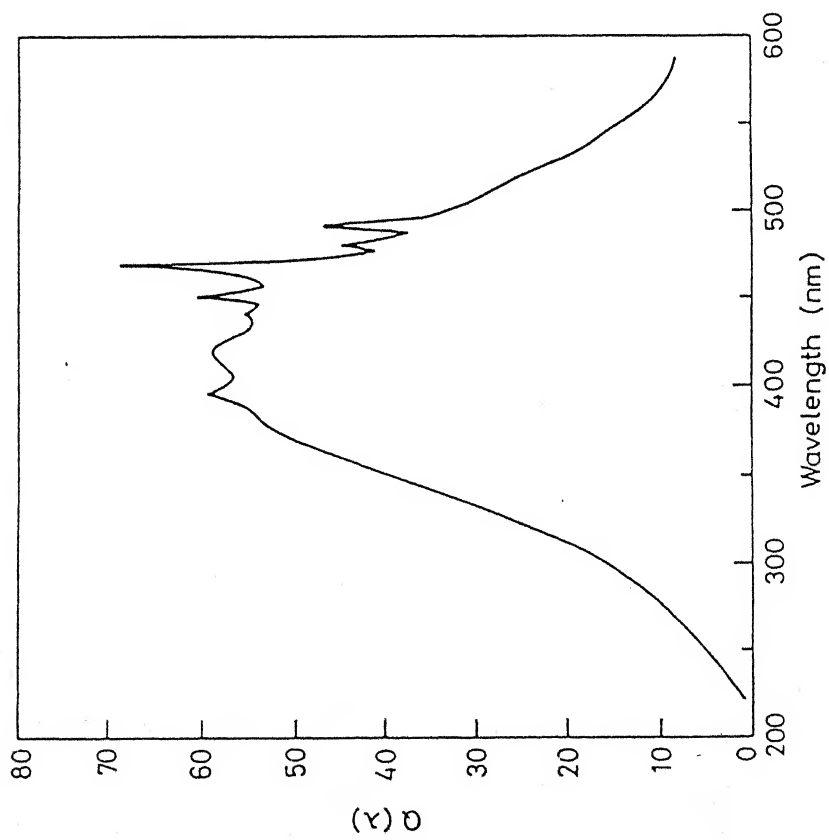
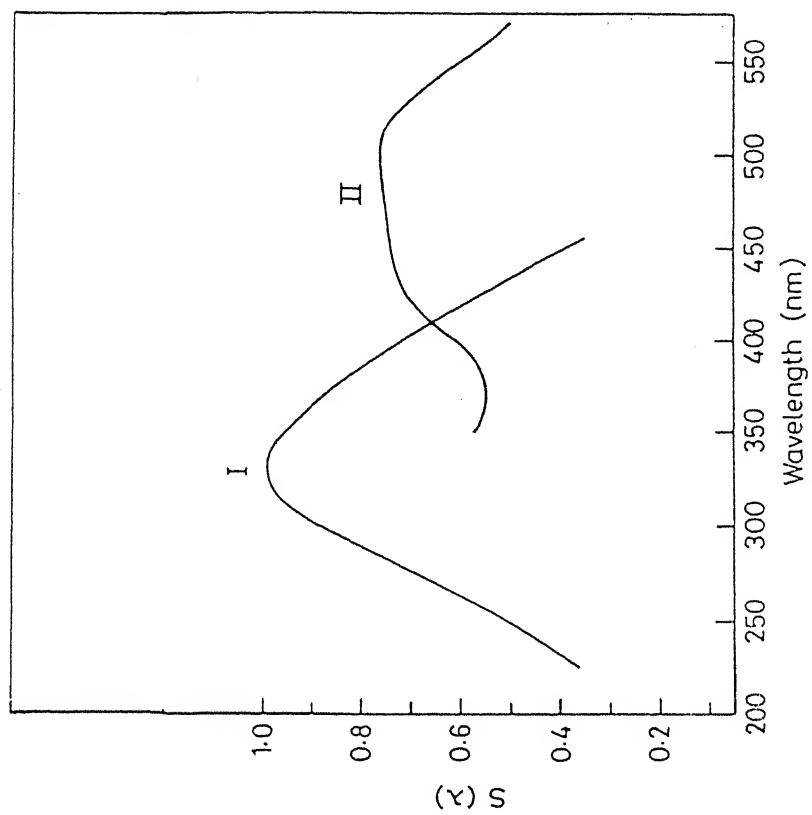


Fig. 2.3 Relative intensity distribution of excitation source. Fig. 2.4 Emission calibration curves : I 300 nm blaze grating  
II 500 nm blaze grating.



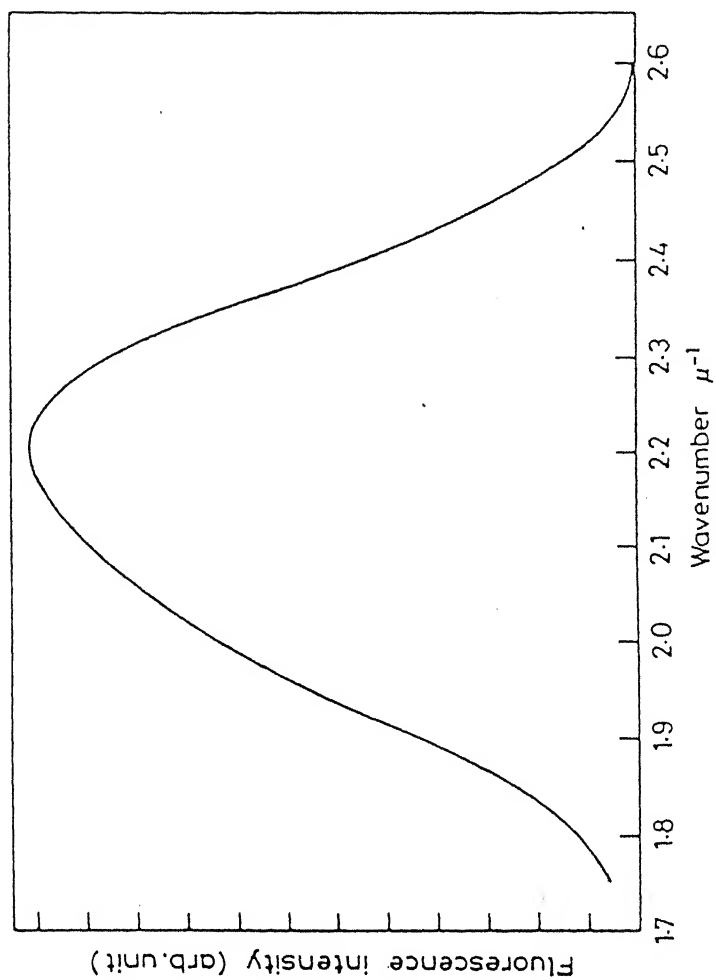


Fig. 2.6 Corrected Fluorescence spectrum of Quinine Sulphate  
( $1 \times 10^{-5} \text{ M}$  in  $0.1 \text{ N H}_2\text{SO}_4$ )

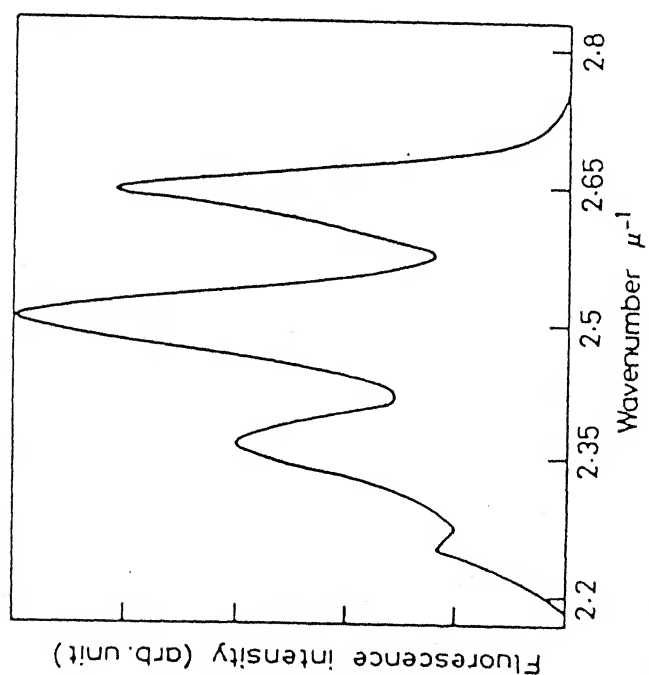
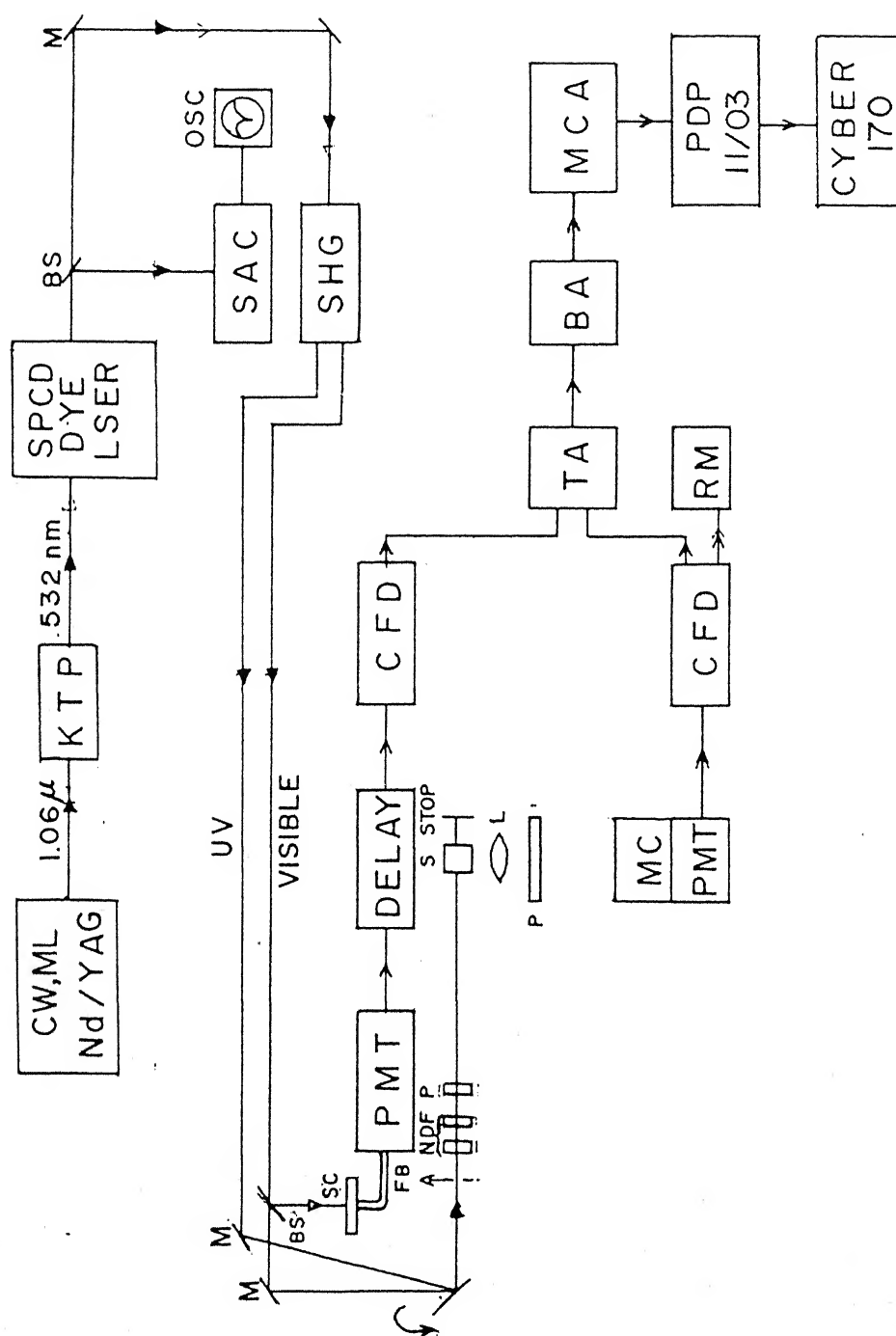


Fig. 2.5 Corrected Fluorescence spectrum of  
Anthracene ( $1 \times 10^{-5} \text{ M}$  in ethanol)

#### 2.3.4 Other Instruments

Picosecond time correlated single photon counting detection system was used to measure the fluorescence lifetimes of monocation and neutral species of 2,3-diaminonaphthalene. It is of Spectra Physics Model (Block diagram is shown in Fig. 2.7), uses a CW Mode locked Nd-YAG/synchronously pumped, cavity dumped dye laser (Rhodamine 6G dissolved in ethylene glycol-ethanol mixture) as the excitation source. The sample contained in a  $1\text{ cm}^2$  quartz cuvette is excited with a train of pulses. The repetition rate normally used is 800 KHz with the average power of 10-25 mW. The pulses have a autocorrelation width of a 10 ps. Fluorescence was collected at right angle to the excitation path through a monochromator and the detection is done on PMT XP2020. The output pulse of PMT is fed into a constant fraction discriminator which provides suitable voltage signals for the time-to-amplitude converter (TAC), Time analyser (Canberra Model 2143). The data from TAC is acquired in multichannel analyser (Tracr Northern Model TN 7200) and fed into a computer to reconvolute to extract the true fluorescence function.

Absorption spectra were recorded on a UV-190 double beam spectrophotometer (Shimadzu) equipped with U-135 chart recorder. The pH of various solution is measured by Toshniwal pH meter model CL 44A. Standard buffer solutions were used for the calibration of the pH meter.



(Fig. 2.7 BLOCK DIAGRAM OF PICOSECOND SPECTROFLUOROMETER)



### CHAPTER-III

#### SOLVENT AND pH EFFECTS ON THE ELECTRONIC SPECTRA OF METHYL, CARBOXYL, AMIDE AND CARBONYL SUBSTITUTED FLUORENES

In this chapter, the effects of solvents and acid concentration on the absorption and fluorescence spectra of some substituted fluorenes have been discussed in great detail. These compounds have been divided into four sections: (i) containing  $-\text{CH}_3$  and  $-\text{CH}_2\text{OH}$  groups, (ii) containing  $-\text{COOH}$ ,  $-\text{COOMe}$  groups at positions 1,2,4 and 9 (iii) containing  $-\text{CONH}_2$  groups at position 1,2 and 4 and lastly (iv)  $-\text{CHO}$ ,  $-\text{COCH}_3$  and  $-\text{COPh}$  groups at position-2.

#### 3.1 FLUORENE AND METHYL SUBSTITUTED FLUORENES<sup>a</sup>

##### 3.1.1 Solvent Effect

The absorption and fluorescence spectral data of fluorene (F), 1-methylfluorene (1MF), 9-fluorenemethanol (9FM) in various solvents and at different acid concentrations are compiled in Tables 3.1 and

---

<sup>a</sup> R. Manoharan and S.K. Dogra, J. Photochem. Photobiol., A: Chem. in press.

3.2 respectively. The spectral characteristics of different species are shown in Fig. 3.1 to 3.3. The results are summarized below:

(i) The absorption spectra of 1MF and 9FM are not very different from that of fluorene<sup>146</sup> in any one solvent. The vibrational structure as well as the band maxima are not affected by the solvent environments.

(ii) The fluorescence spectra of these compounds resemble each other in every respect except a slight red shift (3 to 4 nm) is observed for 1MF and 9FM as compared to fluorene.<sup>147</sup>

It is not expected that groups like  $-\text{CH}_3$  and  $-\text{CH}_2\text{OH}$  will exert significant change in the spectrum of the parent molecule because:

(i) these are not strongly interacting chromophores with the  $\pi$  electron cloud of the fluorene moiety and (ii) these are present either at position-1 or position-9. The former can affect only the short axis polarised transition, whereas the latter one not at all. Since the long wavelength absorption band is long axis polarised, substituent effects are not observed in this band. The perturbation by these groups seems to be slightly more in  $S_1$  state which results in a small red shift (0.3 nm) in the fluorescence spectra. The spectral band maxima as well as the quantum yields indicate that the interaction of solvents with these molecules is not very large. The mirror image relationship and near matching of the maxima of O-O transition of absorption and fluorescence spectra illustrate that the nature of the transition<sup>146</sup> is of  $\pi \rightarrow \pi^*$  character and the emitting and absorbing states are the same.

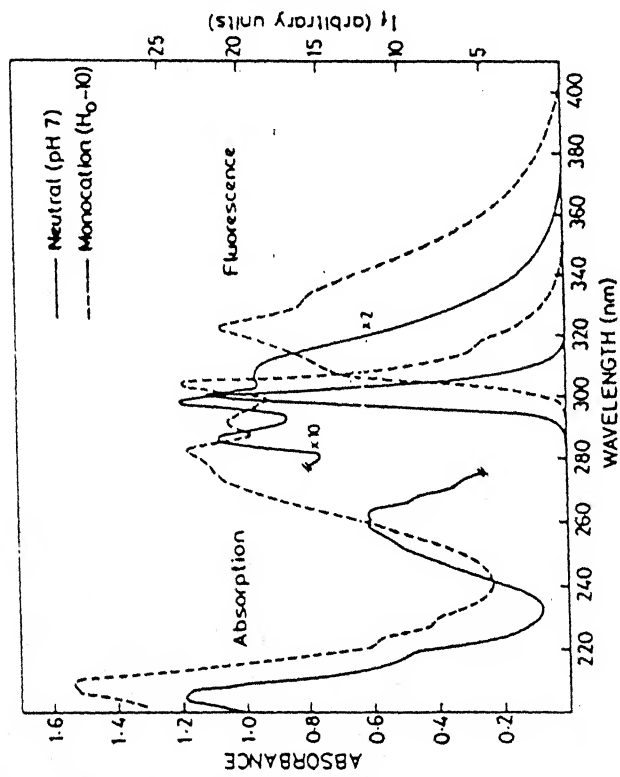


Fig.3.1 Absorption and fluorescence spectra of neutral and monocation species of fluorene.

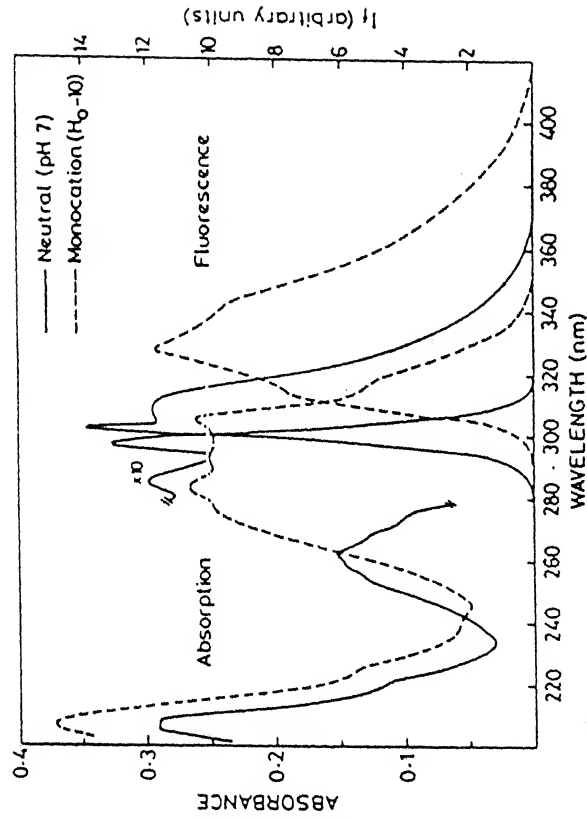


Fig.3.2 Absorption and fluorescence spectra of neutral and monocation species of 1-methylfluorene.

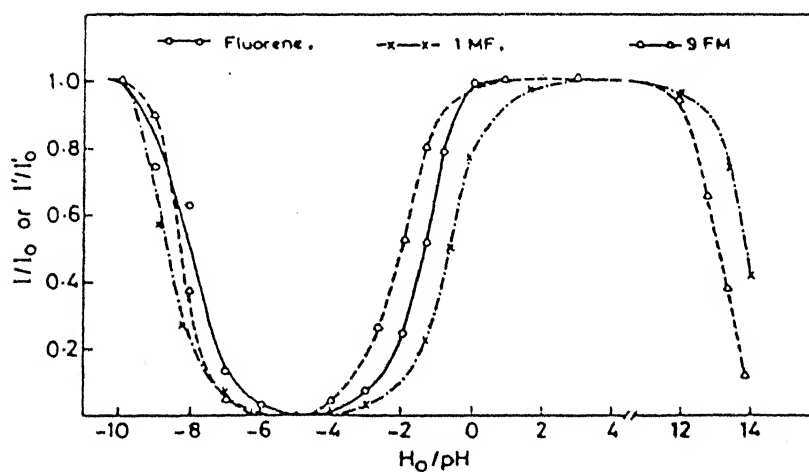
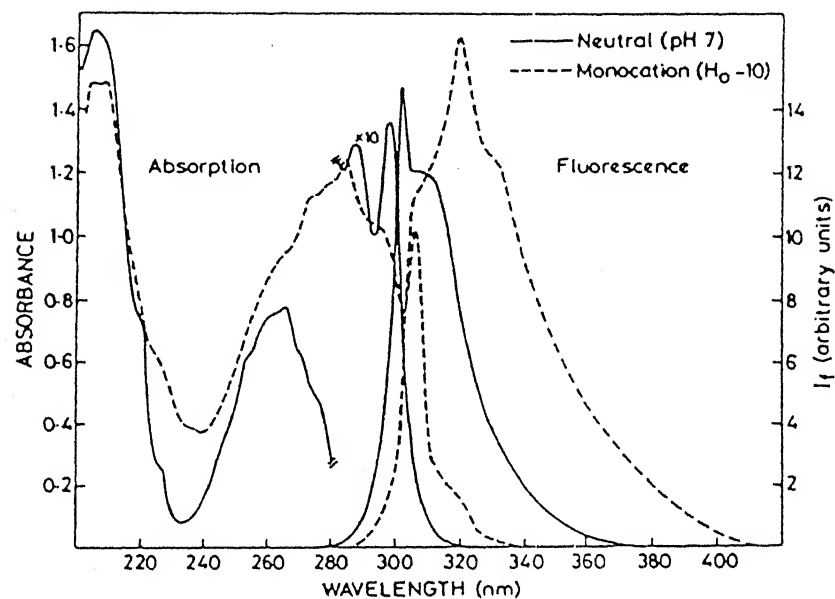


Fig.3.3 Absorption and fluorescence spectra of neutral and monocation species of 9-fluorenmethanol.

Fig.3.4 Fluorimetric titration curves for the various prototropic species of fluorene, 1-methylfluorene and 9-fluorenmethanol.

Table 3.1(contd.)

1	2	3	4	5	6	7	8	9	10
Methanol	297 (3.82)	276 (3.98)	260 (4.22)	300 (3.7)	278 (4.01)	262 (4.22)			
	291 (3.59)	271 (4.11)	255 (4.17)	289 (3.69)	273 (4.11)	255 (4.17)		-	
	287 (3.66)	263 (4.24)			265 (4.24)				
Neutral (pH 7)	296 (3.82)	275 (3.93)	260 (4.14)	299 (3.82)	278 (4.09)	-	299 (4.12)	275 (4.2)	261 (4.47)
	286 (3.75)	270 (4.07)	254 (4.09)	288 (3.78)		254 (4.21)	288 (4.03)	270 (4.30)	257 (4.41)
	-	264 (4.16)	-	-	265 (4.28)	-	-	-	-
Monocation (H <sub>0</sub> -10)	318 (4.07)	295 (4.37)	275 (4.36)	317 (3.5)	285 (4.42)	263 (4.43)	318 (4.06)	282 (4.76)	-
	305 (4.40)	284 (4.40)		306 (4.33)	279 (4.39)		305 (4.78)	273 (4.73)	-
				298 (4.32)	273 (4.38)		293 (4.72)		

Values in paranthesis represent log $\epsilon$ .

Table 3.2. Fluorescence Spectral Data of Fluorene, 1-Methylfluorene and 9-Fluorene-methanol in Different Solvents and at Various Acid Concentration.

Solvent/species	1 MF	9 FM	F
Cyclohexane	302,309 (0.28)	302,309 (0.23)	—
Dioxane	302,309 (0.29)	300,308 (0.22)	—
Acetonitrile	299,308 (0.26)	300,307 (0.20)	—
Methanol	300,306 (0.29)	300,307 (0.24)	—
Neutral (pH 7)	302,308 (0.26)	302,309 (0.30)	299,308 (0.3)
Monocation ( $H_0 - 10$ )	315,326,340 (0.12)	308,322,332 (0.25)	310,322,332 (0.1)

Table 3.3. Acidity Constants of Fluorene, 1-Methylfluorene and 9-Fluorene-methanol.

Equilibrium	$pK_a$	$pK_a^*$		
		ft	a	f
$FH^+ \rightleftharpoons F + H^+$	-8.1	-8.0	-3.9	-3.2
$1MFH^+ \rightleftharpoons 1MF + H^+$	-8.4	-8.6	-3.5	-3.3
$9FMH^+ \rightleftharpoons 9FM + H^+$	-7.8	-8.1	-3.8	-3.9

ft = from fluorimetric titration.

a and f = by Förster cycle method using absorption and fluorescence maxima respectively.

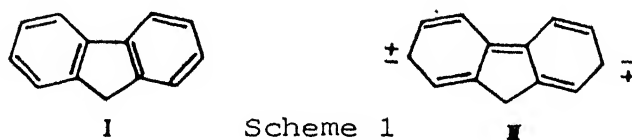
### 3.1.2 Effect of Acid Concentration

The absorption spectra of F, 1MF and 9FM do not change in the range  $H_0$  -6 to pH 14. Below  $H_0$  -6, red shift is observed in all the bands but the vibrational structure is intact. This can be assigned to a monocation formed by the ring protonation at 2-position, because electrophilic substitution in fluorene takes place at this position followed by 7 and 4 positions.<sup>4</sup> The acidity constants (listed in Table 3.3) reveal that the effect of  $-CH_3$  and  $-CH_2OH$  is not much. No change in the spectra of these molecules in the basic region, is consistent with the fact that  $pK_a$  for the deprotonation of  $-CH_2OH$  is above 16<sup>208</sup> and that of  $>CH_2$  of 9 position is  $\approx 23$ .<sup>209</sup>

The effect of acid concentration on the behaviour of the fluorescence spectra is very different from that on the absorption spectra. The fluorescence intensities of the neutral species of 1MF and 9FM are quenched above pH 12 without the appearance of any new fluorescence bands. Although a monoanion fluorescence band of fluorene has been predicted by Vander Donckt et al.<sup>209</sup>, we are unable to detect it, possibly because of the low sensitivity of our equipment. The decrease in the fluorescence intensity could be due to either  $OH^-$  induced fluorescence quenching or the formation of a non-fluorescent monoanion. The latter possibility seems to be correct as the  $pK_a^*$  values for the neutral-monoanion equilibria determined by fluorimetric titration (Fig. 3.4) for 1MF and 9FM (13.9 and 13.1 respectively, Table 3.3) are nearly equal to those of fluorene (reported by Vander Donckt et al.<sup>209</sup>) and N-methyl-2-(hydroxymethyl)benzimidazole.<sup>125d</sup>

The monoanion of the latter compound is also non-fluorescent and its  $pK_a$  value is 13.5, determined with the help of fluorimetric titration; the dissociable proton is from  $-CH_2OH$  group. This indicates that  $>CH_2$  and  $-OH$  groups become stronger acids on excitation.

The fluorescence intensity of IMF is progressively quenched with an increase of acid concentration below pH 2, whereas those of F and 9FM below  $H_0O$ , without an appearance of new fluorescence bands. Invariance of fluorescence intensity with concentration of  $SO_4^{-2}$  (with the addition of  $K_2SO_4$ ) equal to that present in  $H_2SO_4$  used in the region, suggests the proton-induced fluorescence quenching process as a means of deactivation. Similar behaviour has also been noticed for other aromatic hydrocarbons.<sup>128b</sup> The Stern-Volmer constants,  $K_{SV}$  obtained from the plot of  $I_0/I$  vs  $[H^+]$  (shown in Fig. 3.5) and  $\hat{C}_{FM}$  calculated by employing Strickler-Berg<sup>202</sup> equation are listed in the Table 3.4. The data suggest that the higher values of  $k_q$  for F, as compared to naphthalene<sup>128b</sup> ( $\sim 10^6$ ) and anthracene<sup>128b</sup> ( $\sim 10^7$ ) could be due to the contribution of canonical structure (II) in fluorene:



The data further indicate that the presence of  $-CH_2OH$  at position-9 has no effect on  $k_q$  values, whereas  $-CH_3$  group at position-1 may increase the charge density at position-2 and thereby increases the  $k_q$  value. The small values of  $k_q$  observed for these molecules as



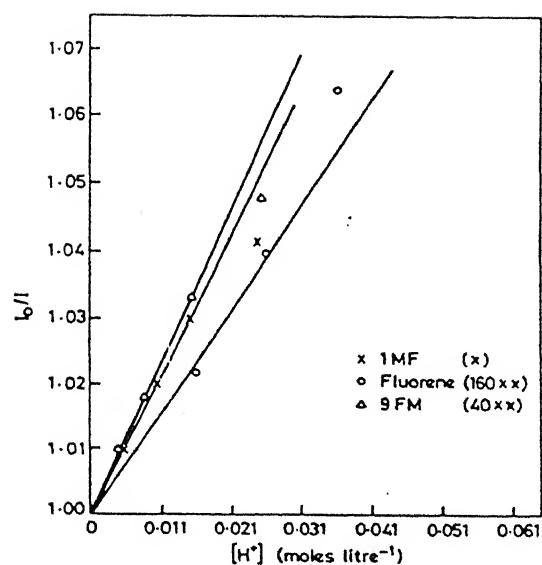


Fig.3.5 Stern-Volmer plots for proton-induced fluorescence quenching of fluorene, 1-methylfluorene and 9-fluorene-methanol.

Table 3.4. Proton-Induced Fluorescence Quenching Kinetic Data for Neutral Species of Fluorene, 1MF and 9FM.

Sample	$K_{sv}$ ( $M^{-1}$ )	$\tau_{FM}$ (ns)	$\tau$ (ns)	$k_q$ ( $M^{-1}s^{-1}$ )
Fluorene	0.036	6	1.8	$2 \times 10^7$
1MF	1.92	10	2.6	$7 \times 10^8$
9FM	0.05	7	2.2	$2 \times 10^7$

compared to arylamines<sup>128b</sup> confirm that charge transfer state is not the lowest energy state in these molecules.

Since there is no correspondance between the decrease and increase in the fluorescence intensity curves of neutral and monocation species, the  $pK_a^*$  values have been obtained from the formation curves of monocations. While fluorimetric titration curves (Fig.3.4) give ground state  $pK_a$  values, Förster cycle calculations<sup>79</sup> show that aromatic hydrocarbons become more basic upon excitation. Near resemblance of  $pK_a^*$  values calculated with absorption and fluorescence data using Förster cycle method, indicate that the solvent relaxation for both the species is not different in  $S_0$  and  $S_1$  states. Fluorimetric titration thus demonstrates that the prototropic equilibrium is not established during the lifetime of the excited state of acid-base pair and the theoretical values for the excited molecules do not correspond to the observable processes. Similar results have also been observed for the protonation reaction of many aromatic hydrocarbons.<sup>210</sup> Mason and Smith<sup>211</sup> have found from the changes in the upper limit for the quantum efficiencies of photochemical hydrogen isotope exchange in aqueous 1M perchloric acid that the radiative deactivation rate of an electronically excited aromatic hydrocarbon is faster than the rate of protonation by a factor of  $\sim 10^5$ . The same explanation seems to hold good for these molecules also.

It is thus concluded that (i) the absorbing and emitting states of these molecules are the same and are of  $\pi \rightarrow \pi^*$  character, (ii) proton-induced fluorescence quenching rate constant for these molecules

is not very large and the presence of  $-\text{CH}_3$  group at 1-position increases the value of  $k_q$  (iii) the excited state prototropic equilibrium between monocation and neutral species is not established during their lifetimes because of the slow rate of protonation and (iv)  $-\text{CH}_2$  group becomes more acidic upon excitation.

### 3.2 CARBOXYLIC ACIDS<sup>a</sup>

The results of 1-fluorenenecarboxylic acid(1FA), -2-carboxylic acid (2FA), -4-carboxylic acid (4FA), -9-carboxylic acid (9FA) and some methyl esters (1FE, 2FE and 9FE) are included in this section.

#### 3.2.1 Solvent Study

The absorption and fluorescence spectra of 1FA, 4FA, 2FA and 9FA recorded in different solvents are depicted in Fig. 3.6 to 3.9. The relevant data together with those of esters are compiled in Tables 3.5 and 3.6 respectively. The absorption spectra of 1FA and 4FA in any one particular solvent, are broad, diffuse and red shifted (except middle band  $\sim 260$  nm) as compared to the structured long wavelength band system of fluorene. As the polarity and hydrogen bonding ability of the solvents (except water) increase, the long wavelength band is progressively blue shifted whereas the middle one is unaffected. In acidic water, while the trend continues for 4FA, 1FA shows red shifted band. It is interesting to note that solvent sensitive

---

<sup>a</sup> R. Manoharan and S.K. Dogra, Spectrochim. Acta, 43A, 91 (1987); J. Photochem. Photobiol., A: Chem. in press.

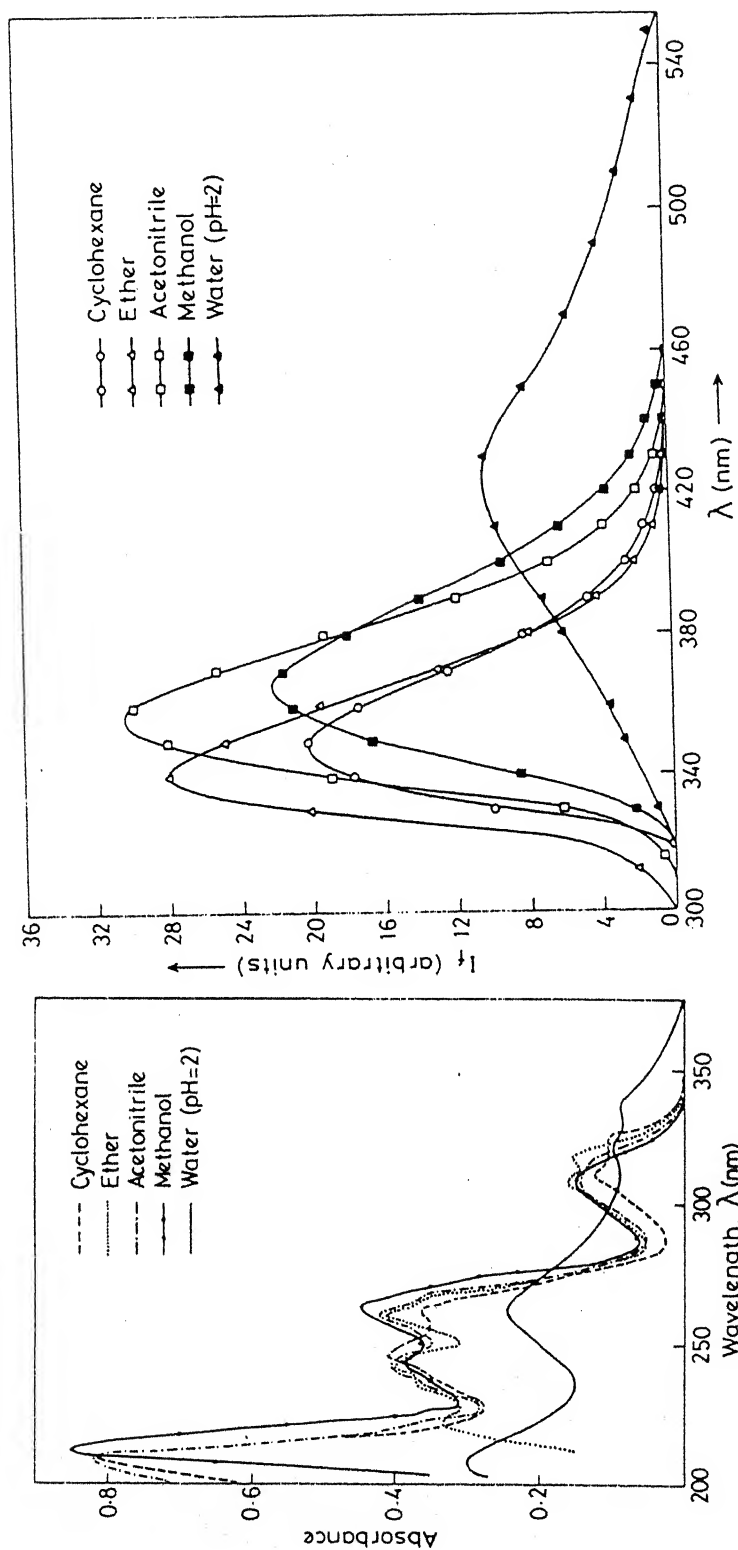


Fig.3.6 Absorption (left panel) and fluorescence (right panel) spectra of 1-fluorene-9-carboxylic acid in different solvents.

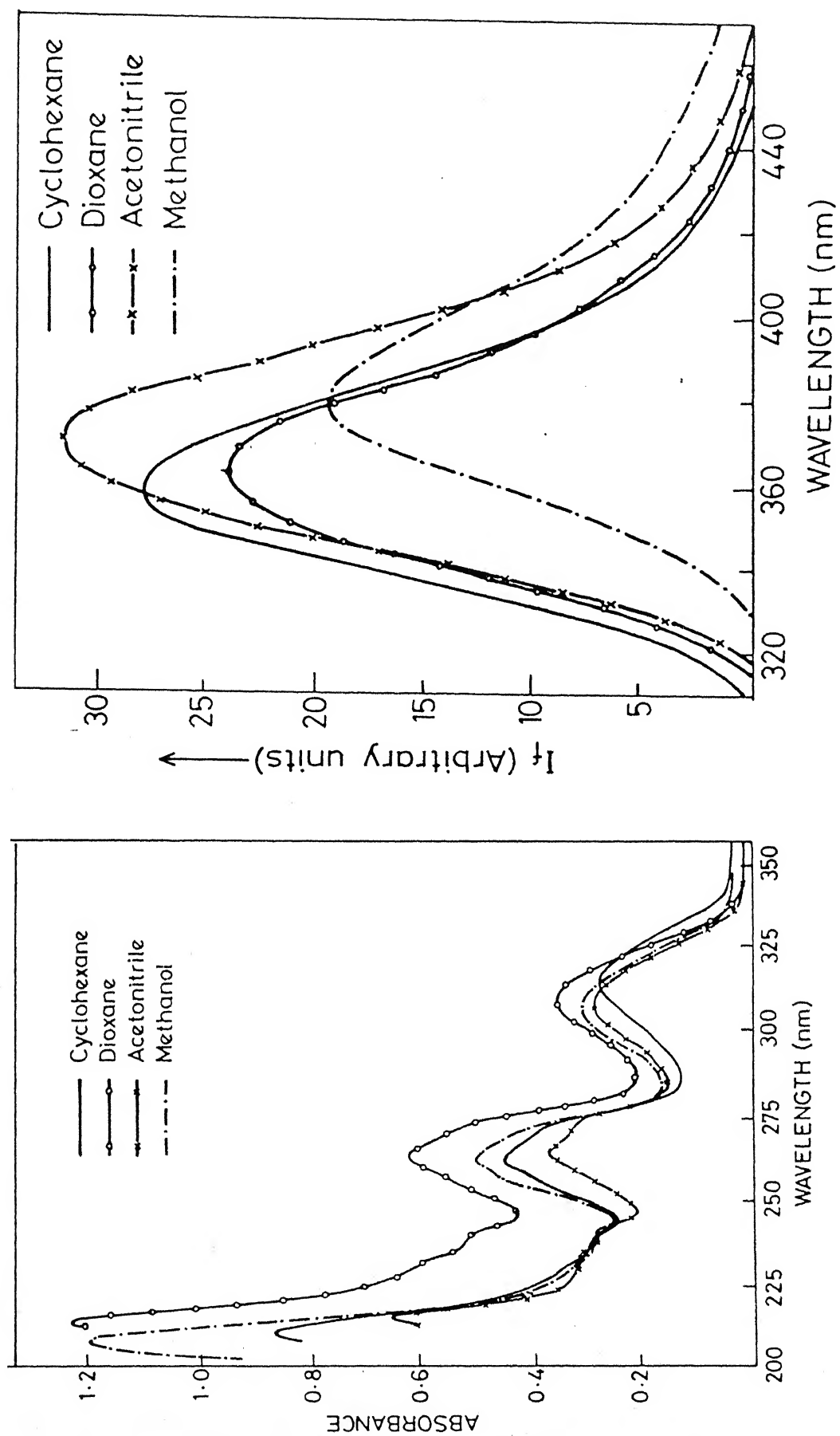


Fig.3.7 Absorption (left panel) and fluorescence (right panel) spectra of 4-fluorene-9-carboxylic acid in different solvents.

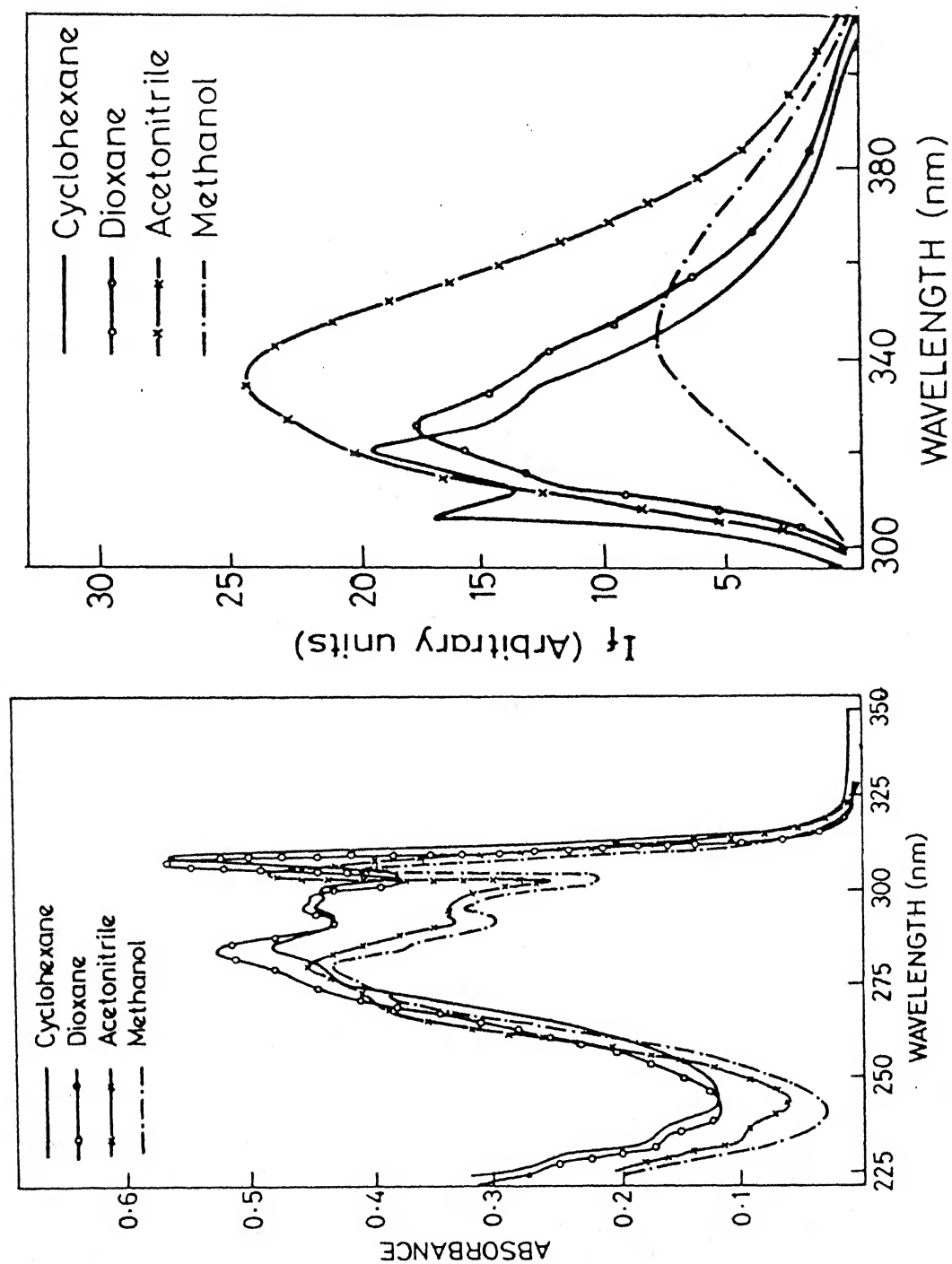


Fig.3.8 Absorption (left panel) and fluorescence (right panel) spectra of 2-fluorene-9-carboxylic acid in different solvents.

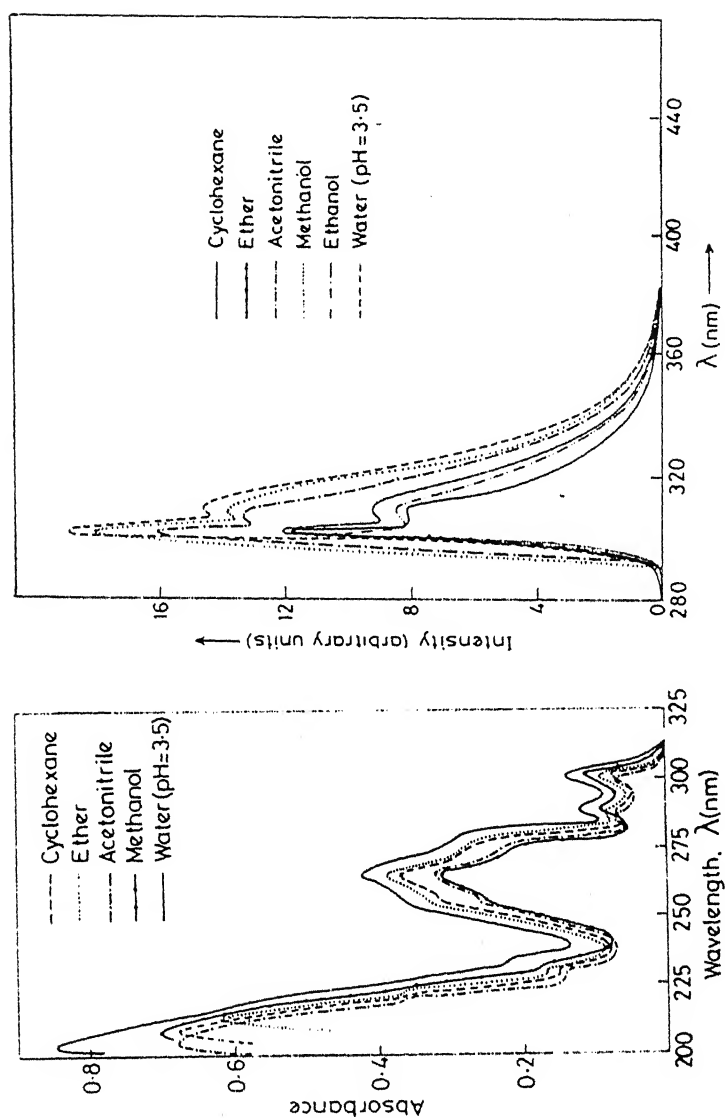


Fig.3.9 Absorption (left panel) and fluorescence (right panel) spectra of 9-fluorene-9-carboxylic acid in different solvents.

Table 3.5. Absorption Spectral Data of 1FA, 1FE, 4FA, 2FA, 2FE, 9FA and 9FE in Different Solvents.

	Cyclohexane	Ether/Dioxane	Acetonitrile	Methanol	Water
	2	3	4	5	6
1FA	322(3.35) 312(3.40) 262(3.83) 247(3.88)	318(3.80) 308(3.82) 262(4.24) 242(4.22)	315(3.75) 309(3.76) 261(4.22) 243(4.20)	- 307(3.76) 261(4.25) 242(4.18)	334(3.66) 320(3.71) 261(3.98) -
1FE	321(3.77) 308(3.81) 268(4.18) 246(4.24)	319(3.76) 307(3.82) 266(4.17) 244(4.22)	315(3.73) 308(3.76) 265(4.15) 244(4.20)	317(3.66) 309(3.70) 266(4.10) 244(4.20)	310(3.71) - 260(4.16) 245(4.2)
4FA	315 272 263 239	309(3.96) 274(4.13) 264(4.21) 239(4.13)	307(3.88) 275(3.93) 265(3.99) 241(3.88)	307(3.87) 270(3.92) 263(4.00) -	305(3.89) - 272(4.05) 262(4.12)
2FA	306 299 294 283 272 236	306(4.45) 297(4.36) 293(4.37) 282(4.43) 271(4.35) 233(3.91)	304(4.44) - 293(4.37) 280(4.41) 270(4.33) 232(3.52)	304(4.38) 297(4.32) 291(4.20) 286(4.31) 279(4.40) 269(4.28)	307(4.07) 297(4.05) - 284(4.04) - 233(3.04)

..contd.



Table 3.5(contd.)

1	2	3	4	5	6
2FE	308 303 293 282 271	309(4.36) 298(4.36) 294(4.35) 282(4.40) 272(4.29)	303(4.46) — 294(4.39) 280(4.40) 270(4.30)	308(4.37) 298(4.38) 292(4.18) 286(4.32) 279(4.43)	309(4.10) 298(4.00) — 284(4.15) —
9FA	301(3.57) 290(3.58) 266(4.26) 257(4.20)	301(3.63) 289(3.61) 267(4.23) 258(4.16)	300(3.55) 289(3.54) 265(4.18) 258(4.13)	301(3.76) 290(3.67) 266(4.19) 258(4.13)	298(3.61) 288(3.63) 266(4.25) 257(4.18)
9FE	301(3.72) 290(3.74) 266(4.28) 258(4.22)	301(3.63) 289(3.65) 265(4.27) 257(4.20)	300(3.63) 289(3.65) 265(4.27) 258(4.20)	300(3.62) 289(3.65) 264(4.25) 257(4.20)	298(3.63) 288(3.69) 265(4.20) 256(4.11)

For 4FA, 2FA and 2FE data are reported for dioxane solutions instead of ether.

Table 3.6. Fluorescence Spectral Data of 1FA, 1FE, 4FA, 2FA, 2FE, 9FA and 9FE in Different Solvents.

Compound	Cyclohexane	Ether/Dioxane	Acetonitrile	Methanol	Water
1FA	349(0.21)	341(0.26)	356(0.31)	365(0.29)	430(0.11)
1FE	340(0.18)	327(0.18)	350(0.17)	360(0.17)	392(0.10)
4FA	358(0.11)	364(0.12)	370(0.17)	380(0.21)	397(0.22)
2FA	332 320(0.21) 305	337 324(0.31) 310	335(0.13)	345(0.18)	365(0.22)
2FE	333 320(0.08) 305	338 324(0.13) 310	333(0.13)	347(0.18)	367(0.48)
9FA	303(0.35) 311	303(0.27) 311	303(0.38) 311	303(0.40) 311	303( - ) 311
9FE	301(0.28) 309	301(0.25) 309	302(0.24) 309	302(0.17) 309	302( - ) 309

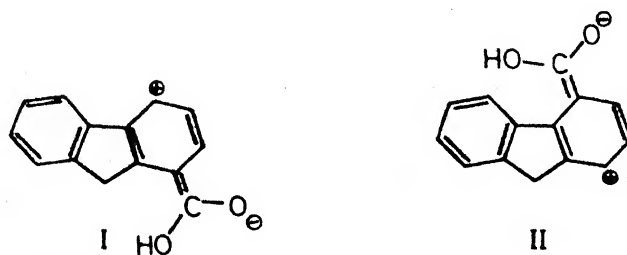
For 4FA, 2FA and 2FE data are reported for dioxane solutions instead of ether.

long and short wavelength bands of 1FA (322 nm, 247 nm respectively), in a given solvent are relatively more red shifted than those of 4FA. The absorption spectrum of 2FA is nicely structured and hardly affected by the solvent environment and matches with that of fluorene, except a small red shift by 3 to 4 nm. The spectral profiles of the esters are identical with those of their respective acids. But for 1FE, in water, absorption band is blue shifted by 24 nm as compared to that of 1FA. Similar to absorption spectra, fluorescence spectra of 1FA, 4FA and 1FE in different solvents are broad, devoid of vibrational structure and red shifted as compared to that of fluorene. Fluorescence spectra of 2FA and 2FE are structured in non polar solvent but vibrational structure is lost in polar solvents.

9-Substituted fluorenes (9FA and 9FE) exhibit absorption and fluorescence characteristics which are quite different from those of other carboxylic acids of fluorene. The spectra of 9FA and 9FE are vibrationally resolved and exactly resemble that of fluorene in all the solvents.

As mentioned earlier (Section 1.7), the absorption spectrum of fluorene consists of three bands. The bands centered at 300 nm and 265 nm are long axis polarised and that of 287 nm is short axis polarised one. Substitution at 1- and 4-positions (along short axis) of fluorene will affect considerably the short axis polarised transitions if these groups are coplanar with fluorene moiety. Similarly substitution at 2-position would predominantly affect the long axis polarised bands. 1FA and 4FA can be structurally compared with 1-naphthoic acid (1NA)<sup>212</sup> and 1-anthroic acid (1AA).<sup>213</sup> The studies on 1NA

suggest that the torsional angle<sup>214</sup> between  $\text{-COOH}$  group and naphthalene ring is  $11^\circ$  and this angle is enough to allow significant resonance interaction between these two groups. The red shifts observed for these acids (1NA,  $2400\text{ cm}^{-1}$ ; 1AA,  $1100\text{ cm}^{-1}$ ; 1FA,  $2300\text{ cm}^{-1}$ ; 4FA,  $1800\text{ cm}^{-1}$ ; 2FA,  $650\text{ cm}^{-1}$ ; 9FA, nearly zero) relative to their parent systems suggest that in the acids studied, the resonance interaction is maximum for 1FA and minimum for 9FA. From the data of Table 3.5, it is possible to conclude that  $\text{-COOH}$  group in 1FA and 4FA is nearly coplanar with respect to fluorene moiety. This leads to significant resonance interaction, thereby 287 nm band is largely red shifted and mixed with 300 nm band. Due to this, the long wavelength band system is broadened. It is concluded that the short axis polarised transition is of lower energy in 1FA and 4FA and long axis one in 2FA and 9FA. This can be further manifested from the fact that the molecular extinction coefficient of the first peak of long wavelength band is less than that of the other peaks in 1FA and 4FA, whereas it is opposite for 2FA and 9FA. The latter trend resembles that of fluorene. The resonance interaction between  $\text{-COOH}$  and the ring introduces charge transfer (CT) character in the short axis polarised state (as suggested by the canonical structures in Scheme 2). As  $\text{-COOH}$  group is



Scheme 2

coplanar, any interaction with solvent will be reflected in the absorption spectrum, as presented in the Table 3.5. Since in 1FA and 4FA, -COOH group is along the short axis, one would expect the spectra of these acids to be identical in position. But the red shift observed in absorption spectrum for the particular acid, as compared to its parent molecule (F), is more for 1FA than 4FA. This is because the hydrogen atoms at position-9 may facilitate the partial rotation of the 1-carboxylic group to have an intramolecular hydrogen bonding. In the case of 1FE, where the hydrogen bonding may be less effective for steric reasons, the absorption spectrum is nearly same as that of 4FA where the intramolecular hydrogen bonding is not possible at all. This is further manifested from the study of dissociation constants (vide infra) i.e. the  $pK_a$  for 1FA is 4.0 and that of 4FA is 3.0.

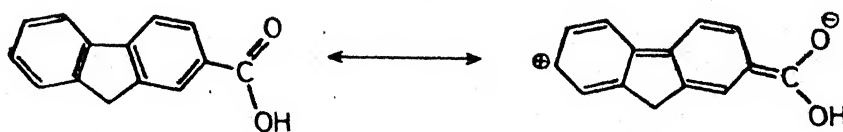
The more diffuseness of the fluorescence spectra of 1FA, 4FA and 1FE could be due to the complete rotation of -COOH group in the  $S_1$  state, thus making this group fully coplanar with the ring. Since the transition moment of the long wavelength absorption band of 1FA seems to be perpendicular to the long axis of fluorene ring, a greater conjugation is expected in  $S_1$  state than in the  $S_0$  state, thereby introducing greater CT character into  $S_1$  state. The exceptionally large red shifted fluorescence band of 1FA in acidic water, and the spectral similarity of 1FE and 4FA confirm the presence of an intramolecular hydrogen bonding in 1FA as proposed for the ground state species. The large Stokes shift (given in Table 3.7) observed for 1FA and 4FA is not only due to the greater difference in the  $S_0$  and  $S_1$  state geometries but also to the greater change in the dipole moment upon excitation. Smaller Stokes shift observed for 1FA as compared

Table 3.7. Stokes Shift ( $\text{cm}^{-1}$ ) Observed for 1FA, 4FA, 2FA and 9FA in Different Solvents and at Various pHs.

Solvent	1FA	4FA	2FA	9FA
Cyclohexane	2400	2600	1430	1070
Ether/Dioxane	2170	4910	1870	1130
Acetonitrile	3650	5550	4000	1240
Methanol	5180	6310	3100	1070
Water	6690	7600	5180	1400
Monoanion	4700	6380	2870	970
Monocation	—	—	4810	—
Dication	—	6630	5130	—

to 4FA in any one solvent further indicates that the difference between the ground and excited state geometry for 1FA is less than that of 4FA and thus is consistent with the earlier conclusion derived for 1FA. In other words, it may be concluded that unlike in 4FA,  $-\text{COOH}$  group at 1-position is nearly coplanar with the fluorene ring even in the ground state, because of an intramolecular hydrogen bonding.

In the case of 2FA and 2FE, molecular models indicate that  $-\text{COOR}$  group is free of any moderating factors. So one would expect large effect on the spectra of these molecules. On the contrary, absorption and fluorescence spectra are structured and these exhibit small Stokes shift in non-polar solvents, indicating that  $-\text{COOR}$  group is not coplanar with fluorene ring, both in  $S_0$  and  $S_1$  states. This kind of behaviour has also been observed for indole-3-acid, even though steric hindrance is absent in this case.<sup>155</sup> The large Stokes shift observed for 2FA and 2FE in polar solvents can not be explained by simple solute-solvent interaction, especially when  $-\text{COOR}$  group is non-planar with the parent moiety. It seems that in polar and protic solvents, the following canonical structures may be stabilized thereby leading to a more planar structure in the  $S_1$  state and thus displays a large Stokes shift. The driving force behind this charge migration



Scheme 3

is the combination of the transition dipole moment of the long wavelength transition, which is long axis polarised and polarity of the solvents. As might be expected, significant hydrogen bonding interaction with the solvent is better transmitted to the ring through coplanar form.

Strikingly different absorption and fluorescence spectral behaviour of 9FA and 9FE (identical with those of fluorene) indicates that there is practically no interaction between -COOR group and fluorene ring. This is clear from the molecular model i.e. as -COOR group is attached to an  $sp^3$  hybridized carbon, the  $\pi$  electron cloud of -COOR group is not in the plane of the  $\pi$  cloud of the fluorene ring to have any significant interaction.

### 3.2.2 Effect of Acid Concentration

Fig. 3.10 to 3.13 depict the absorption and fluorescence spectra of different prototropic species of the acids and the pertinent data are compiled in Table 3.8. For all the acids except 9FA, existence of neutral species below pH 3 and anion after pH 5 was manifested by a blue shift noted from neutral to monoanion species. After pH 14, a small red shift is noted and is not complete even at  $H_{-17}$ , the highly basic condition used. In the acidic region at  $H_0-6$ , absorption spectrum of 1FA is blue shifted and that of 4FA is red shifted indicating the formation of a monocation. Monocations of 2FA and 2FE are formed at  $H_0-8$  resulting in a large red shift in the absorption spectra. On increasing the acid concentration further, 1FA and 4FA show red shift, and 2FA a blue shift in their absorption spectra. Fluorescence spectra



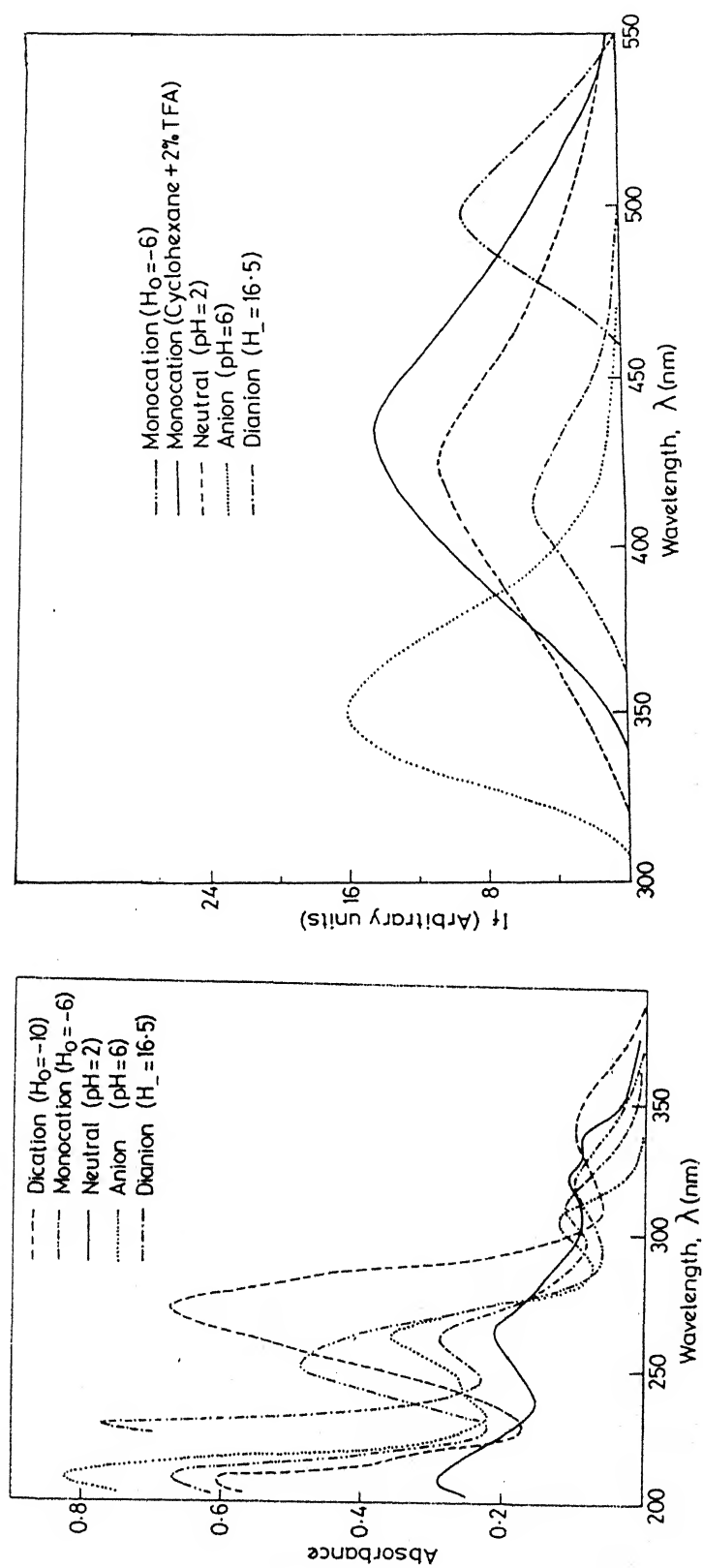


Fig.3.10 Absorption (left panel) and fluorescence (right panel) spectra of different prototropic species of 1-fluorene-carboxylic acid.

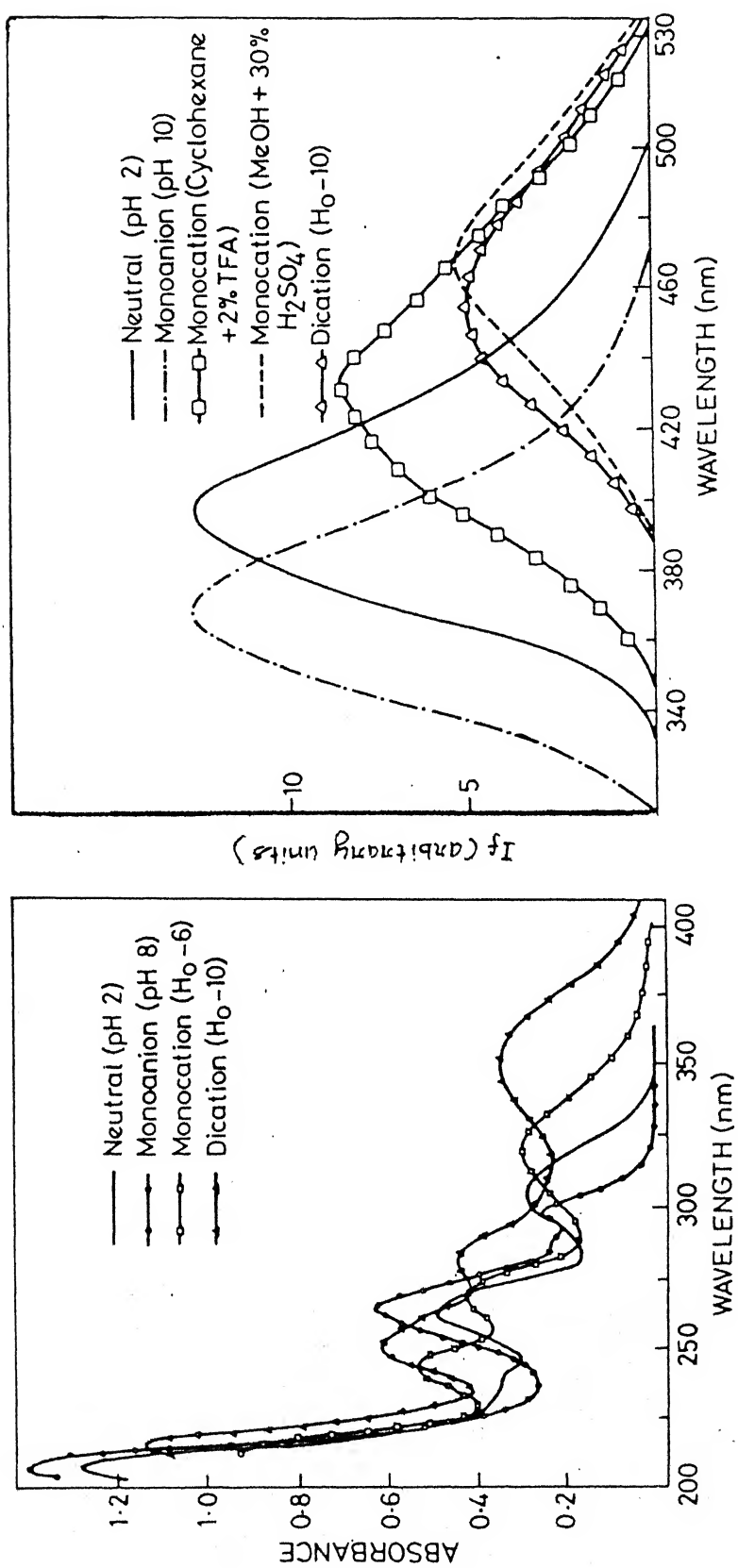


Fig.3.11 Absorption (left panel) and fluorescence (right panel) spectra of different prototropic species of 4-fluorene-2-carboxylic acid.

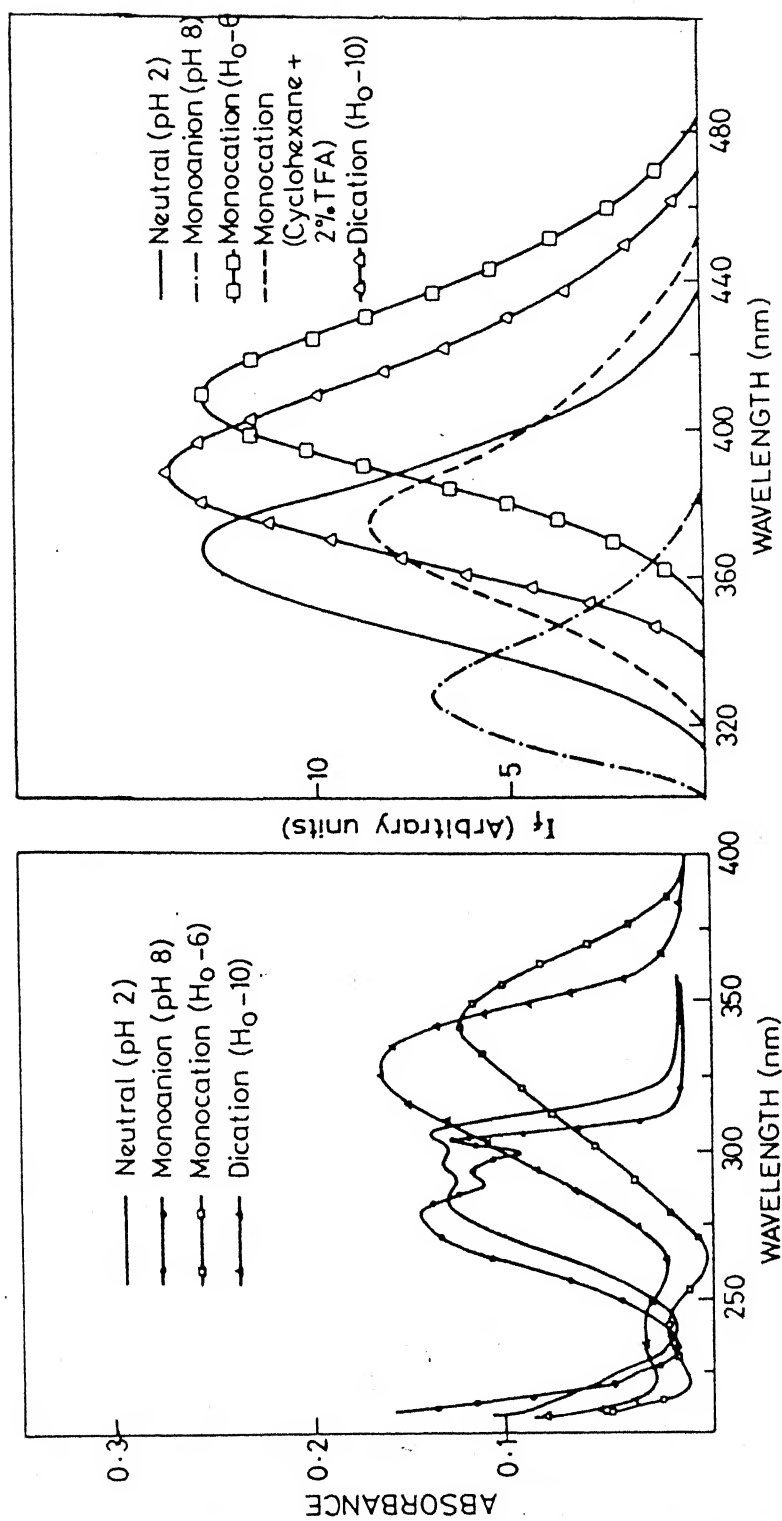


Fig.3.12 Absorption (left panel) and fluorescence (right panel) spectra of different prototropic species of 2-fluorene-1-carboxylic acid.

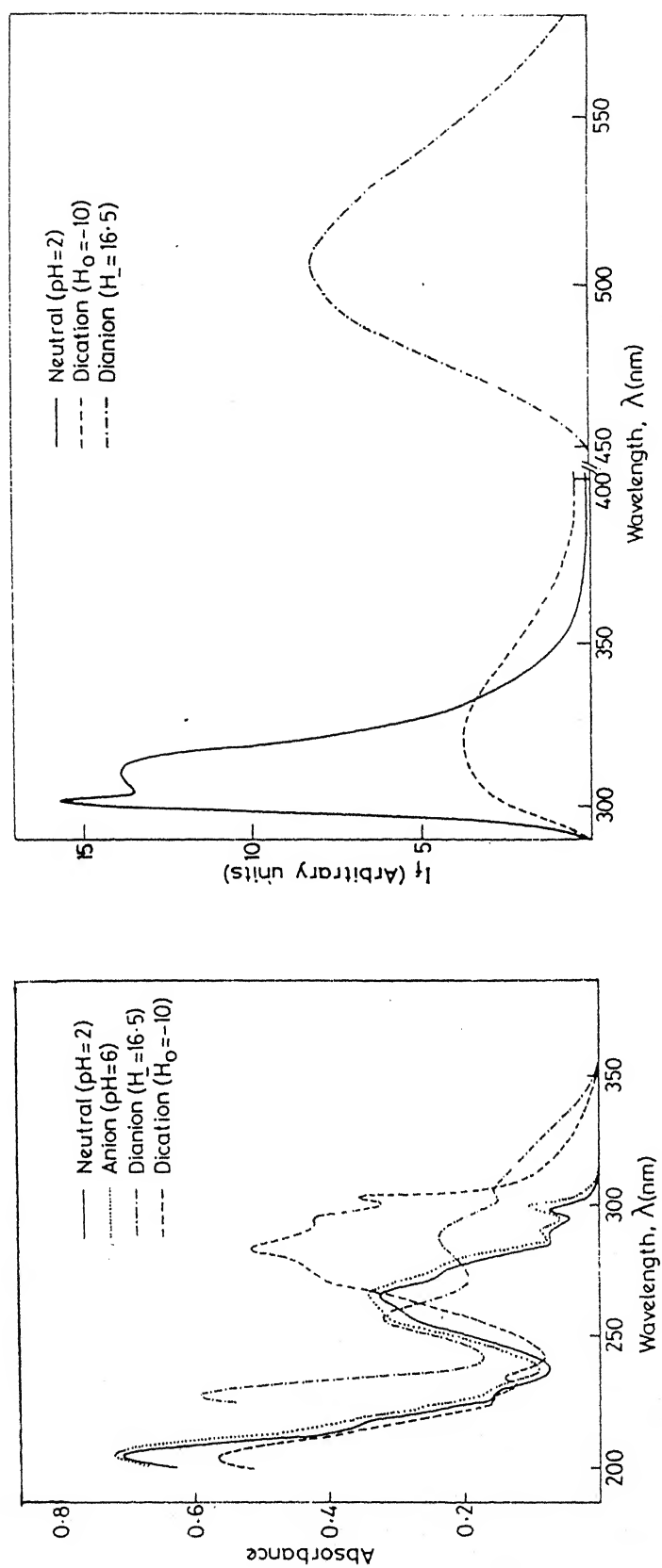


Fig.3.13 Absorption (left panel) and fluorescence (right panel) spectra of different prototropic species of 9-fluorene-9-carboxylic acid.

Table 3.8. Absorption and Fluorescence [in square bracket] Spectral Data of Different Species of Fluorenenecarboxylic Acids and Esters.

Compound	Neutral (pH 2)	Monocation (H <sub>O</sub> <sup>+</sup> -6)	Dication (H <sub>O</sub> <sup>+</sup> -10)	Monoanion (pH 8)*	Dianion (H <sub>16</sub> )
	1	2	3	4	5
1FA	334(3.66) 320(3.71) 261(3.98) [430(0.11)]	319(3.64) 250(4.34) - [498;440 <sup>a</sup> ]	338(3.75) 270(4.47) - -	302 262 246 [352;330 <sup>b</sup> ]	306 260 - [410]
1FE	310(3.71) - 260(4.16) 245(4.2) [392(0.10)]	318(3.72) - 250(4.31) - -	345(3.66) - 270(4.52) - -	- - [352 <sup>c</sup> ]	317 - 275 261 -
4FA	305(3.89) - 272(4.05) 262(4.12) [397(0.22)]	318(3.81) - 271(4.01) 264(4.03) [434 <sup>a</sup> ;468 <sup>d</sup> ]	349(3.95) 305(3.79) 279(4.05) 259(4.18) [454(-)]	298(3.83) 288(3.78) - 265(4.24) [368(0.07)]	- - - -
2FA	307(4.07) 297(4.05) 284(4.04) [365(0.22)]	341(4.04) - 241(3.12) [408(0.19); 373 <sup>a</sup> ]	325(4.16) - 242(3.64) [388(-)]	304(4.04) 296(3.99) 293(4.00) [333(0.02)]	318 294 282 [410]

...contd.

Table 3.8(contd.)

1	2	3	4	5	6
2FE	309(4.10) — 272(4.05) 262(4.12) [367(0.48)]	341(4.0) — — 240(3.11) [410(0.03); 372 <sup>a</sup> ]	326(4.21) — — 241(3.8) [390(—)]	318 294 284 269 [410]	— — —
9FA	298(3.61) 288(3.63) 266(4.25) [303,311]	299(3.33) 288(3.53) 265(4.16) —	303(4.27) 294(4.35) 283(4.48) [321]	300(3.61) 289(3.66) 265(4.25) [303,311 (0.35)]	307(3.9) 288(4.09) — [510]
9FE	300(3.72) 290(3.74) 266(4.28) [302,309]	299(3.29) 288(3.57) 265(4.13) —	302(4.1) 294(4.25) 282(4.35) —	298(3.63) 288(3.67) 265(4.2) [303,311]	325(3.78) 307(3.78) 288(4.03) 262(4.19) [455]

a = in cyclohexane + 2% TFA; b = in cyclohexane + 2% piperidine;

c = monoanion species after hydrolysis at pH 14;

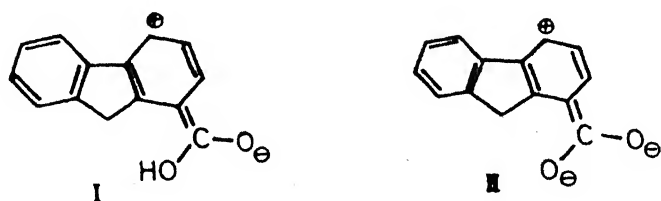
d = in methanol + 30% H<sub>2</sub>SO<sub>4</sub> medium; \* = in 2FE, this data is for the deprotonation of the ring at H<sub>16.5</sub>.

of monoanions are blue shifted as compared to their neutral species. At  $H_{17}$ , except 4FA other compounds give very weak fluorescence band. On increasing the acidity after pH 3, all the acids and esters (except 4FA) display red shifted fluorescence band due to monocation formation. Monocation of 4FA is non-fluorescent in aqueous solution but exhibit intense fluorescence in cyclohexane +2% TFA and methanol +  $H_2SO_4$  media. Similar results have also been observed for the protonation of indole-4-acid.<sup>215</sup> At  $H_{10-8}$ , a new blue shifted fluorescence band is observed at the expense of monocation fluorescence for all the compounds except 1FA, where it is non-fluorescent.

Absorption spectral changes after  $H_{15}$  indicate the presence of a dianion formed by the deprotonation of  $>CH_2$  group at 9-position and  $-COOH$  group of the respective acids. Though very high value of  $pK_a$  ( $\sim 22$ ) has been predicted<sup>209</sup> for the deprotonation of  $>CH_2$ , it is expected to be near  $H_{17}$ , because such a large decrease in the  $pK_a$  value is generally not expected in  $S_0$  state by having an electron withdrawing group. This is further manifested from the  $pK_a$  values for this reaction of 9-ethoxy and 9-cyano substituted fluorenes which are found to be 10 and 11.4 respectively.<sup>216</sup> 1FE undergoes hydrolysis at this basic condition to give  $-COO^-$  species. The weak fluorescence observed for 1FA and 2FA in highly basic solution can be attributed to dianion formation in the  $S_1$  state.

Unlike neutral species, monoanions display structured absorption spectra which closely resemble that of fluorene molecule. Even the molecular extinction coefficient of the first peak of long wavelength band is more than the other peak of this band. This clearly

suggests that  $\text{-COO}^-$  group in these molecules are not coplanar with respect to the fluorene moiety, even at position-1, where some intramolecular hydrogen bonding seems to be present. This is because of the presence of a negative charge on the  $\text{-COO}^-$  group that will inhibit the charge transfer from the ring to the  $\text{-COO}^-$  in  $S_0$  state. This also indicates that the lowest energy transition in the monoanions may be long axis polarised. On the other hand, the fluorescence spectra of monoanions, though blue shifted with respect to the neutral species, are largely red shifted with respect to fluorene and are broad bands. The Stokes shifts observed are also large, but less than that noticed for neutral. This suggests that  $\text{-COO}^-$  group in  $S_1$  state becomes more coplanar as compared to that in  $S_0$  state but not to that extent as for the neutral species. The driving force for this change in the geometry of  $\text{-COO}^-$  group in  $S_1$  state is due to the presence of transition dipole moment, which induces this change as shown in the scheme below. The fluorescence spectrum of monoanion of 2FA is broad and more diffuse

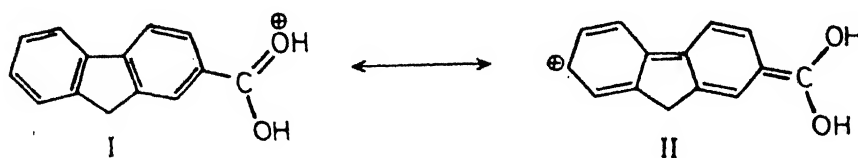


Scheme 4

than absorption spectrum and also red shifted as compared to fluorene fluorescence. It can be explained on the same lines as has been done for 1FA and 4FA. The spectral changes observed in the formation of monoanions are consistent with those observed for the other systems.



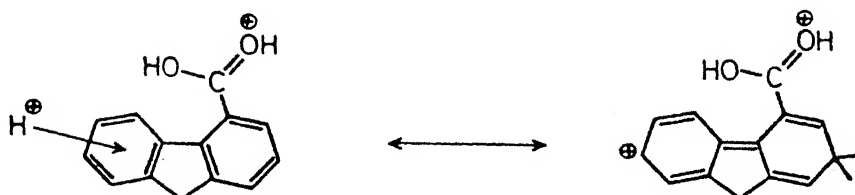
At pH 3, a spectral change observed in all the species, except for esters, suggests the formation of neutral species as suggested earlier. This is further based on the fact that the spectral characteristics of these molecules are similar to those observed in non-aqueous solvents. The spectral behaviour of acids and esters in high acid concentration is rationalized as follows. If  $\pi \rightarrow \pi^*$  is the lowest energy transition, protonation at the carbonyl oxygen results red shift in the spectra. Absorption spectral changes indicate that mono-cations of 2FA and 4FA are carbonyl protonated species. While this protonation in 4FA leads to a normal red shift, 2FA shows largely red shifted band. This large shift of  $\sim 40$  nm in the absorption spectra can not be attributed only to the protonation reaction, because as said earlier,  $-\text{COOH}$  is non planar in the  $S_0$  state. It can be rationalized that subsequent to protonation, a charge reorganization takes place, thereby leading to canonical structure contributing to the stability (shown below). The driving force for this could be the presence of a



Scheme 5

positive charge on the  $-\text{COOH}$  group and the polar medium. The second protonation (after  $\text{H}_0 - 8$ ) results in red and blue shifts in the absorption spectra of 4FA and 2FA respectively. As mentioned earlier (section 3.1.2), the electrophilic attack in fluorene takes place at position-2,

followed by at positions 7 and 4. This leads to the canonical structure (II) (Scheme 6) and thus red shift is noted. A similar behaviour has also been observed for the ring protonation of fluorene. In the



Scheme 6

case of 2FA, the ring protonation will occur at position-7 and thus will inhibit the complete charge transfer as suggested in the Scheme 4. Due to this, blue shift is expected in the absorption spectrum.

Contrary to 2FA and 4FA, 1FA displays a blue shifted absorption band on first protonation. This is also assigned to carbonyl protonated monocation, because this protonation might break the intramolecular hydrogen bonding between -COOH and 9-methylene hydrogen atoms which exists in the neutral species. As expected, the absorption band maximum of the protonated 1FA is same as those of the monocations of 1FE and 4FA. The dication of 1FA is ring protonated species. Prototropic reactions of esters are similar to that of their acids.

Fluorescence spectral studies in high acid concentration has revealed that monocation is of carbonyl protonated species. Monocation of 1FA emits red shifted fluorescence near 498nm and its intensity depends upon the wavelength of excitation i.e. fluorescence is not observed when excited above 310 nm. Though it can not be said precisely from our studies, it is speculated that inter system crossing might be dominant when excited with  $\lambda_{\text{ex}} > 310 \text{ nm}$ . The formation of monocation

is confirmed from the fluorescence measurements in cyclohexane + 2% TFA. The highly blue shifted fluorescence (440 nm) for the monocation in the above non polar medium indicates that solvent relaxation is very minimum. This is in agreement with the studies on 1- and 2-naphthoic acids.<sup>213</sup> In case of 2FA and 2FE, carbonyl protonated monocations are involved in resonance interaction as mentioned in Scheme 3. The large solvent relaxation for this species is manifested by recording the spectrum in cyclohexane + 2% TFA. Monocation of 4FA is non-fluorescent, whereas similar species in non-polar medium is fluorescent and the band maximum is red shifted in comparison to that of the neutral species. The large solvent relaxation is further manifested from the largely red shifted (468 nm) fluorescence band, observed in methanol + 30% (w/w)  $\text{H}_2\text{SO}_4$ . Though it is difficult to assign the reason exactly, the study of Flom and Barbara<sup>43</sup> indicates that the hydrogen bonding interaction leads to the increase in the rate of internal conversion.

The dications of 2FA, 2FE and 4FA are blue shifted and that of 1FA is non-fluorescent. The blue shift observed in the fluorescence spectra of dications can be rationalized in terms of the ring protonation that reduces the conjugation between -COOR group and the ring as explained for the ground state behaviour.

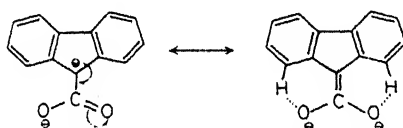
The spectral behaviour of 9FA and 9FE is different from that of other acids and is summarized as follows:

(i) Between  $\text{H}_0$ -6 and pH 14, virtually there is no change in the absorption spectrum which resembles that of fluorene and the reasons mentioned earlier are the same. Since all the reactions involved in this acidity range are on -COOR group, no effect is seen on the

spectrum. The species involved are monoanion, neutral and monocation (carbonyl protonated). No fluorescence is observed from monocation.

(ii) After  $H_0-8$ , the absorption and fluorescence spectra are red shifted and the spectral intensity is continuously increased even upto  $H_0-10$ . This spectral changes can be assigned to the dication formed by the ring protonation preferably at position-2. This assignment is made on the basis that the spectral profiles are identical to those of the ring protonated fluorene (Section 3.1.2).

(iii) Absorption and fluorescence spectra of 9FA and 9FE are largely red shifted in the high basic region ( $H_-17$ ). This change indicates the existence of dianion for 9FA, formed by the deprotonation of  $-COOH$  group and  $>CH$  group at position-9 and monoanion for 9FE formed by the deprotonation of  $>CH$  group. This deprotonation changes the hybridization at this carbon which brings  $-COO^-$  or  $-COOCH_3$  group in plane with the fluorene ring. Now, an intramolecular hydrogen bonding could occur between the substituents at 9-position and hydrogen atoms at 1 and 8 positions as shown below. This can be substantiated



Scheme 7

by the observation of a large red shifted fluorescence (510 nm) for 9FA as compared to that for 9FE (455 nm).

### 3.2.3 Acidity Constants

The acidity constants are given in Table 3.9. The results can be summarized as follows: (i) The  $pK_a$  (4) of 1FA, 2FA and 4FA could not be calculated because the reaction is not complete even at  $H_{17}$ . The  $\text{>CH}$  group in 9FA is more acidic ( $pK_a$  15.2) than any other acids studied. It is due to the presence of an electron withdrawing group ( $-\text{COOH}$ ) at position 9 and thus reduce the charge density at this centre. (ii) Fluorimetric titrations (Fig. 3.14) give the ground state value for neutral-anion equilibrium for the acids.  $pK_a^*$  calculated by Förster cycle method indeed has shown that  $-\text{COOH}$  group becomes weaker acid upon excitation, although this is not accurate as explained below. The fluorimetric curves for this equilibrium suggest that the lifetimes of conjugate acid-base pair are too small to establish the equilibrium within the lifetimes of these species, especially when the concentration of proton is less. This behaviour is generally observed for carboxylic acids.<sup>213</sup> The carbonyl group of acids and esters becomes stronger bases in the excited state. (iii)  $pK_a(1)$  for dication-monocation equilibrium is less than that of similar reactions of fluorene.<sup>213</sup> This is due to the presence of positive charge on carbonyl group which reduces the basicity of the molecule, (iv) Förster cycle method could not be employed for the prototropic reactions of 9FA because either there is no change in the spectra or geometrical changes are involved in the formation of certain species. The geometry change of  $-\text{COOH}$  group limits the application of Förster cycle calculation for other acids also.

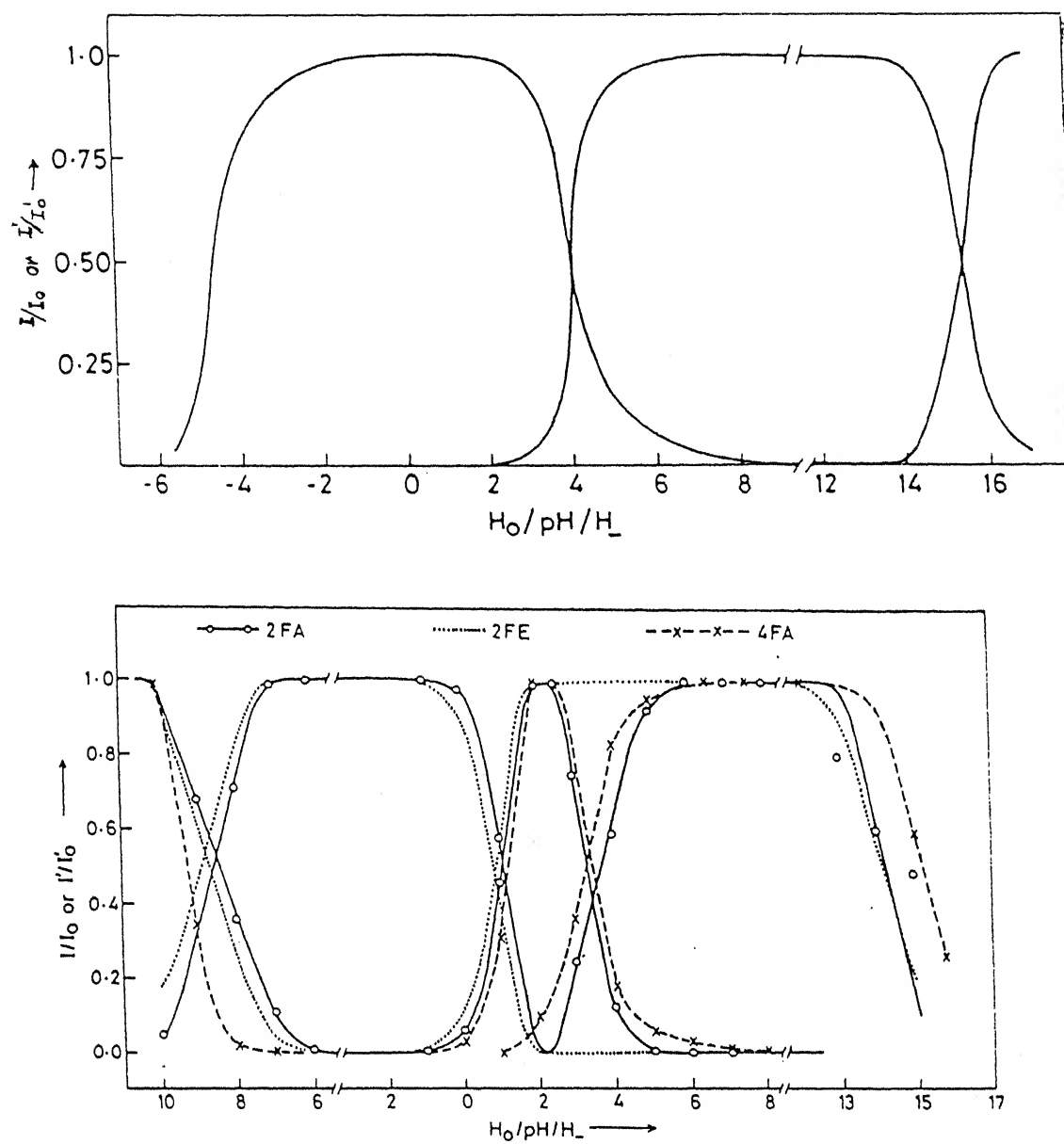
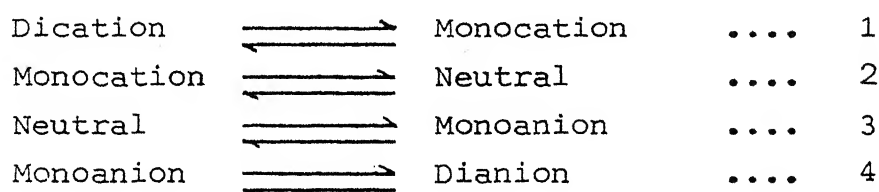


Fig.3.14 Fluorimetric titration curves for different prototropic species of 1-fluorencarboxylic acid (upper panel) and 2-,4-fluorencarboxylic acids (lower panel).

Table 3.9. Acidity Constants of Fluorenecarboxylic Acids and Esters for the Following Equilibria.



Compound/ Equilibrium		Spectroscopic method		Förster cycle method	
		$S_0$	$S_1$	a	f
1FA	1	<-10	-		
	2	-4.75	-4.6		
	3	4.0	4.1		
	4	>16	15.5		
4FA	1	<-10	-9.3	5.9*	-
	2	-4.3	1.2	-1.9	-
	3	3.0	3.3	4.6	7.2
	4	>16	15.3	-	-
2FA	1	<-10	-8.5	-3.0*	-2.4*
	2	-6.0	1.1	0.8	0.1
	3	3.2	3.4	3.87	8.7
	4	>16	14.6	-3.2*	11.8*
2FE	1	<-10	-8.8	-2.8*	-2.6*
	2	-6.1	0.8	0.3	0.1
	4	>16	14.3	-1.8*	-6.0*
9FA	1	-7.9	-8.0		
	2	-	-		
	3	3.9	-		
	4	15.2	13.7		

a, f : by using absorption and fluorescence data respectively.

\* :  $\Delta pK_a = [pK_a(S_1) - pK_a(S_0)]$ .

From the above study the following conclusions can be drawn:

- (i) The long wavelength absorption bands of 2FA and 2FE, and their various protonated species are long axis polarised whereas, in 1FA and 4FA it is composed of long and short axes polarised transitions.
- (ii) The charge transfer interaction of  $\text{-COOH}$  and  $\text{-COO}^-$  groups with the parent molecule of 1FA and 4FA is large in the  $S_1$  state as compared to  $S_0$  state, thereby making these groups more planar in the  $S_1$  state. Similar interaction for 2FA is minimum in both  $S_0$  and  $S_1$  states in the non polar solvents. The  $\text{-COOH}$  group (in polar and protic solvents) and  $\text{-COOH}_2^+$  of 2FA are coplanar in  $S_1$  state.
- (iii) The  $\pi$  electronic interaction between  $\text{-COOH}$  group and the fluorene ring of 9FA is minimal so long  $>\text{CH}_2$  is not deprotonated. The large red shift observed in the absorption and fluorescence band maxima of dianion of 9FA is due to the coplanarity of  $\text{-COO}^-$  group with the fluorene moiety and the intramolecular hydrogen bonding from the positions 1 and 8 of fluorene moiety.

### 3.3 CARBOXAMIDES<sup>a</sup>

This section describes the spectral characteristics of three fluorenamides such as 1-fluorenamide (1Fam), 2-fluorenamide (2Fam) and 4-fluorenamide (4Fam).

#### 3.3.1 Solvent Study

The absorption and fluorescence spectra of 1Fam, 2Fam and 4Fam

---

<sup>a</sup> R. Manoharan and S.K. Dogra, communicated.



recorded in different solvents are portrayed in Fig. 3.15 and the relevant data are compiled in Table 3.10.

Absorption bands of 1FAM are broad and the maxima are red shifted in comparison to those of fluorene. Absorption spectrum of 2FAM resembles that of fluorene in both profile and position (though slightly red shifted by 3-4 nm), but for 4FAM, the long wavelength band is a broad one at the same position of fluorene fluorescence. The spectrum of 2FAM is structured in non-polar solvents, but the structure is lost in polar solvents. On the other hand, fluorescence bands of 1FAM and 4FAM are broad and are red shifted with respect to that of fluorene. Unlike absorption, fluorescence spectra are solvent dependent which are progressively red shifted on increasing the polarity and hydrogen bonding ability of the solvents. Absorption and fluorescence spectral maxima of any one amide in any one solvent are blue shifted with respect to the corresponding acids and the shifts are very large especially for 1FAM in water. The nature of the transitions observed in all the amides are the same as observed in case of fluorene and the corresponding acids. This is based on the fact that (i) the molecular extinction coefficients of these bands are either nearly equal to or greater than those of fluorene molecule and (ii) fluorescence emission is observed at room temperature, establishing Kasha's rule.<sup>30</sup> Like corresponding acids, long wavelength band in 1FAM and 4FAM is composed of two differently polarised transitions. This is because, as  $-\text{CONH}_2$  group is substituted along the shorter axis of the molecule, the short axis polarised transition (280 nm) gets more stabilized and mixes with the relatively unaffected long axis polarised

Table 3.10. Absorption and Fluorescence Spectral Data of 1Fam, 2Fam and 4Fam in Different Solvents and at Various Acid Concentrations.

Solvent/pH	1Fam		2Fam		4Fam	
	$\lambda_a (\log \epsilon)$	$\lambda_f (\phi_f)$	$\lambda_a (\log \epsilon)$	$\lambda_f (\phi_f)$	$\lambda_a (\log \epsilon)$	$\lambda_f (\phi_f)$
1	2	3	4	5	6	7
Cyclohexane	314 305 274 269 262 258 241	328 (0.01)	306 298 294 283 270 235	307 322 335 (0.01)	300 290 275 265 255	347 (0.01)
Dioxane	313(3.62) 304(3.75) — 274(3.91) 262(4.12) — 239(4.08) 235(3.80)	323 334 (0.01)	307(4.32) 295(4.24) 282(4.37) 271(4.36) 234(4.26)	311 323 (0.01)	298 289 275 264 254	352 (0.01)
Acetonitrile	313(3.64) 303(3.73) — 262(4.08) 239(4.00)	338 (0.02)	305(4.20) 294(4.16) 281(4.25) 271(4.19) 233(3.75)	325 (0.01)	297 288 275 263 253	360 (0.01)

...contd.

Table 3.10(contd.)

1	2	3	4	5	6	7
Methanol	314(3.68) 304(3.78) — 261(4.21) 250(4.09) 239(3.90)	352 (0.11)	304(4.41) 293(4.39) 281(4.45) 270(4.37) 233	338 (0.16)	296 288 275 262 —	380 (0.1 )
Neutral (pH 6)	315(3.64) 303(3.76) 261(4.30) 243(4.21) — —	382 334 <sup>a</sup> (0.33)	304(4.36) 294(4.35) 282(4.39) 269(4.33) — —	360 <sup>a</sup> 323 <sup>a</sup>	296 288 261 — — —	395 <sup>a</sup> 352 <sup>a</sup> (0.23)
Monocation (H <sub>O</sub> <sup>-4</sup> )	322(3.64) 314(3.63) 254(4.47)	408 <sup>*</sup> 395 <sup>b</sup> 400 <sup>c</sup>	313(4.46) 288(4.24) 277(3.95)	396 <sup>b</sup> 362 <sup>c</sup> 365 <sup>c</sup>	316 303 290 263 245	433 <sup>b</sup> 390 <sup>c</sup> 395 <sup>c</sup>
Dication (H <sub>O</sub> <sup>-10</sup> )	320(4.08) 283(4.47) 268(4.61) 238(4.21)	— 368 <sup>a</sup>	316(4.57) 292(4.4 ) 242(3.66)	372 <sup>a</sup> 360 <sup>a</sup>	313 297 272 254	— 390 <sup>a</sup>
Anion <sup>d</sup>	—	—	—	—	325 314 285 263	—

\* In cyclohexane + 2% TFA medium; a: 77 K; b: H<sub>O</sub><sup>-4</sup>, 77 K; c: H<sub>O</sub><sup>-4</sup>, 77K;  
d: 1 FAM and 2 FAM get precipitated after pH 14.

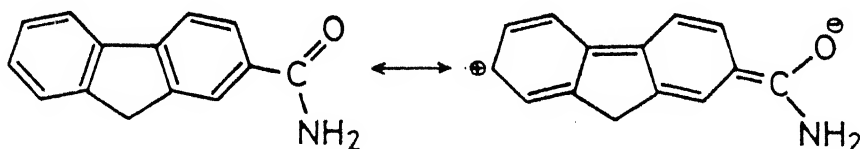
transition ( $\sim 300$  nm). The red shift observed in the long wavelength band of 1FAM, in comparison to 4FAM, in any given solvent could be attributed to the intramolecular hydrogen bonding between the  $-\text{CONH}_2$  group at position-1 and hydrogen atoms of the position-9. On the other hand, the blue shift observed for 1FAM corresponding to the long wavelength band of 1FA, indicates more favourable hydrogen bonding involving  $-\text{OH}$  group rather than  $-\text{OCH}_3$  or  $-\text{NH}_2$  group. In the case of 2FAM, one would expect the long wavelength transition to be affected appreciably but the structured absorption spectrum indicates that  $-\text{CONH}_2$  group is not coplanar with the fluorene ring in the ground state. The small red shift of 3 to 4 nm could be due to the inductive effect of  $-\text{CONH}_2$  group.

The broad, featureless, red shifted fluorescence of 1FAM and 4FAM as compared to that of fluorene can be explained as has been done for the acids i.e. a complete rotation of  $-\text{CONH}_2$  group into the plane of the fluorene ring takes place and this results in an enhanced resonance interaction between the two moieties. Fluorescence spectrum of 2FAM in non-polar solvents is vibrationally resolved, which shows only one vibrational mode ( $1420\text{ cm}^{-1}$ ), that also appeared in the absorption spectrum. The mirror image symmetry observed between the absorption and fluorescence spectra of 2FAM in non-polar solvents indicates that the absorbing and emitting states are the same. The Stokes shift (recorded in Table 3.11) observed for 2FAM in non-polar solvent reveals that the geometry of the molecule in  $S_1$  state is not very different from that in  $S_0$  state. As  $-\text{CONH}_2$  group in 2-position is free of any steric interaction, one would have expected large effect on the

Table 3.11. Stokes Shift ( $\text{cm}^{-1}$ ) Observed for 1FAM, 2FAM and 4FAM in Different Solvents and at Various Acid Concentrations.

Solvent/species	1FAM	2FAM	4FAM
Cyclohexane	1360	110	4515
Dioxane	2010	420	5160
Acetonitrile	2365	2020	5890
Methanol	3540	3310	7470
Water	5570	5120	8470
Monocation	—	6696	—
Dication	—	4764	—

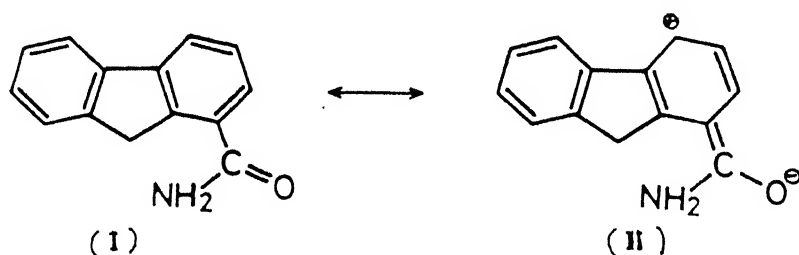
spectral transitions than other amides. But the otherwise results indicate that  $-\text{CONH}_2$  group in 2FAM is not in the same plane of fluorene, in both  $S_0$  and  $S_1$  states in non-polar solvents. The vibrational structure appeared in non-polar solvent is lost in polar and hydrogen bonding solvents. Similar to 2FA, the large Stokes shift observed for 2FAM in the latter solvents can not be attributed only to the simple solute-solvent interaction, especially when  $-\text{CONH}_2$  group is non-planar. In polar and hydroxylic solvents, the following canonical structure may be stabilized, thereby leading to a more polar and planar structure



Scheme 8

in  $S_1$  state and thus displays a large Stokes shift. The driving force behind this charge migration is the combination of transition dipole moment of the long wavelength transition, which is long axis polarised and the polarity of the medium. As might be expected, significant hydrogen bonding interaction with the solvent is better transmitted to the ring through coplanar form. The Stokes shift observed under the above environment for 1FAM and 4FAM are greater than that of 2FAM in any one solvent. This reveals the increased charge migration from the ring to the amide group in  $S_1$  state. The preferential increase of Stokes shift for 4FAM over 1FAM in one particular solvent might be due to the greater geometry difference between  $S_0$  and  $S_1$  states of 4FAM than 1FAM. This is consistent and can be seen from the long wavelength absorption band maxima of the two amides.

The blue shift observed in the absorption and fluorescence spectra of amides with respect to their acids is because of the presence of an amino group, a better charge donor than hydroxy group at the carbonyl group. Due to the increased charge density at the carbonyl function of amide than acid group, the canonical structure (II) is not important in the resonance hybridization as compared to that of 1FA.



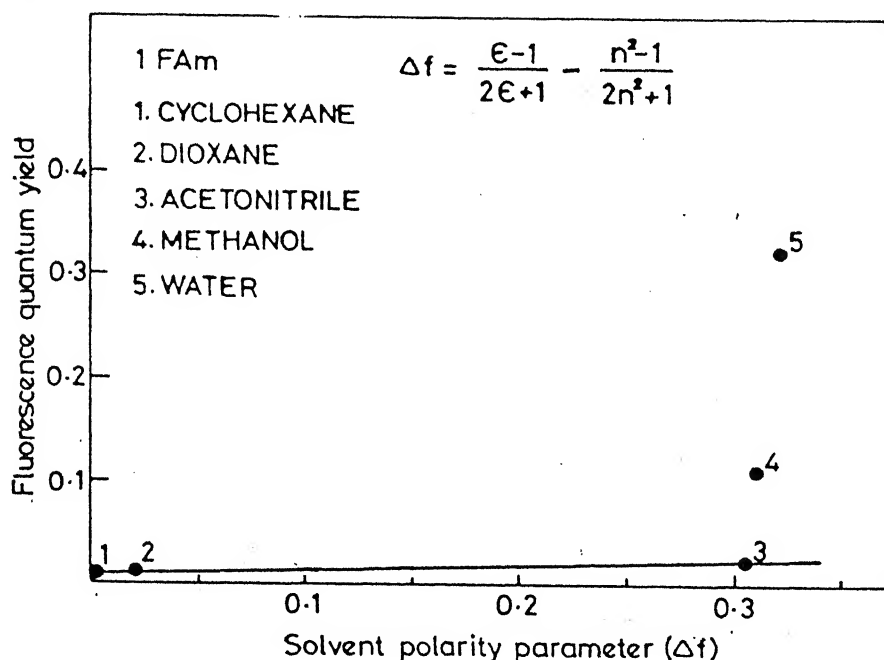
Scheme 9

Amides are weakly fluorescent in non-polar and aprotic polar solvents. But the quantum yield is increased dramatically in hydroxylic solvents (as shown below; scheme 10). This kind of fluorescence activation by hydroxylic solvents can be explained as follows: In presence of the above solvents, the energy gap between  $^1n\pi^*$  and  $^1\pi\pi^*$  singlet states increases. This will decrease the vibronic coupling<sup>a</sup> between the two singlet states and hence reduces the Spin-Orbit coupling between  $^1\pi\pi^*$  and lowest  $^3\pi\pi^*$  states, thereby prefers fluorescence

---

<sup>a</sup> Spin-Orbit coupling between  $^1n\pi^*$  and  $^3\pi\pi^*$  is greater than between  $^1\pi\pi^*$  and  $^3\pi\pi^*$ . Vibronic coupling between the higher lying  $^1n\pi^*$  introduces  $n\pi^*$  character into the lowest  $^1\pi\pi^*$  state thereby facilitates the interaction between  $^3\pi\pi^*$  state. A decrease in vibronic coupling removes the  $n\pi^*$  character.<sup>217</sup>

over intersystem crossing as a means of deactivation of excited states.<sup>217</sup> This means of fluorescence activation is preferred over the reversal of  $^1\pi\pi^*$  and  $^1n\pi^*$  singlet states, as observed in ketones and aldehydes because it has been shown that  $^1\pi\pi^*$  is the lowest energy singlet state in amides and carboxylic acids.



Scheme 10

### 3.3.2 Effect of Acid Concentration

The absorption and fluorescence spectra of different species of amides are illustrated in Fig. 3.16 and the data are compiled in Table 3.10. While the absorption spectra of amides (except 4FAM which indicates small red shift) show no prototropic equilibrium in the high basic medium, fluorescence intensities of amides start decreasing without the appearance of any new fluorescence band. All the amides are neutral species upto pH 1 and display progressively red shifted absorption spectra in the acid concentration  $H_0$  0 to  $H_0-6$  (Fig.3.17



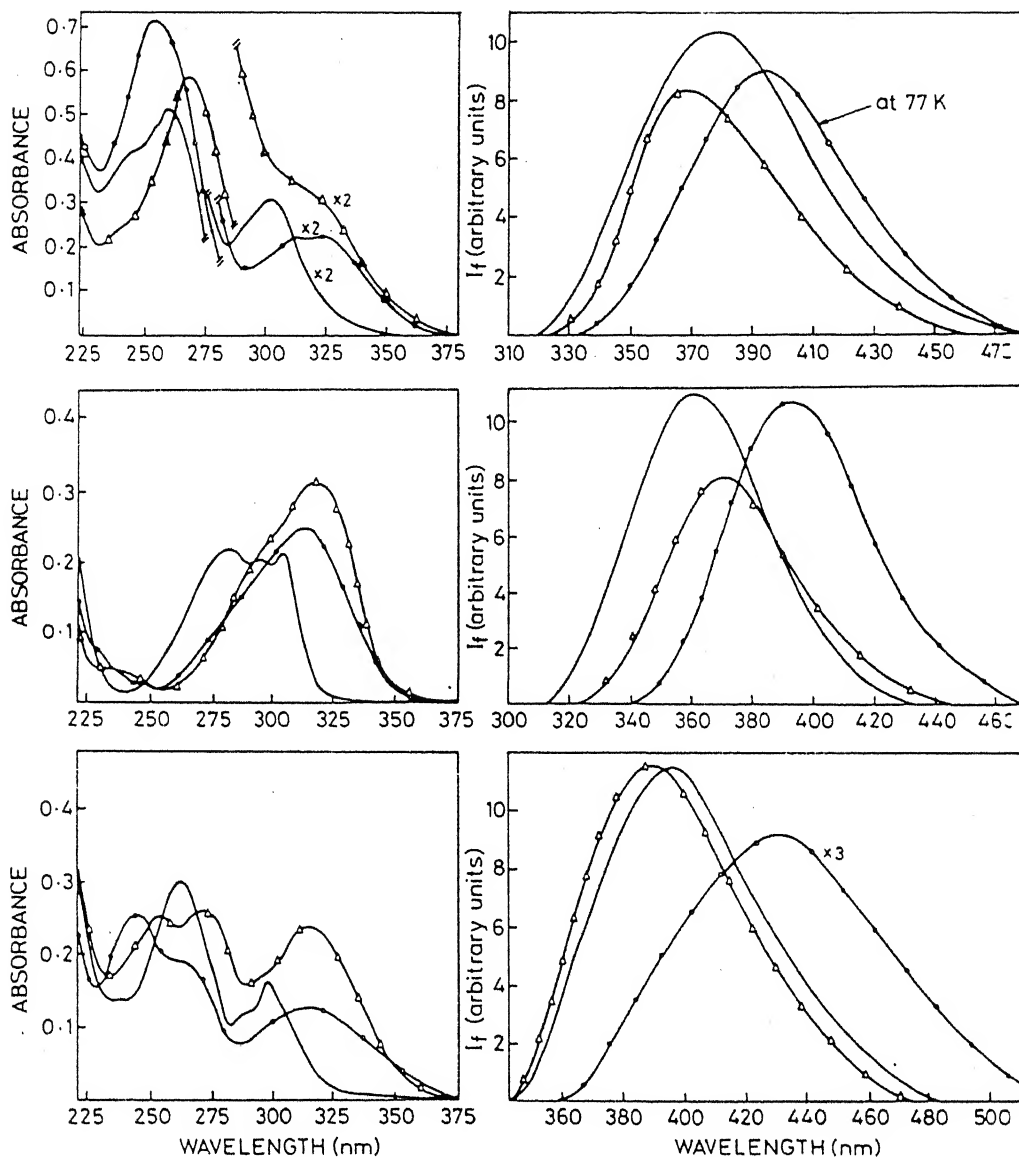


Fig.3.16 Absorption (left panel) and fluorescence (right panel) spectra of different prototropic species of 1-, 2-, and 4-fluorenamide (— neutral, -o-o- monocation, -Δ-Δ- dication).

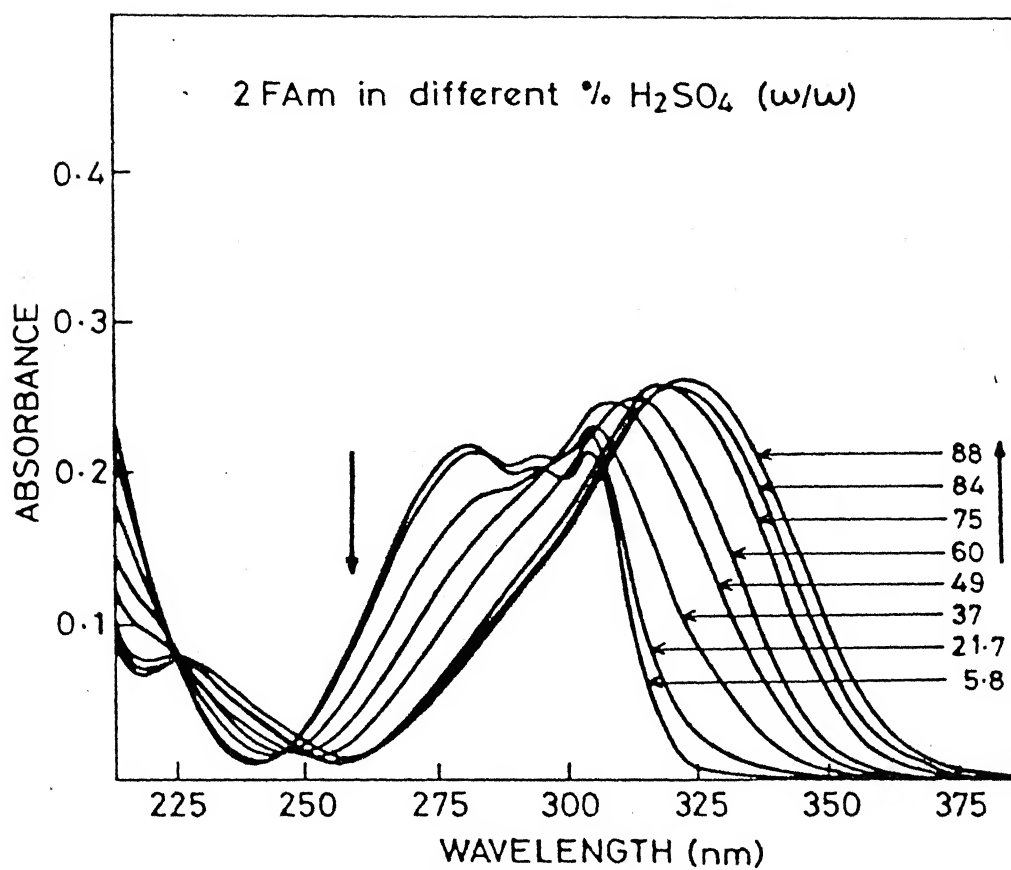


Fig.3.17 Absorption spectra of 2-fluorenamide in different % (w/w) sulfuric acid.

shows for a typical case of 2FAM). This is due to the formation of monocation. A blue shift is noticed after  $H_0-7$ , indicating the formation of dication. Similarly, the fluorescence spectra of the monocations of 2FAM and 4FAM are red shifted as compared to that of neutral species. 1FAM is non-fluorescent in aqueous medium at 298K and fluorescent in cyclohexane +2%TFA medium. Fluorescence emission of monocation and dications of amides at low temperature (77 K) reveal that the first protonation results in a red shift and the second, a blue shift in the fluorescence spectra.

The protonation equilibria of amides are interesting because of (i) their controversial protonation sites,<sup>156-171</sup> (ii) the inapplicability of  $H_0$  scale,<sup>163-166</sup> and (iii) the medium effects.<sup>168</sup> Two different opinions are afloat about the site of protonation. Liler<sup>157</sup> has favoured the site to be Nitrogen centre. This is based on the fact that, (i) the hydroxide catalyzed reaction is faster than the hydronium ion catalyzed one<sup>158-160</sup> and (ii) the  $pK_a$  values for the prototropic reactions ( $\sim -2$ ) are not consistent with the  $pK_a$  values ( $\sim -7$ ) of the similar reaction of other carbonyl groups of the carboxylic acids and esters.<sup>161,162</sup> Theoretical studies have suggested oxygen protonation in the gas phase but find that increasing 'pyrimidization' of the  $NH_2$  group, which might occur in solution, increases the nitrogen and decreases the oxygen basicity. Based on the observations that absorption spectral changes of amides in aqueous sulfuric acid involve two processes (one a red shift with a clear isobestic point and the other a progressive red shift), Liler<sup>157</sup> has proposed the N-protonation in aqueous  $H_2SO_4$  solution and O-protonation,

as a result of tautomerization in concentrated acid solution. But more recently, Yates et al.<sup>166</sup> identified the first change to be a prototropic reaction at the carbonyl oxygen, rather than at the nitrogen centre of amide group and the second change to be the medium effect on the protonated species. Even the separation of these two changes has been made by these workers.

Based on the studies<sup>218</sup> from our laboratory on 2-benzimidazolone and 3-indazolinone we speculate the protonation to be at the carbonyl oxygen. In the case of molecule (I), the first protonation in aqueous



Scheme 11

solution (where this structure is more stable) should have occurred at pH 4 and the monocation should have formed by protonating  $>\text{NH}$  group adjacent to benzene ring. But the  $\text{pK}_a$  value observed for this reaction is  $-2.1$ . This value is in the right region for carboxamides which proves that the protonation has occurred at the carbonyl oxygen rather than at  $>\text{NH}$  group. Further, protonation of the monocation of molecule (I) lead to reorganization of bands resulting in benzimidazole structure as inferred from the absorption spectrum of dication. If the protonation had occurred at  $>\text{NH}$  group, structural reorganization to have benzimidazole moiety would have also required the migration of proton from  $-\text{NH}_3^+$  to the carbonyl oxygen atom which is unfavourable

than simple charge migration in the case of protonation at the carbonyl group. Similar results also exist for molecule (II) as well as for N-methyl-2-benzimidazolone and N,N-dimethyl-2-benzimidazolone.<sup>218</sup>

As mentioned earlier, the protonation of amides do not obey Hammett's acidity scale. This is stemmed from the fact that slopes of  $-\log I (= -\log [BH^+]/[B])$ , where  $[BH^+]$  and  $[B]$  are the concentration of acid and conjugate base) Vs  $H_0$  plot were far from unity as required by Hammett's equation (section 2.2.2). It led Yates et al.<sup>194</sup> to propose a new acidity scale,  $H_A$  to determine thermodynamically meaningful equilibrium constants. Medium effects on the acidic and/or basic species also result deviation from 'unit slope requirement'. Indeed, slopes (reported in Table 3.12) obtained by plotting  $-\log I$  values Vs  $H_A$  (in the range 5-84% (w/w)  $H_2SO_4$ ) are less than unity. This indicates that medium effect is operative in the prototropic reactions of amides. As described earlier, the first process (in the range 5-60% (w/w)  $H_2SO_4$ ) with clear isosbestic point is the prototropic reaction and the second process (in the range 60-84% (w/w)  $H_2SO_4$ ) is the medium effect on the spectral characteristics of protonated species of amides which causes a red shift with the loss of isosbestic point. Plots were made by taking the experimental points within the range 5.8 to 60% (w/w)  $H_2SO_4$  by using both the scales that is, by neglecting the region where medium effect is supposed to have been observed. Plots of  $H_A$  Vs  $-\log I$  have given unit slopes and the calculated  $pK_a$  values are in good agreement with literature values when expressed in Amide scale. Similar plots using  $H_0$  values did not give unit slope demonstrating that  $H_0$  scale is not valid for the protonation reactions of amides.

Table 3.12. Ground State  $pK_a$  of Monocation-Neutral Equilibria of Amides, Using Different Data (see text).

Compound	Scale	a	b	Difference in Hydration number (see text)
1Fam	$H_O$	Slope 0.46	Slope 0.63	
		$pK_a$ -2.75	$pK_a$ -2.15	(n-r) = 2.25
	$H_A$	Slope 0.68	Slope 0.99	$pK_a$ -1.87
		$pK_a$ -2.25	$pK_a$ -1.85	
2Fam	$H_O$	Slope 0.29	Slope 0.78	
		$pK_a$ -4.1	$pK_a$ -2.25	(n-r) = 2.58
	$H_A$	Slope 0.68	Slope 1.0	$pK_a$ -1.95
		$pK_a$ -2.55	$pK_a$ -1.97	
4Fam	$H_O$	Slope 0.62	Slope 0.68	
		$pK_a$ -3.3	$pK_a$ -2.45	(n-r) = 2.16
	$H_A$	Slope 0.88	Slope 1.0	$pK_a$ -2.2
		$pK_a$ -2.6	$pK_a$ -2.0	

a = Considering the eqbm within the range 5.8% - 84%  $H_2SO_4$  (w/w).

b = Within the range 5.8% - 60%  $H_2SO_4$  (w/w).

Lovell and Schulman<sup>219</sup> have proposed that the failure of Hammett's acidity scale to describe the prototropic reaction of amides is because of the different hydration requirements of the prototropic reactions of the amides relative to those of the dissociation of the primary anilines used as indicators to establish  $H_0$  scale. The following equation has been derived to calculate  $pK_a$  values.

$$H_0 - \log [B]/[BH^+] = pK_a - (n-r) \log a_w$$

where  $(n-r)$  is the difference in the hydration requirements as described above and  $a_w$  is the activity of water. The slopes as well as the intercepts from the plot of the magnitude in the left hand side Vs  $-\log a_w$  have been listed in Table 3.12. The activity of water,  $a_w$  values were taken from a curve constructed from the data of Giaque et al.<sup>220</sup> The  $pK_a$  values obtained as the intercept of the above plot agree nicely with the ones calculated using  $H_A$  scale (listed in Table 3.12). The slopes,  $(n-r)$  also obtained from the plots indicate that two fewer water molecules are involved in the dissociation reaction of these three protonated amides than dissociation reaction of ammonium ions used in the establishment of  $H_0$  scale.

The acidity constants in  $S_0$  and  $S_1$  states have been calculated by spectrophotometric and fluorimetric methods (titration curve shown in Fig.3.18) and are presented in the Table 3.13. Förster cycle method has also been employed wherever applicable to calculate  $pK_a^*$  values. The  $pK_a^*$  values obtained for the dication-monocation equilibria are consistent with the ring protonated reactions of fluorene-carboxylic

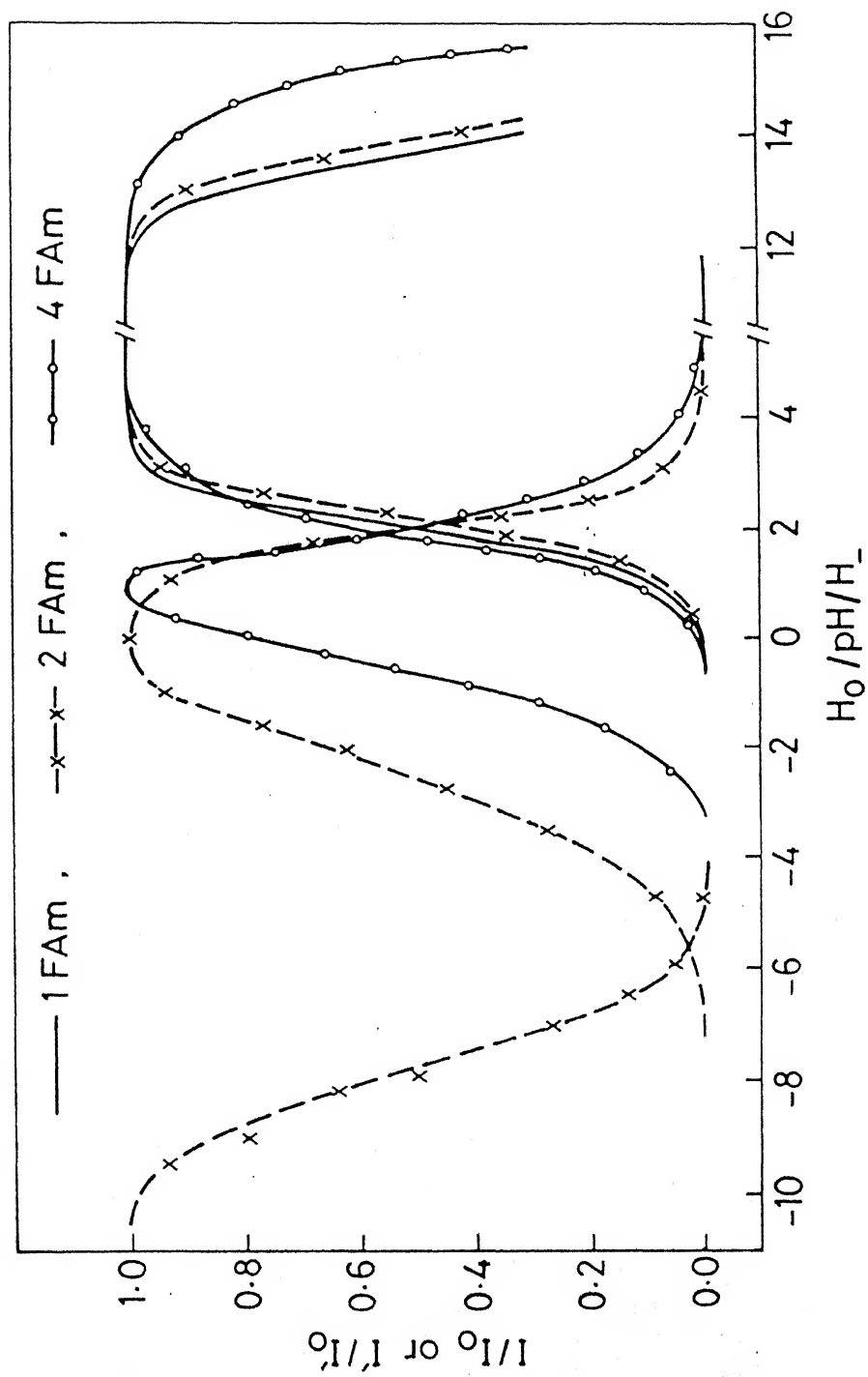


Fig.3.18 Fluorimetric titration curves for different prototropic species of 1-,2-, and 4-fluorenamide.



Table 3.13. Acidity Constants of Fluorenamides in the Ground and First Excited Singlet States.

Equilibrium	$pK_a(S_0)$	$pK_a^*(S_1)$	Förster cycle method $pK_a(S_1)$		
			a	f	av
$1FamH_2^{+2} \rightleftharpoons 1FamH^+ + H^+$	-8.5				
$1FamH^+ \rightleftharpoons 1Fam + H^+$	-1.87	2.1	-0.4	7.8*	3.7
$1Fam \rightleftharpoons 1Fam^- + H^+$	>16	13.8	-	-	-
$2FamH_2^{+2} \rightleftharpoons 2FamH^+ + H^+$	-8.3	-7.8			
$2FamH^+ \rightleftharpoons 2Fam + H^+$	-1.95	2.0	1.6	3.3	1.8
$2Fam \rightleftharpoons 2Fam^- + H^+$	>16	13.6	-	-	-
$4FamH_2^{+2} \rightleftharpoons 4FamH^+ + H^+$	-8.1	-			
$4FamH^+ \rightleftharpoons 4Fam + H^+$	-2.2	1.8	1.8	5.6*	3.0
$4Fam \rightleftharpoons 4Fam^- + H^+$	>16	15.3	-	-	-

\* using low temperature spectral data.

acids studied. The excited state dissociation constants for the monocation-neutral equilibria show that amide group becomes more basic in the  $S_1$  state. The  $pK_a^*$  value for the dication-monocation equilibrium has been calculated only for 2FAM, as the dications of other amides are non-fluorescent at 298 K. The results show that the rate of protonation is so small that the prototropic equilibrium is not established in  $S_1$  state. These results are similar to that observed for F, 1MF and 9FM. Thus similar explanation can be given. The decrease in the fluorescence intensity after pH 12 can not be attributed to any particular process. It may be due to either hydroxyl-induced fluorescence quenching or the formation of a non-fluorescent monoanion of the amide.

The fluorescence quenching of monocation is in general agreement with the reports of Watkins,<sup>221</sup> and Hussain and Wyatt.<sup>222</sup> The proton-induced fluorescence quenching rate constant ( $k_q$ ) could not be calculated for the lack of experimental lifetimes of monocation. The Strickler-Berg equation<sup>202</sup> can not be employed as the lowest energy transition is congested of two transitions.

The fluorescence maxima observed for the species at 77 K are blue shifted with respect to the room temperature measurements indicating the minimum solvent relaxation at low temperature. The monocations of amides which show proton-induced fluorescence quenching at 298 K exhibit intense fluorescence at low temperature (77 K) in the same acid concentrations. These results illustrate that fluorescence quenching is diffusion controlled and is thus dynamic in nature at room temperature.

The fluorescence maxima of the dications are blue shifted with respect to the spectra of monocations indicating the resonance break down after the formation of dication, as explained for the respective carboxylic acids.

In conclusion, it can be said that, (i) the long wavelength transition of 2FAM is long axis polarised whereas those of 1FAM and 4FAM are composed of the long and short axes polarised transitions, (ii) the  $-\text{CONH}_2$  group of 1FAM and 4FAM are coplanar in both  $S_0$  and  $S_1$  states whereas in 2FAM it is non planar in  $S_0$  and  $S_1$  states in non polar solvents but attain coplanarity in polar and hydroxylic solvents, (iii) the Hammett's acidity scale is not applicable for the protonation reaction of amides and medium effect is observed in aqueous sulfuric acid solution, (iv) amides are stronger acids on excitation and (v) proton-induced fluorescence quenching is observed for the monocations of the amides.

### 3.4 ALDEHYDE AND KETONES

In this section, the effects of solvents and pH on the absorption and fluorescence spectra of 2-fluorenaldehyde (2FAl), 2-acetylfluorene (2AcF) and 2-benzoylfluorene (2BeF) are described.

#### 3.4.1 Solvent Effect

The absorption spectral data of 2FAl, 2AcF and 2BeF in different solvents are given in Table 3.14. The long wavelength absorption bands of these compounds are intense, red shifted as compared to that

of fluorene.<sup>146</sup> The absorption spectra of all these carbonyls are vibrationally resolved in cyclohexane. But as the polarity or hydrogen bonding ability of the solvent increases, the vibrational structure is lost while the band maximum is nearly unaffected. The absorption spectra of these carbonyls are identical in profile in any one solvent and in water, the band maximum of 2BeF is at longer wavelength and that of 2AcF is at shorter wavelength. These compounds fluoresce in none of the solvents employed, except water. The fluorescence emission in water is intense and the maxima are broad and red shifted as compared to that of fluorene.<sup>147</sup>

As described in section 1.7, the absorption bands of fluorene with maxima at 300 nm and 265 nm are long axis polarised and that at 285 nm is short axis polarised one. Further, the first vibrational peak of the long wavelength band is more intense than the other peaks. Carbonyl substituents at 2-position of fluorene are expected to impart substantial effect on the long axis polarised transitions than short axis polarised ones. Infact, the data of Table 3.14 clearly reveal that the long axis polarised absorption bands (300 nm and 265 nm) are largely red shifted such that the latter one completely mixes with the short axis polarised band centered at 285 nm. In effect, the long wavelength absorption band of 2FAl, 2AcF and 2BeF is composed of three transitions i.e. the 265 nm absorption band of fluorene is completely displaced toward red and it may be appearing as a shoulder at 288 nm. The large molecular extinction coefficient value, which is similar to 265 nm band of fluorene also confirms this assignment. The loss of vibrational structure on increasing the polarity and

Table 3.14. Absorption and Fluorescence Spectral Data of 2FA1, 2AcF and 2BeF in Different Solvents and at Various Acid Concentrations.

	2FA1		2AcF		2BeF	
	$\lambda_a$ (loge)	$\lambda_f(\phi_f)$	$\lambda_a$ (loge)	$\lambda_f(\phi_f)$	$\lambda_a$ (loge)	$\lambda_f(\phi_f)$
1	2	3	4	5	6	7
Cyclohexane	318(4.53)		313(4.52)		313	
	313(4.44)		304(4.39)		-	
	304(4.42)	-	300(4.41)	-	293	-
	298(4.39)		293(4.40)		245	
	291(4.35)		287(4.38)			
	241(3.74)		279(4.30)			
	232(3.82)		238(3.58)			
Dioxane	318(4.42)		314(4.40)		313	
	-		-		-	
	307(4.39)		303(4.38)		293	
	-		292(4.34)		250	
	293(4.29)	-	288(4.32)	-		-
	243(3.84)		279(4.21)			
	234(3.84)		239(3.68)			
Acetonitrile	316(4.43)		312(4.40)		314	
	-		-		-	
	306(4.40)	-	303(4.17)	-	293	-
	-		291(4.09)		250	
	293(4.30)		285(4.05)			
	241(3.66)		238(3.46)			
	234(3.79)					

...contd.

Table 3.14(contd.)

1	2	3	4	5	6	7
Methanol	316(4.43) — 306(4.38) — 292(4.28) 241(3.67) 233(3.76)	—	309(4.46) — 301(4.44) — 289(4.39) — 238(3.57)	—	315 — 295 — 250	—
Neutral (pH 5)	318(4.44) 295(4.24) 242(3.79)	408 (0.02)	313(4.46) 292(4.29) 242(3.67)	400 (0.02)	(320) 325(4.39) 320(4.40) 298(4.18) 254(4.15)	* 400
Monocation (H <sub>2</sub> O <sup>+</sup> -8)	413(4.54) 279(3.76) 290(3.57)	468	402(4.62) 266(3.81) 243(3.66)	460	434(4.68) 310(4.39) 274(4.10) 262(4.05) 253(4.00)	* 485 500
Monocation (cyclohexane + 2 TFA)	234 321 300	420	329 321 297	415	330 — 298	415
Dication <sup>+</sup> (H <sub>2</sub> O <sup>+</sup> -10)	384 260 240	435	379 260 247	422	408 — 316 305 274 263	467

<sup>+</sup> Equilibrium is not complete

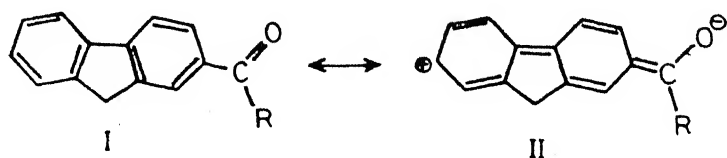
\* in 20%ethanolic solution

hydrogen bonding ability of the solvents can be explained on the basis of the increased solute-solvent interactions. As discussed earlier, the absorption spectra of these carbonyls are red shifted with respect to that of fluorene. The red shift observed is in the order  $2\text{AcF} < 2\text{FAl} < 2\text{BeF}$  which is exactly in the same order of the electron withdrawing ability of these groups  $-\text{COCH}_3 < -\text{CHO} < -\text{COPh}$ .

Fluorescence spectral studies show interesting phenomenon as is commonly observed for the aromatic carbonyls. The apparent lack of fluorescence of 2FAl, 2AcF and 2BeF in hydrocarbon and aprotic polar solvents constitute the best argument for an  $S_1$  state of  $n\pi^*$  type. The lowest energy triplet state of 2-acetylfluorene is of  $\pi\pi^*$  type.<sup>151</sup> Probably this might be the lowest triplet states for 2FAl and 2BeF also. As the Spin-Orbit Coupling<sup>3</sup> between  $^1n\pi^*$  and  $^3\pi\pi^*$  states is very much greater than that between  $^1\pi\pi^*$  and  $^3\pi\pi^*$  states, intersystem crossing is preferred as a means of excited state deactivation for these carbonyls, in all the solvents except in water. In hydroxylic solvents, hydrogen bonding of the solvent with the non-bonded electron pairs of the carbonyl group raises the energy of  $^1n\pi^*$  state while the polarising effect of hydrogen bonding and the gross dielectric properties of solvents lower the energy of  $^1\pi\pi^*$  state to the point where it becomes the lowest excited singlet state, favouring fluorescence over intersystem crossing as a means of deactivation of  $S_1$  state. So it may be concluded that  $^1n\pi^*$  is the lowest energy transition in non-polar solvents whereas  $^1\pi\pi^*$  is the lowest energy transition in water. Since the molecular extinction coefficient of

$^1n\pi^*$  transition is generally very small, it appears that it is overlapped by the strong  $^1\pi\pi^*$  one.

The large Stokes shift ( $\sim 7000\text{ cm}^{-1}$ ) observed for these carbonyls as compared to that of fluorene ( $1100\text{ cm}^{-1}$ ) in water can not be explained by simple substituent effect alone, so it is probable that these substituents attain coplanarity with the fluorene ring upon excitation. This geometry relaxation stabilizes the dipolar structure (II) in the  $S_1$  state, resulting a highly Stokes shifted fluorescence emission from all the carbonyls studied.



Scheme 12

#### 3.4.2 Effect of Acid Concentration

Fig. 3.19 to 3.21 represent the absorption and fluorescence spectra of different species of 2FA1, 2AcF and 2BeF respectively. The pertinent data are reported in Table 3.14. All the carbonyls studied behave similarly in the acid concentrations. In the region pH 3 to pH 14, carbonyls exist as neutral species both in  $S_0$  and  $S_1$  states. The absorption spectra exhibit progressive red shift with increase in the concentration of acid and at  $H_0-5$ , a highly red shifted, broad band is appeared. This change indicates the formation of monocations. On increasing the acid concentration further, a red shifted absorption band starts appearing and its intensity reaches



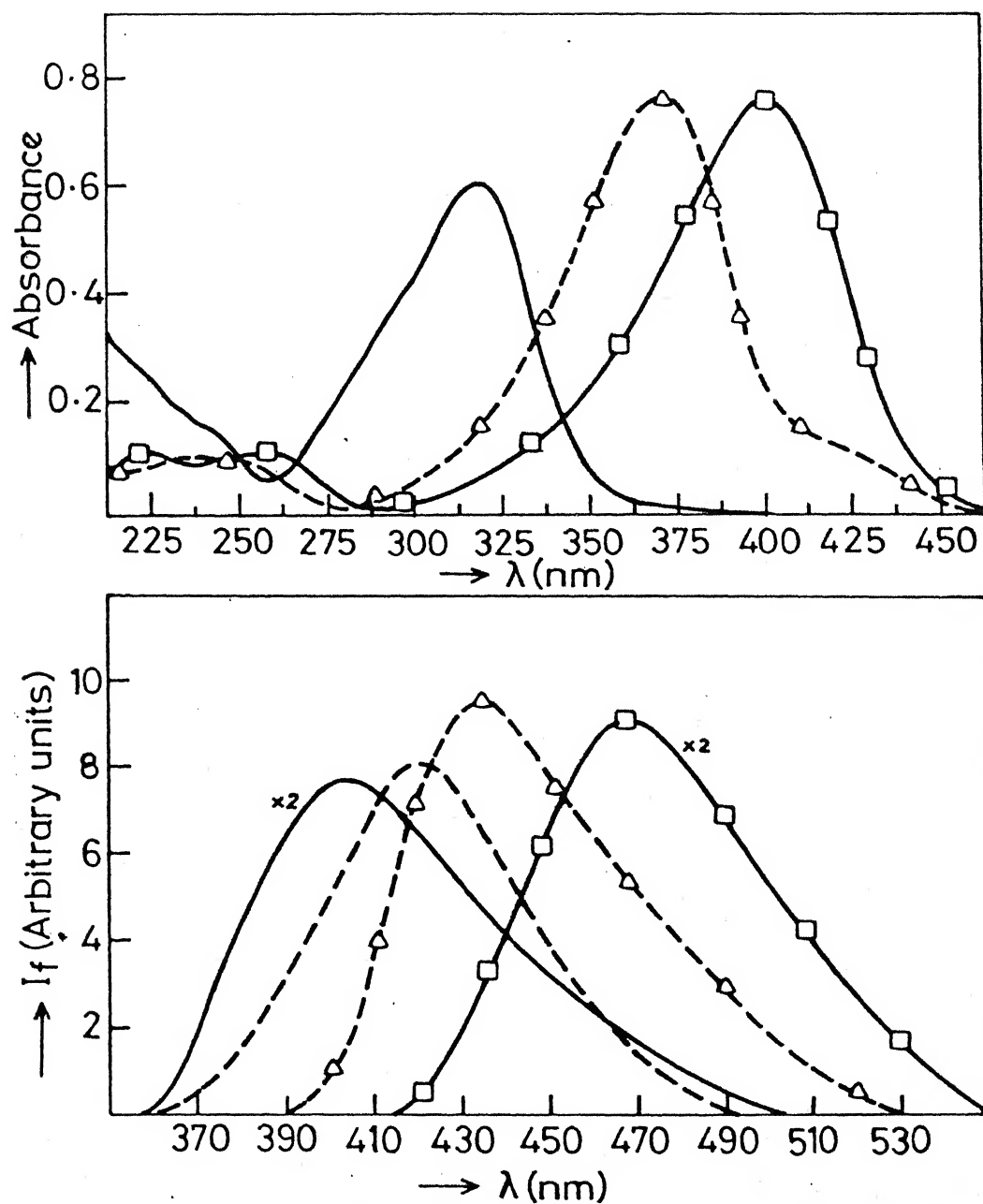


Fig.3.19 Absorption (upper panel) and fluorescence (lower panel) spectra of different prototropic species of 2-fluorenaldehyde. (— neutral, —□—□— monocation, --Δ--Δ-- dication, --- monocation in cyclohexane medium).

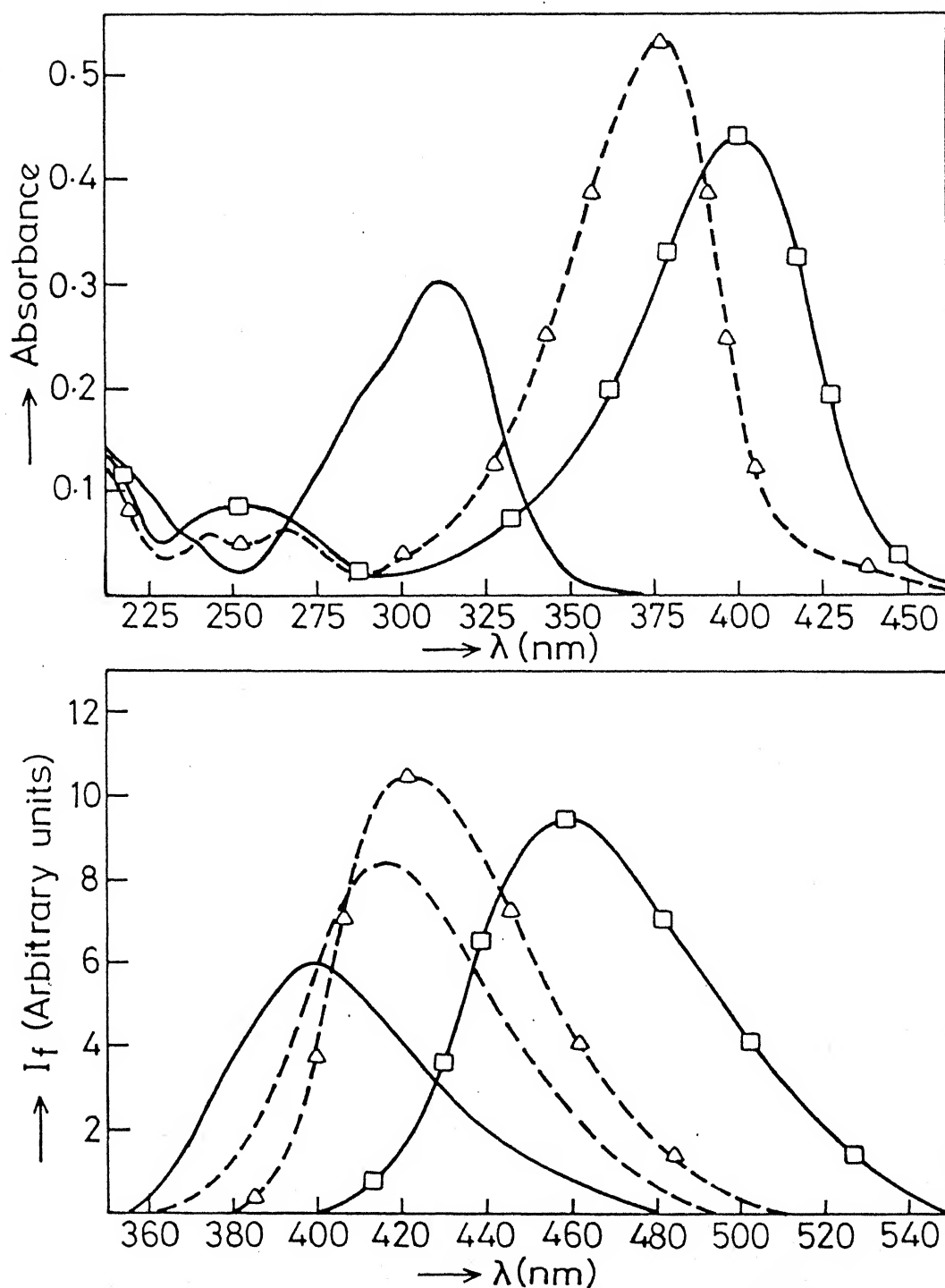


Fig.3.20 Absorption (upper panel) and fluorescence (lower panel) spectra of different prototropic species of 2-acetylfluorene. (— neutral, --□--□-- monocation, --△--△-- dication, - - - monocation in cyclohexane medium).

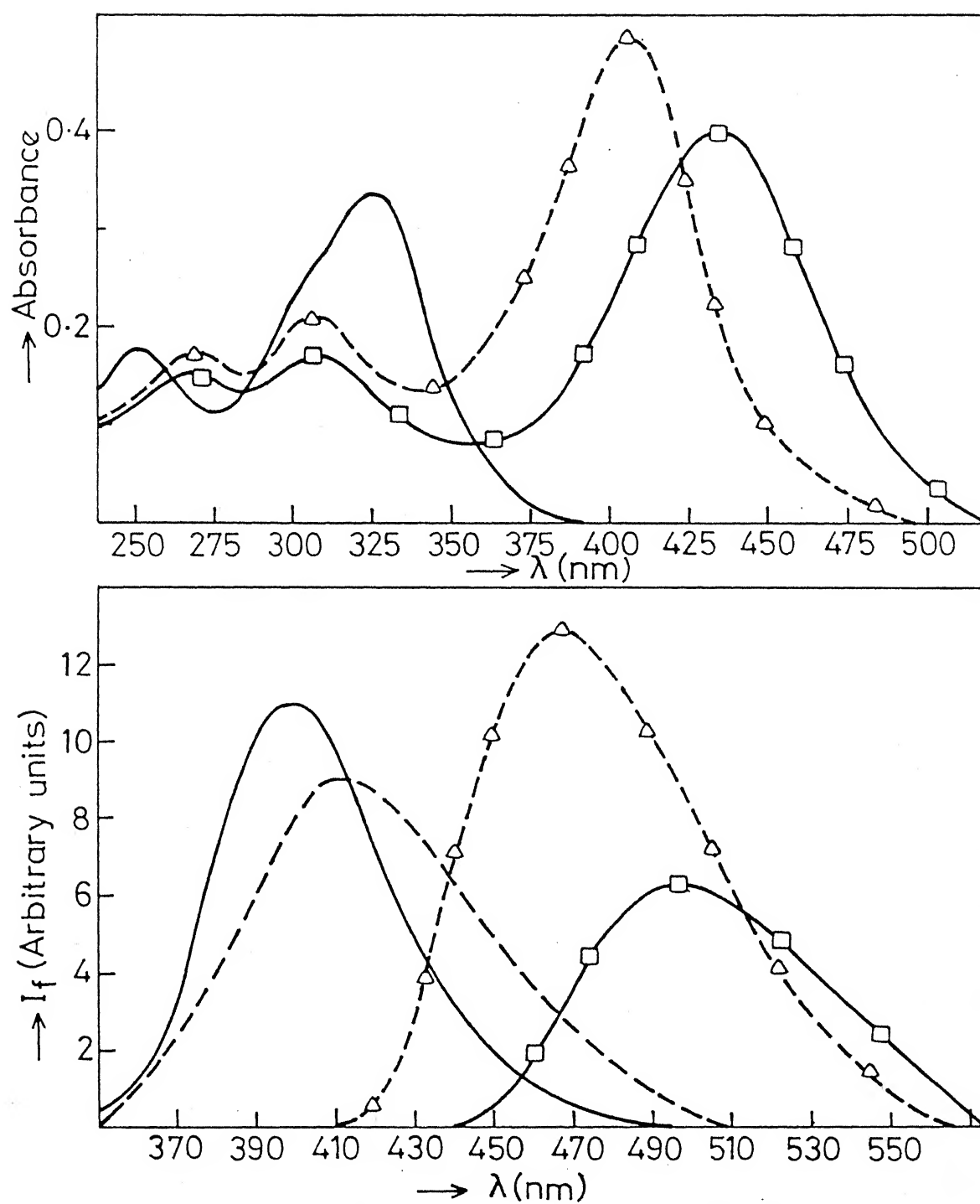


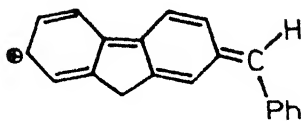
Fig.3.21 Absorption (upper panel) and fluorescence (lower panel) spectra of different prototropic species of 2-benzoylfluorene. (— neutral, —□—□— monocation, --△--△-- dication, - - - monocation in cyclohexane medium).

saturation value at  $H_O-8$ . After  $H_O-8$ , the spectra are continuously blue shifted even upto  $H_O-10$ . Due to the poor solubility of 2BeF, the above study was carried out in 20% ethanolic solution. In the basic region at  $H_-15$ , all the carbonyls get precipitated out. The intensity of fluorescence spectra of the neutral species of 2FA1, 2AcF and 2BeF is decreased continuously on increasing the acid concentration from pH 3, without the appearance of any new fluorescence band. Fluorescence is completely absent at  $H_O-3$  but after  $H_O-4$ , a new red shifted fluorescence band appears and the intensity is increased upto  $H_O-8$ . Like absorption, fluorescence spectra are also blue shifted in the acid concentration  $H_O-9$  and  $H_O-10$ .

If  $\pi \rightarrow \pi^*$  transition is the lowest energy transition, protonation on carbonyls results red shift in the electronic spectra. As mentioned earlier, the lowest energy transition in these carbonyls is of  $\pi\pi^*$  type in water. The data in Table 3.14 indicate that monocation species of these carbonyls are formed by the protonation at the oxygen centre. The large red shift observed for monocation as compared to neutral species, can not be explained by simple protonation. It seems that subsequent to protonation, charge reorganization takes place resulting in more stable canonical structures. In the carbonyls studied, the monocation of 2BeF show large red shift and it might be due to more effective stabilization of the carbonium ion. (shown in page 118).

During the study on a series of substituted acetophenones, Stewart and Yates<sup>221</sup> noticed interesting feature in the plots of, difference in the molecular extinction coefficient of ionized and

unionized species,  $(\epsilon_i - \epsilon_u)$  Vs  $H_O$ . While, p-methoxyacetophenone gave sigmoid titration-like curve, 2-acetylfluorene and p-phenylacetophenone showed two inflection points one at -5.5 and the other



Scheme 13

at -9 (as shown in Fig. 3.22). These results, they interpreted as the result of large increase in the molecular extinction coefficient in going from unionized to ionized form of these compounds. It was also proposed that in 96 % (w/w)  $H_2SO_4$ , 2-acetylfluorene exist as a monocation and the absorption maximum of this monocation of 2AcF was reported to be 379 nm. But the systematic study on the prototropic reactions of 2AcF shows that the species at 96 % (w/w)  $H_2SO_4$  is infact the dication and the absorption maximum is exactly the same as that of the reported species by Stewart and Yates.<sup>221</sup> At this acid concentration, the carbonyls exist as dications rather than monocation. This is consistent with the observation that 2FA (section 3.2.2) and 2FAM (section 3.3.2) also exist as dications at this acid concentration. From our studies, it is also clear that the inflection noticed by Stewart and Yates<sup>221</sup> is not because of a large change in the molecular extinction coefficients but the formation of dications. Thus at  $H_O$  -9, the dications are formed by protonating the carbonyl group and the ring. The blue shift observed in the absorption and

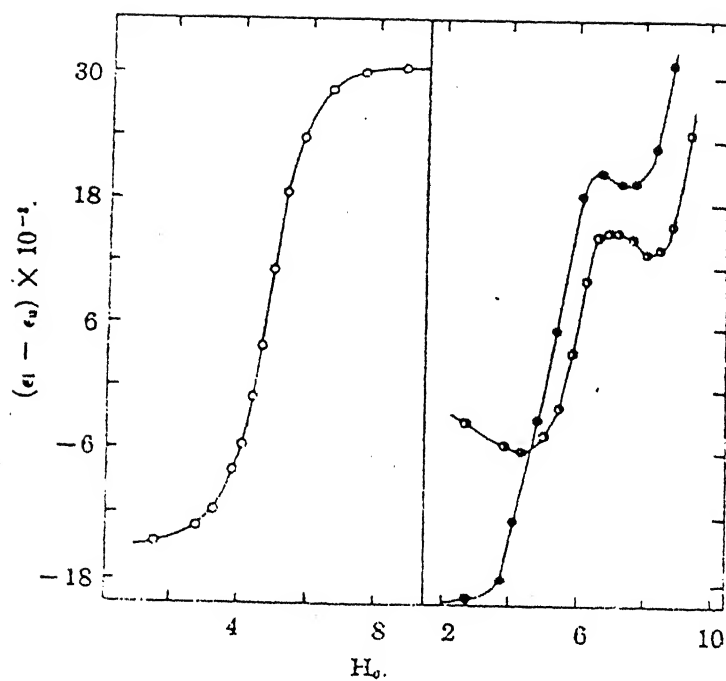


Fig.3.22 Plot of  $(\epsilon_i - \epsilon_u)$  Vs  $H_0$  for p-methoxyacetophenone ( $\circ$ — $\circ$ — $\circ$ ), 2-acetylfluorene ( $\bullet$ — $\bullet$ — $\bullet$ ) and p-phenylacetophenone ( $\circ$ — $\circ$ — $\circ$ ).

fluorescence spectra is consistent with those of 2FA and 2FAM and can be explained on the same lines (section 3.2.2 and 3.3.2 respectively).

In accord with carbonyl protonation, fluorescence spectra of carbonyls also result in red shift on first protonation. Fluorescence intensity of the neutral species is quenched prior to the formation of monocations. This is attributed to proton-induced fluorescence quenching of neutral species because the same amount of  $\text{SO}_4^{-2}$  (which present in this region), added with the addition of  $\text{K}_2\text{SO}_4$ , do not quench the fluorescence of the monocation. Proton-induced fluorescence quenching constant could not be calculated as the long wavelength absorption bands of all these carbonyls are composed of more than one transitions.

The absorption and fluorescence spectral changes observed for different prototropic species of 2FAl, 2FAc and 2BeF are exactly similar to those of 2FA and 2FAM.

### 3.4.3 Dissociation Constants

Like aromatic carboxamides, these carbonyls also show interesting features in their protonation reactions: (i) Medium effect is observed in the prototropic reactions of carbonyls, (ii) Hammett's acidity function ( $H_0$ ) fails to describe the prototropic behaviour of aldehydes and ketones. It has been observed by Bonner and Phillips<sup>193</sup> that the plot of  $H_0$  Vs  $-\log I$  for benzophenones do not give unit slope as required by Hammett equation (section 2.2.2).

This failure of Hammett's scale to describe the prototropic behaviour of benzophenones led these workers to propose a new acidity scale, which uses a set of substituted benzophenones as indicators. Thermodynamically meaningful  $pK_a$  values can be obtained by using this acidity function and the values obtained for 2FAl, 2AcF and 2BeF are shown in the Table 3.15. The slopes have been calculated after the correction for medium effect is made. The medium effect can be reasonably corrected by reading absorbance values at  $\lambda_{max}$ , characteristics of each medium rather than at a fixed wavelength for all media.<sup>193</sup> The unit slope obtained for 2FAl, 2AcF and 2BeF clearly indicate that Benzophenone Hammett's scale is valid for all these carbonyls. The trend observed in the  $pK_a$  values of these is in good agreement with those of 2-benzaldehyde (-7.4), 2-acetophenone (-6.5) and 2-benzophenone (-5.7).<sup>89</sup>

As the fluorescence of neutral species of carbonyls is quenched prior to the formation of monocation,  $pK_a^*$  for this equilibrium has been obtained from the formation curves of monocation (Fig. 3.23; Table 3.16). This gives the ground state  $pK_a$  values for all the carbonyls. As pointed out by Ireland and Wyatt,<sup>222</sup> this might be due to the fact that proton-induced fluorescence quenching of the neutral species is so efficient at this acid concentration that 'excited monocation is not formed in the encounter: this could amount to a case of a non-adiabatic reaction in which electronic energy is lost during the transfer of a proton to the excited base'. The same explanation can be given for these compounds also. Though nothing can be said conclusively from our study, it may be pointed out that the proton-



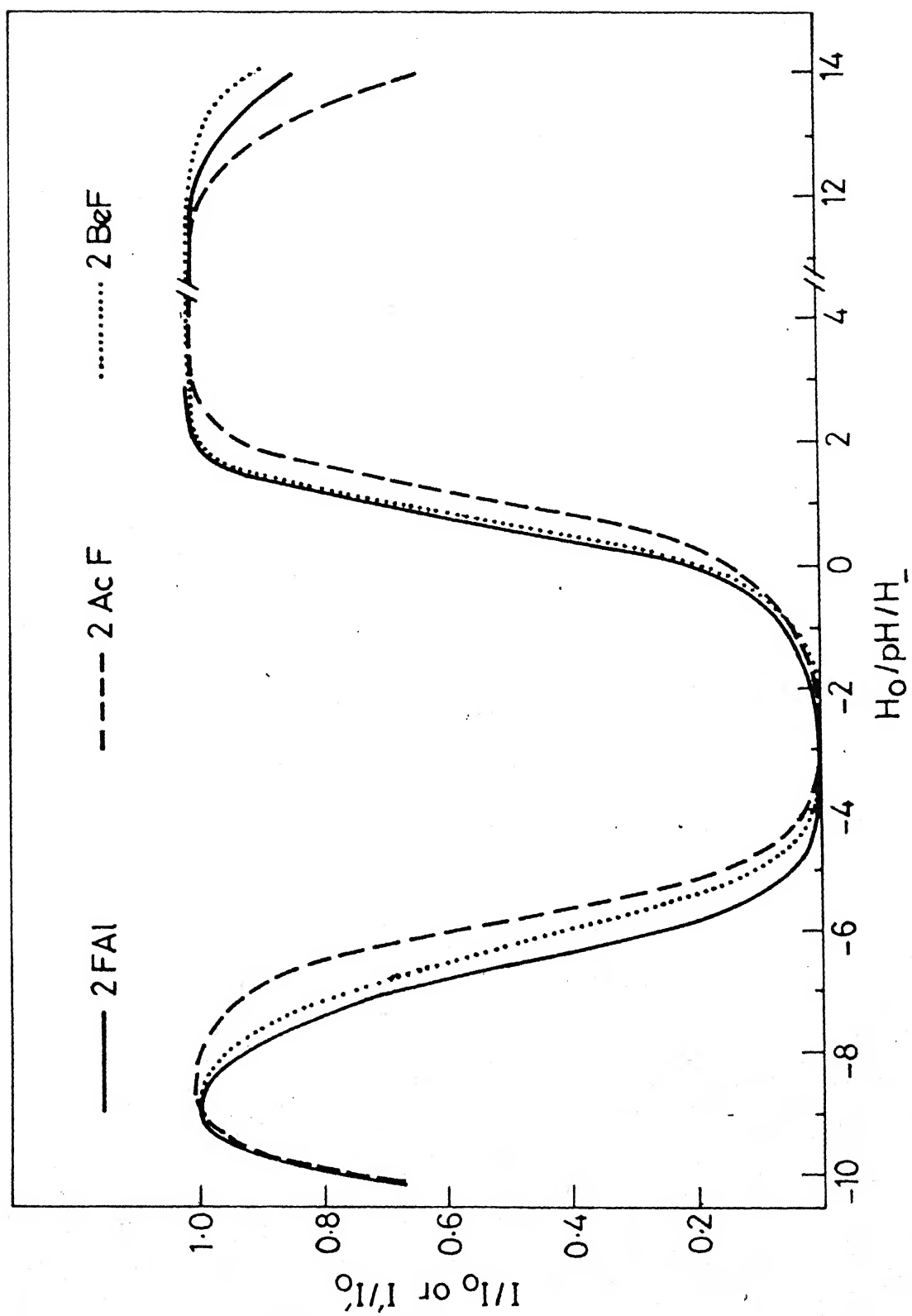


Fig.3.23 Fluorimetric titration curves for the prototropic species of 2-fluorenaldehyde, 2-acetylfluorene and 2-benzoylfluorene.

Table 3.15. Acidity Constants of Monocation-Neutral Equilibrium.

Compound		$H_O$ scale	$H_O$ (Benzophenone scale)
2 FA1	Slope	0.54	1.04
	$pK_a$	-7.3	-6.5
2 AcF	Slope	0.59	1.00
	$pK_a$	-6.2	-5.6
2 BeF	Slope	0.56	0.95
	$pK_a$	-6.4	-5.2

Table 3.16. Acidity Constants of 2FA1, 2AcF and 2BeF:  
Determined by Absorptiometric and Fluorimetric  
Titrations.

Equilibrium	2FA1	2AcF	2BeF
$pK_a(S_0)$	-6.5	-5.6	-5.2
Monocation-Neutral			
$pK_a(S_1)$	-6.6	-5.7	-6.2

$pK_a(S_1)$  represent apparent values because equilibrium is not established in the  $S_1$  state (see text).

induced fluorescence quenching of the neutral carbonyls is solvent dependent. It is well known that the carbonyls become strongly basic on excitation and this monocation fluorescence band can be observed in 2 % (v/v) TFA + cyclohexane medium. This acidity of TFA in cyclohexane amounts to protonate the carbonyl group in the excited singlet state. Our results (Table 3.14) also show that the red shifted fluorescence of the carbonyls in cyclohexane + 2 % (v/v) TFA is because of the carbonyl protonated monocations. If the proton-induced fluorescence quenching had not been solvent dependent one would not have observed fluorescence band for the monocations in non-polar medium as the similar band is absent in water for the same acidity.

The ground and excited state dissociation constants for dication-monocation equilibrium can not be calculated because the prototropic reactions are not complete.

From this study, it can be concluded that: (i) The long wavelength absorption band of 2FA1, 2AcF and 2BeF is composed of three transitions. (ii) The lack of fluorescence from these carbonyls is because,  $^1n\pi^*$  is the lowest energy transition in all the solvents employed except water. (iii) Literature anomaly regarding the assignment of species is removed i.e. at 96%  $H_2SO_4$  medium, 2AcF exist as dication, not the monocation. (iv) Hammett's acidity function fails to describe the prototropic behaviour of carbonyls hence benzo-phenone Hammett's acidity scale is used to get thermodynamic  $pK_a$  values. (v) The neutral species of these carbonyls undergo proton-induced fluorescence quenching.

## CHAPTER-IV

### EFFECTS OF SOLVENTS AND pH ON THE ELECTRONIC SPECTRA OF 2,7-DIAMINO- FLUORENE AND RELATED DIAMINES

Spectral characteristics of bifunctional molecules having electron donating and electron withdrawing groups have been studied extensively.<sup>175-178</sup> Similar studies on molecules having both either electron donating groups or electron withdrawing groups are scarce.<sup>179-183</sup> For example, during the prototropic reactions of 9,10-phenanthroline, Schulman et al.<sup>179</sup> have noticed red shifts in absorption spectra on each protonation (a normal trend) but the fluorescence spectrum followed an anomalous behaviour i.e. a large red shift was followed by a blue shift on protonations. This has been explained by the fact that large solvent relaxation is observed in case of monocation in  $S_1$  state as compared to that for dication. This kind of behaviour led us to carry out the systematic study on molecules containing both electron donating groups. Six molecules have been selected i.e. 2,7-diaminofluorene, 2,3-diaminonaphthalene, o-, m-, p-phenylenediamines and 9,10-diaminophenanthrene. The results and discussion on the effect of solvent and pH on the absorption and fluorescence spectra of these

molecules are presented in this chapter. Depending upon the parent molecule, these have been discussed in four sections.

#### 4.1 2,7-DIAMINOFLUORENE<sup>a</sup>

##### 4.1.1 Effect of Solvent

The absorption and fluorescence spectra of DAF in different solvents are depicted in Fig. 4.1 and the pertinent data are compiled in Table 4.1. As compared to fluorene,<sup>146</sup> the absorption maxima of all the bands of DAF are largely red shifted in any one particular solvent (300 to 340 nm, 264 to 290 nm). The long wavelength absorption band is unresolved whereas the middle one is structured in less polar solvents but in more polar solvents all the bands become broad and diffuse. The absorption spectrum is red shifted upon moving from cyclohexane to acetonitrile but blue shifted in methanol and water as solvents. On the other hand, fluorescence spectrum is a large red shifted broad band, as compared to the structured fluorescence spectrum of fluorene.<sup>147</sup> Starting from cyclohexane as one goes to water, the fluorescence spectrum is regularly red shifted and the quantum yield is unaffected in these solvents, except in water.

In DAF, as both the amino groups are present along the long axis of fluorene molecule, the interaction will be maximum with the ring and hence the long axis polarised transitions will be affected much more than the short axis polarised ones. It is observed that

---

<sup>a</sup> R. Manoharan and S.K. Dogra, Can. J. Chem., 65, 2013 (1987).

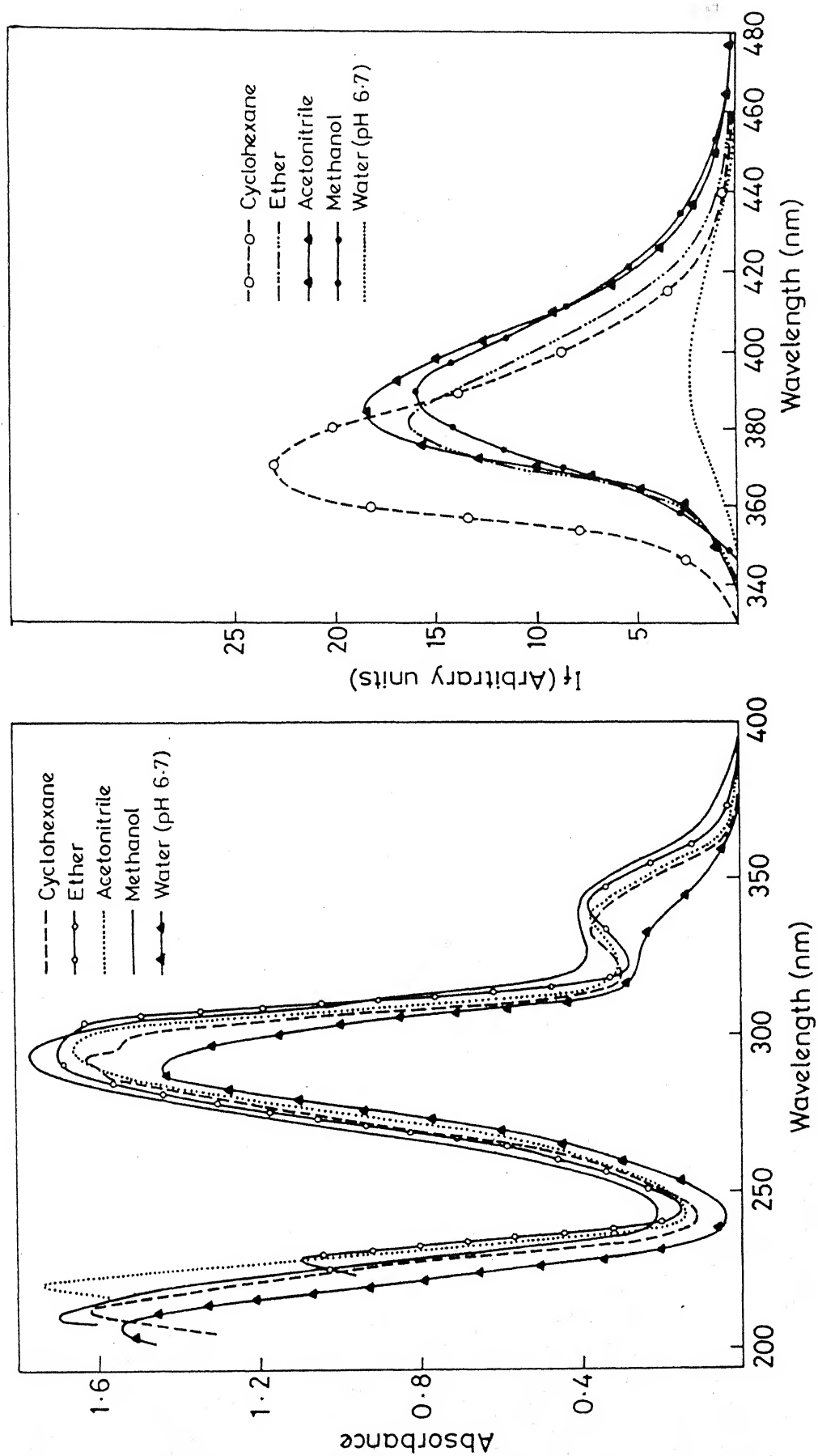


Fig.4.1 Absorption (left panel) and fluorescence (right panel) spectra of 2,7-diaminofluorene in different solvents.

Table 4.1(contd.)

1	2	3
Water (pH 8)	328.5(3.79)	395(0.03)
	—	
	289.5(4.38)	
	207 (4.59)	
Monocation (pH 4)	317.5(3.86)	410(0.42)
	289.5(4.26)	
	202.5(4.47)	
Dication ( $H_O -4$ )	297 (3.93)	300(0.07)
	(s)290 (3.75)	310
	285.5(3.81)	
	(s)275 (3.94)	
	(s)270 (4.12)	
	262 (4.29)	
	(s)252.5(4.25)	
	(s)217.5(4.08)	

$\epsilon$  is in cubic decimeters per mole per centimeter.

the long wavelength band is structureless and red shifted as compared to that of fluorene.<sup>146</sup> Though a bathochromic shift is observed in  $\sim 260$  nm band system of fluorene, it is vibrationally structured in non-polar solvents but it is lost in more polar solvents, indicating the strong solute-solvent interaction. The absorption spectral shifts of DAF in more polar or hydrogen bonding solvents are consistent with the characteristic behaviour of the amino<sup>223</sup> or hydroxy<sup>224</sup> groups i.e. amino group acts as a proton donor to proton acceptor solvents and preferably as a proton acceptor if the solvent possess both proton donor and acceptor properties, in  $S_0$  state. Ether is acting as a proton acceptor, acetonitrile a dispersive, whereas methanol and water as proton donors. In the  $S_1$  state, since the charge migration increases from  $-NH_2$  group to the ring, it reduces the charge density at the nitrogen atom and thus behaves as a proton donor. This is further manifested from the increased acidity of  $-NH_2$  group on excitation (vide infra). The increase in Stokes shift with an increase in the polarity or hydrogen bonding ability of the solvents indicates that the dipole moment of the molecule increases upon excitation. The decrease in the fluorescence quantum yield of the neutral DAF in water suggests that the strong interactions with water might increase the rate of radiationless process.<sup>43</sup>

#### 4.1.2 Effect of Acid Concentration

Fig. 4.2 depicts the absorption and fluorescence spectra of the different prototropic species of DAF and the relevant data are listed in Table 4.1. The absorption spectrum of DAF is blue shifted near pH 5, indicating the formation of a monocation by protonating one of



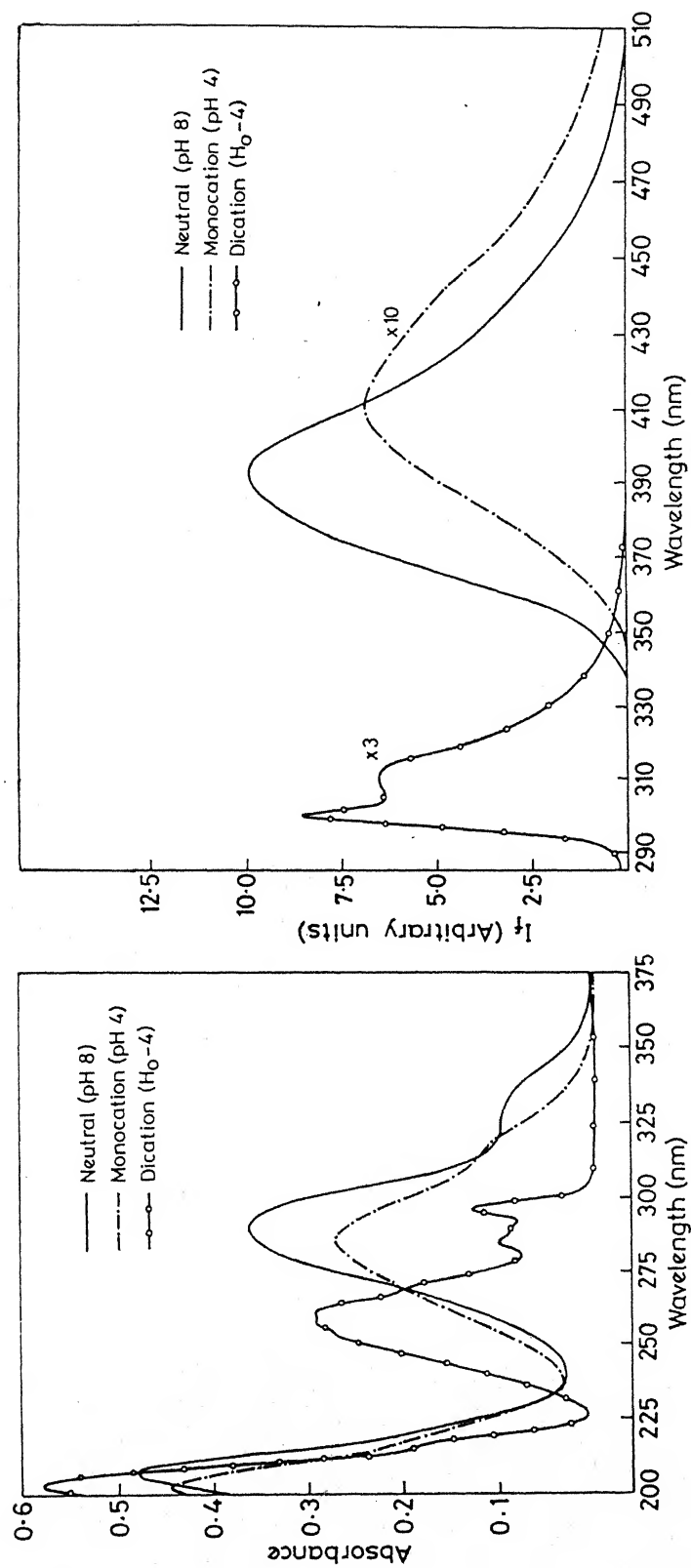


Fig.4.2 Absorption (left panel) and fluorescence (right panel) spectra of different prototropic species of 2,7-diaminofluorene.

the amino groups, and a further blue shift noticed at  $H_o-4$  suggests the formation of a dication by protonating the second amino group also. This is confirmed by their spectral resemblance with 2-amino-fluorene<sup>152</sup> and fluorene<sup>146</sup> respectively. No further change is noticed even at  $H_o-10$ . In the basic region at  $H_-16$ , a red shift is noted only in the long wavelength absorption band which corresponds to the formation of a monoanion by deprotonating  $-NH_2$  group rather than  $>CH_2$  group. This can be rationalized on the basis that only the long axis polarised transition is affected and secondly the expected  $pK_a$  value of the deprotonation reaction of  $-NH_2$  group nicely agrees with the literature values ( $\sim 16$ ),<sup>223</sup> whereas that of  $>CH_2$  in fluorene is close to 22.

The effect of  $pH > 12$  on the fluorescence spectra suggests the formation of a non-fluorescent monoanion (deprotonation of  $-NH_2$  group). The  $pK_a^*$  value calculated from the fluorimetric titration curve is 13.9 which is in agreement with the literature report that  $-NH_2$  group becomes strongly acidic on excitation.<sup>116,125</sup> In the weakly basic medium, the neutral species of DAF is weakly fluorescent (395 nm). On increasing the acid concentration, the intensity of 395 nm band decreases while an intense red shifted (410 nm) fluorescence is observed. Again, the intensity of 410 nm band decreases nearly to 10% of its maximum value at  $pH\ 0.5$ , when a large blue shifted, structured band appeared at 310 nm. This blue shifted band attains the maximum fluorescence intensity by  $H_o-4$ , but a further increase of acidity, decreases the intensity without resulting in any new fluorescence band. The fluorescence spectra with maxima at 410 nm and 310 nm correspond to monocation and dication species respectively. This

assignment is based on their spectral similarities to those of 2-aminofluorene<sup>152</sup> and fluorene<sup>147</sup> respectively. These species are further confirmed by getting the excitation spectral profiles, monitored at the above mentioned emission maxima, which are identical with the absorption spectra of the species present in  $S_0$  state.

Acidity constants of DAF in  $S_0$  and  $S_1$  states have been calculated and are listed in Table 4.2. The  $pK_a$  values for the monocation-neutral equilibrium,  $pK_a(2)$  and the dication-monocation equilibrium,  $pK_a(3)$  are 5.8 and 3.6 respectively. The literature values for the same equilibria are 4.96 and 3.6 respectively.<sup>143</sup> Since the latter values have been determined in 70 % (v/v) ethanol-water solution, these can not be compared with our data. The  $pK_a(2)$  value is higher and the  $pK_a(3)$  is lower than that observed for the aromatic amine protonation ( $\sim 4.5$ ). This increased basicity of these amino groups as compared to aromatic monoamines can be explained from the following Canonical structure, i.e. at any one particular moment, the charge



Scheme 1

density at one of the amino groups will be more than that of the other, but on average the charge density will be equal at both of the amino groups. This is because of their locations at symmetrical positions in fluorene ring. Once one of the amino groups is

Table 4.2. Acidity Constants of 2,7-DAF in the Ground and First Excited Singlet State.

Equilibrium		$pK_a$	$pK_a^*$	$pK_a^*$ (Förster cycle)		
				a	f	av
DAF	$\rightleftharpoons$ DAF <sup>-</sup> + H <sup>+</sup>	>16	13.9	-	-	-
DAFH <sup>+</sup>	$\rightleftharpoons$ DAF + H <sup>+</sup>	5.8	5.3	3.6	7.7	5.7
DAFH <sub>2</sub> <sup>+</sup>	$\rightleftharpoons$ DAFH <sup>+</sup> + H <sup>+</sup>	3.6	-3.0	-1.0	-12.9	-6.9

a, f - from absorption and fluorescence data respectively.

av - average of a and f.

Table 4.3. Prototropic Species of 2,7-DAF in Cyclohexane.

Medium	$\lambda_a$	$\lambda_f$
Cyclohexane	334	369
	299	
	283	
	262	
Cyclohexane + 0.001 % TFA	305	324
	292	
	275	
	260	
Cyclohexane + 2% TFA	298	305
	289	
	285	
	262	

protonated, the presence of  $-\text{NH}_3^+$  group decreases the charge density at the other amino group, resulting in a very low  $\text{pK}_a(3)$  value.

The  $\text{pK}_a^*$  values obtained by various methods do not agree. The Förster cycle method using absorption data shows the normal trend in  $\text{pK}_a^*(2)$  value, i.e.  $-\text{NH}_2$  becomes more acidic upon excitation, but fluorescence spectra predict otherwise. Fluorimetric titration method has given the ground state  $\text{pK}_a$  value. In general, protonation on aromatic amines give blue shift in both absorption and fluorescence spectra if  $\pi \rightarrow \pi^*$  is the lowest energy transition.<sup>116</sup> While the absorption spectral change conforms this, fluorescence spectrum of the monocation of DAF is anomalously red shifted. Because of this, Förster cycle calculations using absorption and fluorescence data predict the opposite trends in the basicity of DAF. The evaluation of the ground state  $\text{pK}_a(2)$  from the fluorimetric titration infers that the relative lifetimes of neutral and monocation must be too short for the proton transfer to occur appreciably within their lifetimes, especially at very low proton concentration.

The anomaly in the fluorescence spectrum of the monocation can be explained as follows. In general, charge migration from the amino group to the aromatic ring increases on excitation. In the case of monocation of DAF, this charge migration from the second amino group at position-7 of the fluorene ring will be facilitated by the presence of positive charge on  $-\text{NH}_3^+$  group. This charge migration in the monocation will be more than that present in the case of neutral. This charge transfer increases the dipole moment of the monocation in the  $S_1$  state. Due to this, the relaxation energy of the solvent cage

from the  $S_0$  configuration to the equilibrium excited state configuration might be so much greater for the monocation such that the blue shift, which one would normally expect for the protonation reaction of amino group is out weighed by the solvent stabilization of monocation. This results a red shift in the fluorescence spectrum of the monocation as compared to neutral species. In the case of dication, since both the lone pairs of the amino groups are protonated they can not perturb the  $\pi$  electron cloud of the fluorene molecule. Thus the spectral profile resembles with that of the parent fluorene molecule.

The above explanation for the monocation can be verified, if the monocation spectrum is recorded in non-polar medium, for example cyclohexane, where the solvent relaxation is negligible. In fact, the data of Table 4.3 reaffirm the above point. The absorption spectra of the monocation and the dication obtained by adding different amounts of trifluoroacetic acid (TFA) in cyclohexane match with those obtained in aqueous  $H_2SO_4$  acid, whereas the fluorescence spectra are different. The results obtained in the fluorescence measurements are similar to the normal behaviour of the aromatic amines, thereby confirming the above explanation i.e. a blue shift (324 nm) is observed for the fluorescence spectrum of monocation of DAF. The greater polarity of the monocation can further be proved from the Stokes shift observed in non-polar and polar media. For example, in cyclohexane the Stokes shifts of neutral, monocation and dication species are  $2670\text{ cm}^{-1}$ ,  $1920\text{ cm}^{-1}$  and  $770\text{ cm}^{-1}$  respectively, whereas in water these are  $5120\text{ cm}^{-1}$ ,  $7100\text{ cm}^{-1}$  and  $340\text{ cm}^{-1}$  respectively. The large discrepancy between the Stokes shift for  $DAFH^+$  in cyclohexane and

water must be due to the solvent relaxation because, the change in solvent can not change the vibrational relaxation to such a large extent. Further, the large Stokes shift for  $\text{DAFH}^+$  in water suggests that this species is stabilized in  $S_1$  state much more than in  $S_0$  state, relative to the species with which it is in prototropic equilibrium. Thus, as suggested by Schulman et al.<sup>179</sup> the Förster cycle method using the average of absorption and fluorescence maxima will not be useful for this equilibrium.

Fluorimetric titration between the monocation and dication equilibrium shows no correspondance between the decrease and increase in the fluorescence intensities of monocation and dication species respectively. This is due to the proton-induced fluorescence quenching of the monocation before it is being protonated to form dication. Due to this, the  $\text{pK}_a^*$ (3) value is calculated from the formation curve of the dication (Fig. 4.3) and the value indicates that the dication is more acidic in the  $S_1$  state. Förster cycle calculations using fluorescence data do not yield reasonable value because of the unusual red shift in the monocation fluorescence and thus should not be considered seriously. Since monoanion of DAF is non-fluorescent, the  $\text{pK}_a^*$  for the neutral-monoanion equilibrium is determined from the decrease in the fluorescence intensity of the neutral species and is listed in Table 4.2. The value agrees with the similar behaviour of other aromatic amines and indicates that  $-\text{NH}_2$  group becomes stronger acid on excitation.

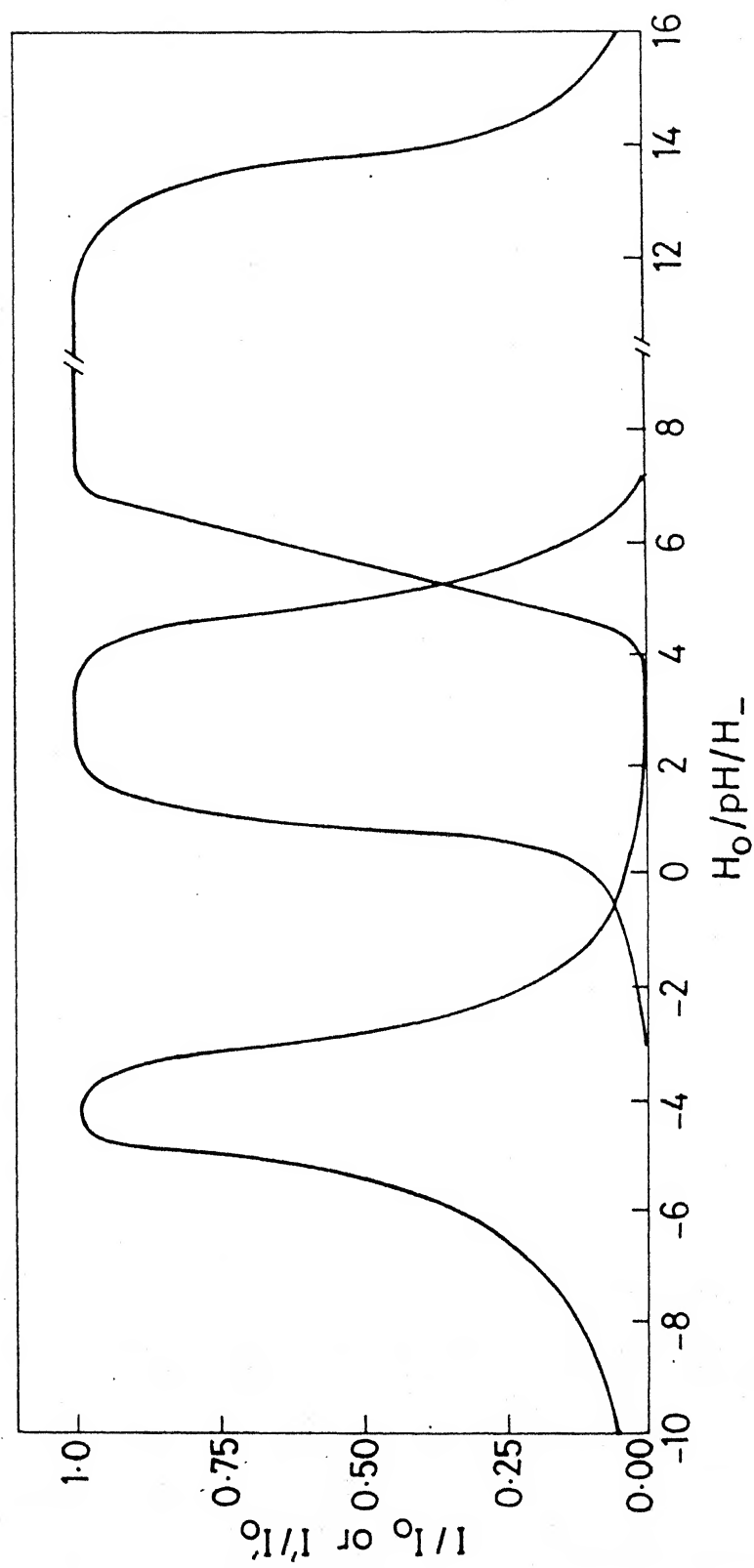


Fig.4.3 Fluorimetric titration curves for different prototropic species of 2,7-diaminofluorene.



#### 4.1.3 Proton-Induced Fluorescence Quenching

The lack of correspondance between the decrease and increase in the fluorescence intensities of monocation and dication respectively is attributed to proton-induced fluorescence quenching. This is because  $\text{SO}_4^{-2}$  ion concentration (produced by the addition of  $\text{K}_2\text{SO}_4$ ) equivalent to that obtained by the addition of  $\text{H}_2\text{SO}_4$ , do not quench the fluorescence of monocation. The model suggested by Shizuka et al.<sup>122d</sup> can be transformed into a simple Stern-Volmer equation under the conditions that the lifetime of monocation is smaller than that of dication and the concentration of  $\text{H}^+$  is too small to have any backward protonation reaction (section 2.2.4). Stern-Volmer quenching constant  $K_{sv}$  has been obtained from Stern-Volmer plot (shown in Fig. 4.4) and natural lifetime, calculated from appropriate absorption envelope and corrected fluorescence spectra using Strickler-Berg equation. The value of  $k_q$  ( $3.6 \times 10^8 \text{ dm}^3 \text{ mol}^{-1} \text{ s}^{-1}$ ) obtained from  $K_{sv}$  and  $\tau_f$  ( $= \tau_{FM} \times \phi_f$ ) is less than that of  $k_q$  generally observed for the neutral amines ( $\sim 10^9 \text{ dm}^3 \text{ mol}^{-1} \text{ s}^{-1}$ ).<sup>128</sup> This is due to the positive charge already present on the molecule.

It can be concluded that the anomalous red shift of monocation as compared to the neutral is due to the large solvent relaxation in  $S_1$  state. Thus the fluorescence data can not be used to calculate  $\text{pK}_a^*$  values for both the prototropic equilibria by Förster cycle method.

The unusual behaviour observed in the fluorescence spectrum of the monocation of DAF stimulated our interest in the diamino compounds.

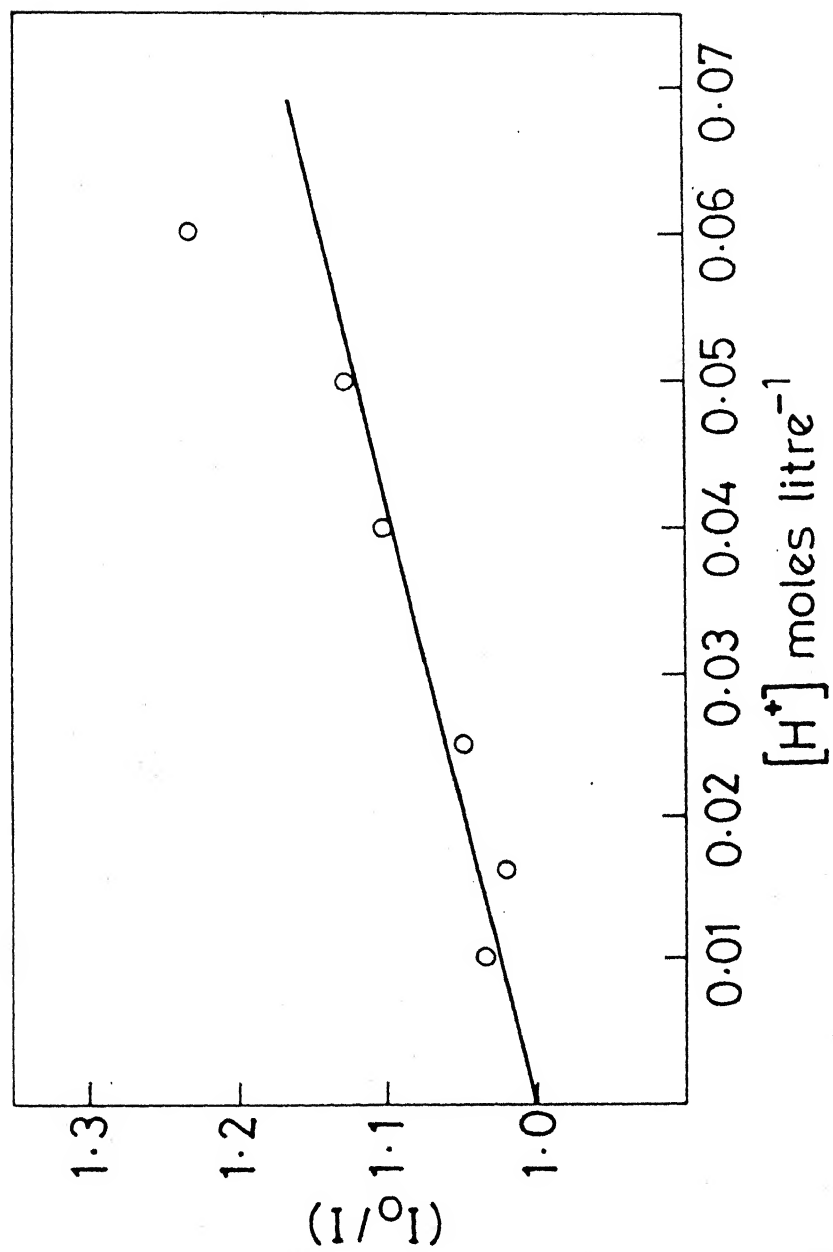


Fig.4.4 Stern-Volmer plot for proton-induced fluorescence quenching of monocation of 2,7-diaminofluorene.

The further study was carried out in some other structurally related diamines and are discussed in the following sections.

## 4.2 2,3-DIAMINONAPHTHALENE<sup>a</sup>

### 4.2.1 Solvent Study

The absorption and fluorescence spectra of DAN recorded in different solvents are shown in Fig. 4.5 and the relevant data are entered in Table 4.4. The absorption and fluorescence spectra of the neutral species of DAN and 2-aminonaphthalene (2AN) are also depicted in Fig. 4.6 for comparison. The absorption band maxima of DAN and 2AN are similar except that the molar extinction coefficient of the long wavelength band of DAN is nearly twice that of 2AN. Unlike the broad long wavelength band of 2AN, vibrational structure ( $960 \pm 40 \text{ cm}^{-1}$ ) is noticed for DAN and the band becomes diffuse in most of the polar solvents used. Like any other aromatic amine, absorption spectrum of DAN is red shifted on increasing the polarity of the solvents but blue shifted in hydroxylic solvents. The fluorescence spectra, with vibrational structure ( $\sim 950 \text{ cm}^{-1}$ ) observed only in cyclohexane are broad and regularly red shifted in the above solvent environments. Further, the fluorescence maximum of DAN in water (384 nm) is at short wavelength than that observed for 2AN (414 nm).

Molecular model depicted below clearly indicates that both of the amino groups are present along the axis which will affect the long

---

<sup>a</sup> R. Manoharan and S.K. Dogra, communicated.

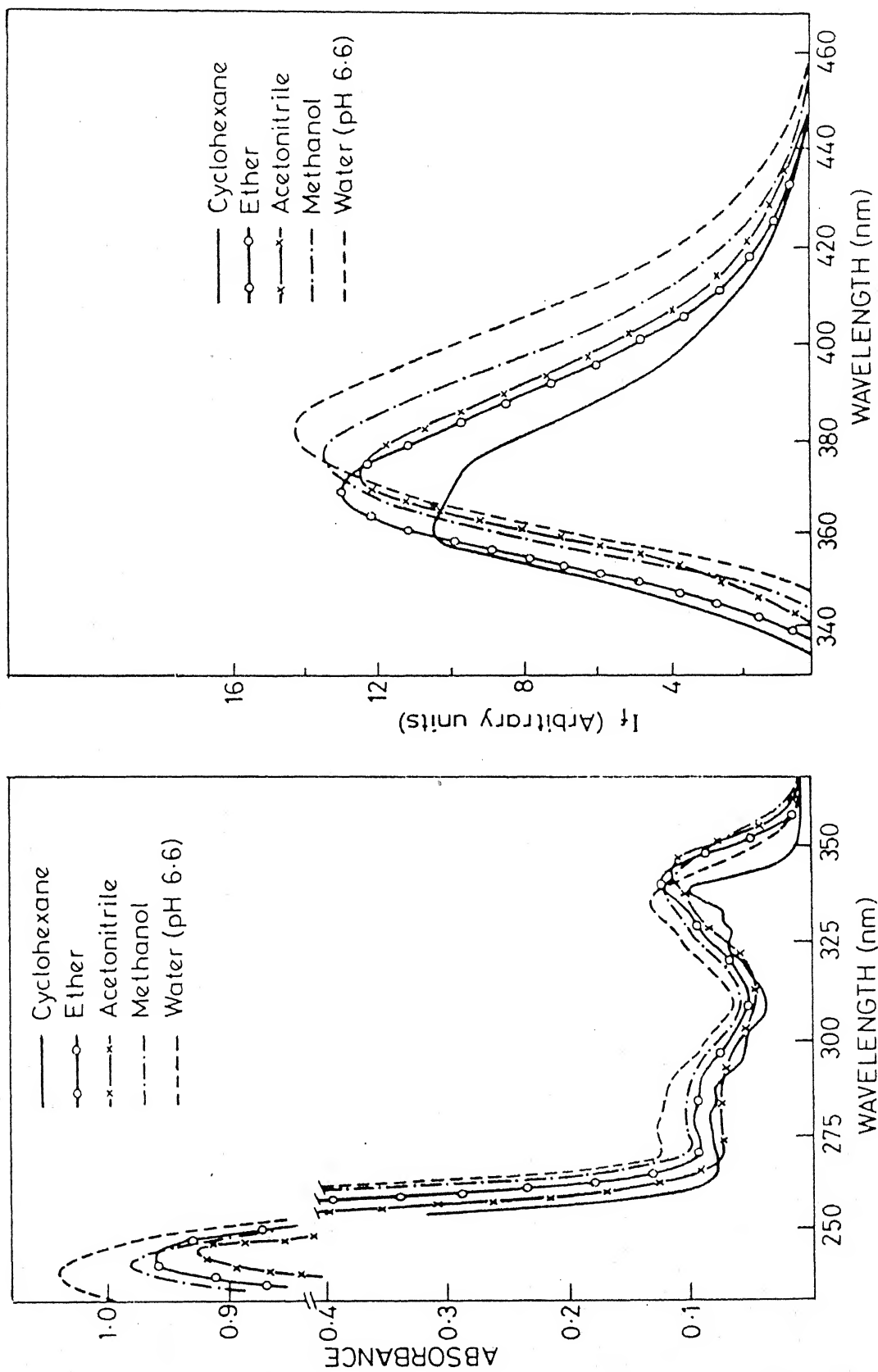


Fig.4.5 Absorption (left panel) and fluorescence (right panel) spectra of 2,3-diaminonaphthalene in different solvents.

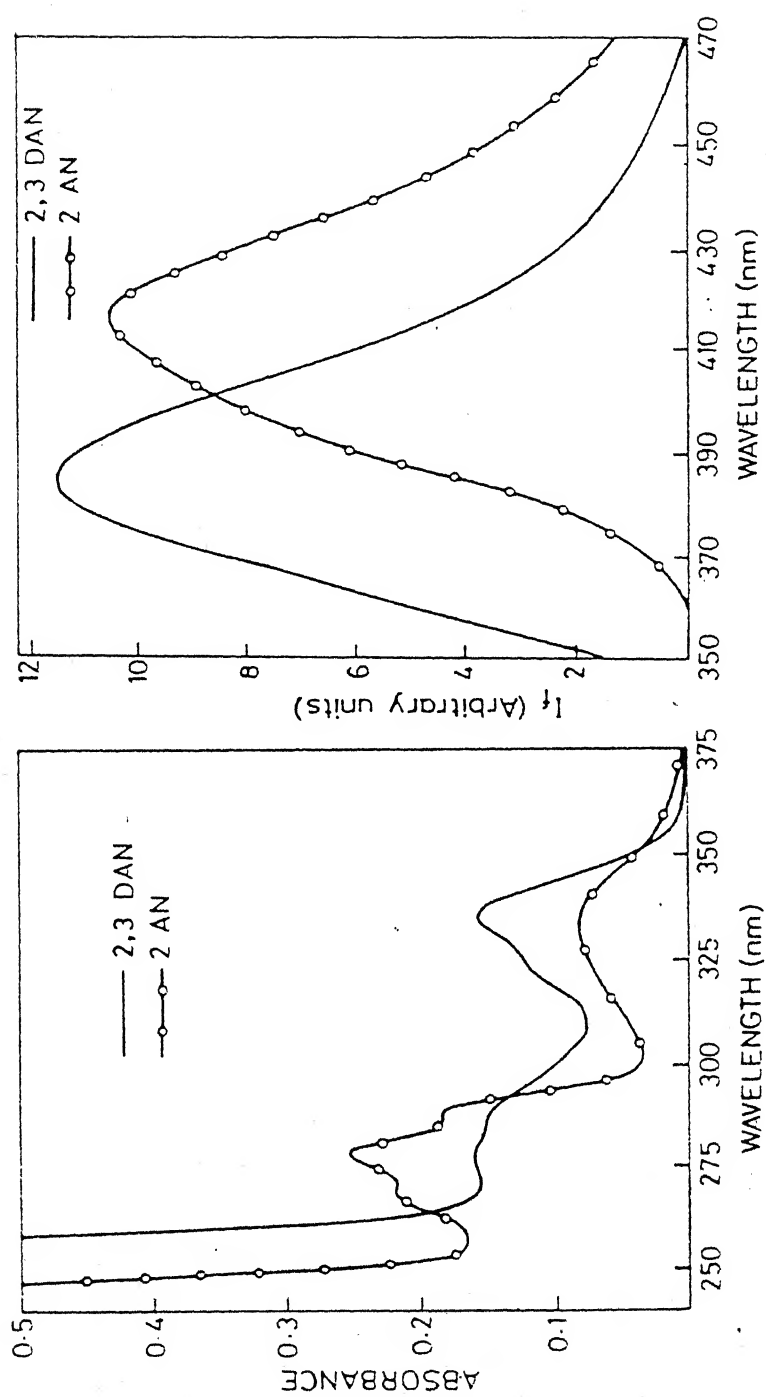


Fig.4.6 Absorption (left panel) and fluorescence (right panel) spectra of neutral species of 2,3-diaminonaphthalene and 2-aminonaphthalene.

Table 4.4. Absorption and Fluorescence Spectral Data of 2,3-DAN  
in Different Solvents and at Various Acid Concentrations.

	$\lambda_{ab} (\log \epsilon_{max})$	$\lambda_f (\phi_f)$
1	2	3
Cyclohexane	337.5	
	330	
	327.5	362
	300	375 (0.42)
	288	
	276.5	
	241.0	
Ether	341.4 (3.77)	
	—	
	328.5 (3.61)	
	290 (3.59)	371 (0.57)
	280 (3.62)	
	245.8 (4.72)	
Acetonitrile	343.4 (3.76)	
	—	
	329.3 (3.63)	
	292.5 (3.59)	374 (0.56)
	281.0 (3.62)	
	246.8 (4.71)	
Methanol	340.5 (3.71)	
	—	
	326.0 (3.62)	
	288.5 (3.59)	377 (0.54)
	277.5 (3.60)	
	245.0 (4.70)	
		..contd.

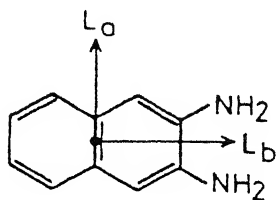
Table 4.4(contd.)

1	2	3
Neutral (pH 7)	335 (3.60)	
	(sh) 324 (3.47)	
	-	
	287.5(3.53)	384(0.64)
	273.5(3.58)	<sup>a</sup> 370
	-	
	235.0(4.66)	
Monocation (pH 2.0)	332.5(3.34)	
	-	
	288 (3.53)	400(0.91)
	272.5(3.69)	<sup>a</sup> 390
	267.5(3.63)	<sup>b</sup> 395
	231.2(4.62)	
Dication (H <sub>0</sub> -7)	315 (2.73)	- <u>a</u>
	301 (3.02)	358 360(s)
	(s) 288.5(3.43)	344 (0.037) 354
	279 (3.59)	- 341
	266.5(3.57)	329 328(s)
	(s) 256.0(3.43)	318 325
	221 (4.7 )	314 314
Monoanion (H <sub>-</sub> 15) <sup>*</sup>	345 (3.53)	
	315 (3.64)	486(0.27)
	247.5(4.06)	
	228 (4.37)	
Dianion (H <sub>-</sub> 16.5)	-	400( - )

a - at 77 K; b - in cyclohexane + 0.01%TFA medium;

\*Ground state equilibrium is not complete at this basic condition, because  $pK_a > 16$ . Absorption data are for the absorption spectrum of DAN at <sup>a</sup>this basic condition.

wavelength transition ( $^1A \rightarrow ^1L_b$ ) more than the short axis polarised ( $^1A \rightarrow ^1L_a$ ) one. But it appears from the data of Table 4.4 that the



Scheme 2

two amino groups are twisted with respect to the naphthalene ring. This conclusion is based on the following facts: (i) If the amino groups are in the plane of the naphthalene ring, one would have observed the absorption and fluorescence maxima of DAN at longer wavelength than those of 2AN. This observation indicates that the net effect of the two amino groups on the absorption spectrum of naphthalene is of about equal degree to that of the one amino group in 2AN, whereas the similar effect on the fluorescence spectrum is even less than that of the amino group in 2AN. This comparison is really valid because of the similarity of their band shapes, as is clear from the Figure 4.6. For DAN and 2AN, the full band width at half maximum of absorption and fluorescence spectra are ( $3.0 \times 10^3 \text{ cm}^{-1}$ ,  $3.5 \times 10^3 \text{ cm}^{-1}$ ;  $3.2 \times 10^3 \text{ cm}^{-1}$ ,  $3.0 \times 10^3 \text{ cm}^{-1}$  respectively) nearly equal. The increase in the molar extinction coefficient of only the  $^1L_b$  band results from an increase in the dipolar length of DAN along the long axis. (ii) The vibrational structure appeared in the absorption spectrum would have been absent, because in 2AN, the long wavelength band is really a broad one. (iii) Though the solvent interaction is observed with DAN, the presence of vibrational structure even in water proves that the



lone pairs are not perturbing the  $\pi$ -electron cloud of the naphthalene ring very much. (iv) The fluorescence spectrum of DAN in cyclohexane displays a vibrational mode ( $\sim 950 \text{ cm}^{-1}$ ) which appear in the long wavelength absorption spectra. This mirror image symmetry between the fluorescence and long wavelength absorption bands demonstrate that the emitting and absorbing states are the same i.e.  $^1L_b$ .

(v) Similar behaviour i.e. the lack of additive effect on the spectral shifts and appearance of vibrational structure are also observed in the case of 2-hydroxy and 2-methoxy-3-naphthylamines<sup>225</sup> indicating that the hydroxy or methoxy and the amino groups are twisted with respect to the naphthalene ring.

The solvent study indicates that DAN acts as a proton acceptor in  $S_0$  state and proton donor in  $S_1$  state. It can be explained as has been done for other diamines. The loss of vibrational structure in the fluorescence spectrum with increasing solvent polarity is due to their increased interaction in the  $S_1$  state.

#### 4.2.2 Effect of Acid Concentration

The absorption and fluorescence spectra of DAN at different acid concentration are portrayed in Fig. 4.7 and the data are tabulated in Table 4.4. At pH 2, the long wavelength absorption band is slightly blue shifted and the middle band ( $\sim 288 \text{ nm}$ ) is not affected much. This species is assigned to a monocation, formed by protonating one of the amino groups, because the long wavelength band of monocation is nearly same as that of 2AN (334 nm, 2AN<sup>+</sup>; 333 nm, DANH<sup>+</sup>). With a further increase in the acid concentration ( $H_0 -6$ ), the absorption

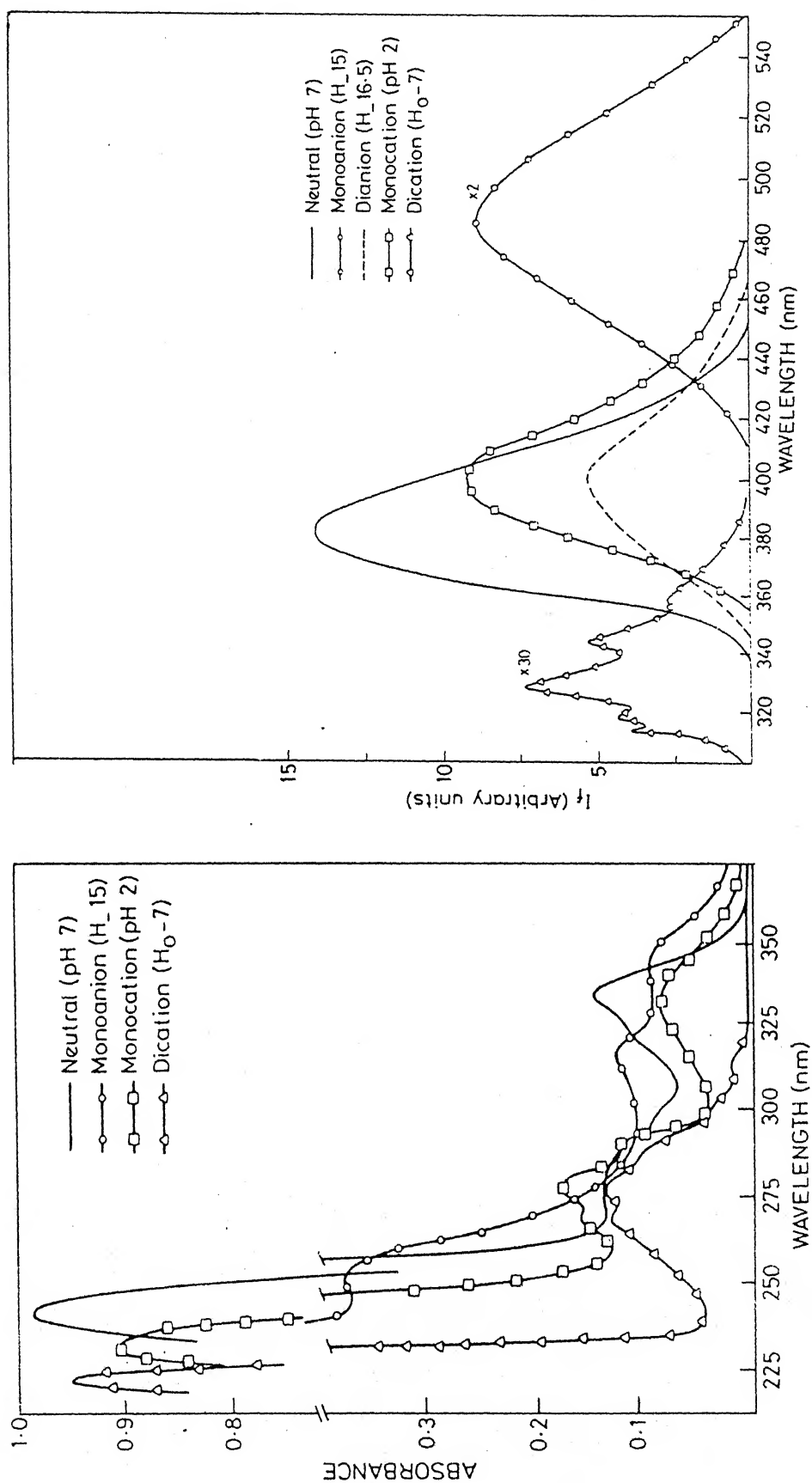


Fig.4.7 Absorption (left panel) and fluorescence (right panel) spectra of different prototropic species of 2,3-diaminonaphthalene.

spectrum is largely blue shifted and the profile exactly resembles that of naphthalene<sup>226</sup> in position and intensity. This indicates the formation of dication by protonating both of the amino groups. At H<sub>15</sub>, the red shift noticed in the spectrum might indicate the appearance of a monoanion formed by deprotonating -NH<sub>2</sub> group. But this equilibrium is not complete even at H<sub>17</sub>, the highly basic medium employed.

The various prototropic species involved in the excited singlet state are the same as obtained in S<sub>0</sub> state but the fluorescence spectral behaviour of the monocation is different. The fluorescence spectrum of the monocation of DAN is red shifted, which is anomalous in comparison to the behaviour of aromatic amines but similar to that observed for 2,7-diaminofluorene. The fluorescence spectrum of the monocation recorded in cyclohexane containing  $1 \times 10^{-2}\%$  (v/v) TFA as well as at low temperature (77 K, aqueous H<sub>2</sub>SO<sub>4</sub> medium) are also red shifted compared to that of the neutral species (375 nm to 395 nm in cyclohexane medium and 370 nm to 390 nm in low temperature solid glass). Since this is at variance with the results of monocation of DAF in non-polar medium, the red shifted fluorescence of the monocation can not be attributed to the solvent relaxation as has been done in the case of DAF. So it forces us to look for an entirely different explanation to account for the red shift in the fluorescence spectra, on first protonation of DAN. Comparing the fluorescence spectra of the neutral species of DAN and 2AN the spectrum of DAN is at shorter wavelength (384 nm) as compared to that of 2AN (414 nm) because the amino groups are twisted with respect to the naphthalene

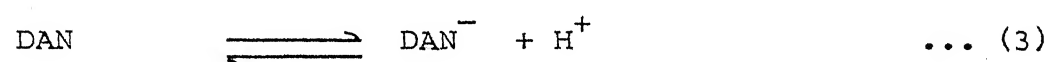
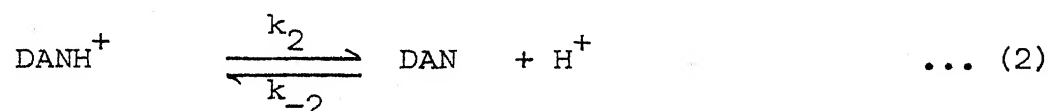
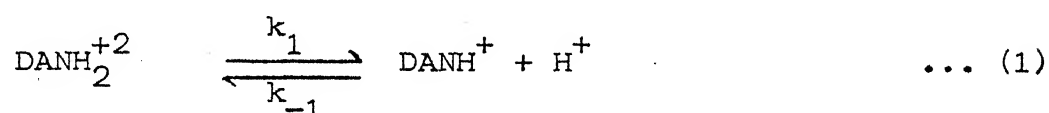
ring and thus have minimum repulsion between the lone pairs of adjacent amino groups. This behaviour can be explained as follows: The protonation of one of the amino groups will remove the lone pair of  $\text{-NH}_2$  group. Due to this it may be possible that repulsion between the two groups may decrease and thus the fluorescence spectrum should resemble that of 2AN species. As said earlier, the fluorescence spectrum of neutral 2AN is red shifted as compared to neutral DAN, hence the fluorescence spectrum of the monocation of DAN will be red shifted to that of neutral DAN. This red shifted fluorescence could be partly due to solvent relaxation of the monocation and partly to the rotation of the two groups ( $\text{-NH}_2$ ,  $\text{-NH}_3^+$ ). But the rotation of the groups to become coplanar with the naphthalene ring is still not completed effectively in  $S_1$  state as  $\lambda_{\text{max}}$  ( $\text{DANH}^+$ ) is still lower than  $\lambda_{\text{max}}$  (2AN).

Similar to other aromatic diamines studied, fluorescence intensity of the monocation is decreased on increasing the acid concentration, without the appearance of any new band, even though the dication is formed in  $S_0$  state. Only after  $H_0 -4$ , a highly blue shifted naphthalene like fluorescence is observed, due to the formation of dication by protonating both of the amino groups. In basic solution ( $H_-14$ ), a large red shifted fluorescence band is observed and can be assigned to the monoanion of DAN. The fluorescence spectrum of the monoanion is also blue shifted (480 nm) in comparison to the monoanion of 2AN (520 nm) and thus a similar explanation is plausible as described in the case of monocation of DAN. At  $H_-16.5$ , a very large blue shifted fluorescence (400 nm) is noticed at the

expense of 480 nm band and it is at the same position as that observed for 2AN under the same basic conditions.<sup>235</sup> This spectral change is attributed to the formation of dianion by deprotonating one of the amino groups and an aromatic centre. The second deprotonation is speculated to be from the aromatic ring rather than second amino group because similar deprotonation has been proposed for 2AN on the basis of the results of deprotonation reaction of N,N'-dimethyl-2-naphthylamine which lack dissociable amino protons.<sup>227</sup>

#### 4.2.3 Acidity Constants

The ground and excited state  $pK_a$  values for the following prototropic reactions have been determined and are compiled in Table 4.5.



A smaller  $pK_a(2)$  value for DAN (3.4) than for the similar reaction of 2AN (4.1) may be due to the steric hindrance provided by the adjacent amino groups. A similar effect is also observed in the case of o-phenylenediamine and 9,10-diaminophenanthrene (section 4.3 and 4.4) but not in m- and p-phenylenediamines and DAF, where these amino groups are separated. The values of  $pK_a(1)$  and  $pK_a(3)$  are consistent with the values for aromatic amines. The Förster cycle method do not yield reasonable value of  $pK_a(1)^*$  and  $pK_a(2)^*$  because of the geometry

Table 4.5. Acidity Constants of DAN in the Ground and First Excited Singlet States.

Equilibrium			$pK_a(S_0)$	$pK_a(S_1)$
$DANH_2^{+2}$	$\rightleftharpoons$	$DANH^+ + H^+$	0.7	-5.3
$DANH^+$	$\rightleftharpoons$	$DAN + H^+$	3.4	<sup>a</sup> 3.35
$DAN$	$\rightleftharpoons$	$DAN^- + H^+$	>16	12.9

<sup>a</sup>apparent value.

Table 4.6. Lifetime of Monocation at Different Acid Concentration.

pH	$\tau$ (ns)
2.0	17.4
1.8	17.1
1.1	17.4
0.2	18.0

changes accompanying in the prototropic reactions. Fluorimetric titration curves (Fig. 4.8) of the monocation and neutral species give the ground state value, indicating that the prototropic equilibrium is not established in  $S_1$  state. This suggests that there is no interconversion between  $DAN^*$  and  $DANH^+*$  during the lifetime of the excited states. Further, the observation of the same inflection points for the fluorimetric titrations of monocation and neutral species clearly indicates that no proton-induced fluorescence quenching of neutral DAN takes place. This observation is unusual because this phenomenon is generally observed for the aromatic amines <sup>223</sup> prior to the protonation. This is due to the fact that the decay rate of DAN ( $\sim 2 \times 10^8 \text{ s}^{-1}$ ) is faster than  $k_{-2}[H^+]$  at concentration of proton around  $10^{-4}$  to  $10^{-3} \text{ M}$ . Because at this concentration of acid, the value of  $k_{-2}[H^+]$  would be  $10^6$  to  $10^7 \text{ s}^{-1}$  assuming that  $k_{-2}$  is equal to the diffusion controlled rate constant ( $\sim 10^{10} \text{ M}^{-1} \text{ s}^{-1}$ ). Similar behaviour has also been observed in other compounds (vide infra). As mentioned earlier, proton-induced fluorescence quenching was observed for  $DANH^+$ , so  $pK_a(1)^*$  was calculated from the formation curve of  $DANH_2^{+2}$  and found to be -5.3, clearly indicating that  $DANH_2^{+2}$  is stronger acid in  $S_1$  state. Similarly the  $pK_a(3)^*$ , calculated from the fluorimetric titrations (Fig. 4.8) is found to be 12.9 showing that the amino group becomes stronger acid on excitation. This is consistent with the similar results obtained for aromatic amines. The equilibrium constant for monoanion-dianion equilibrium can not be determined because the formation of species is not complete even at  $H_2O$ , the highly basic medium used.

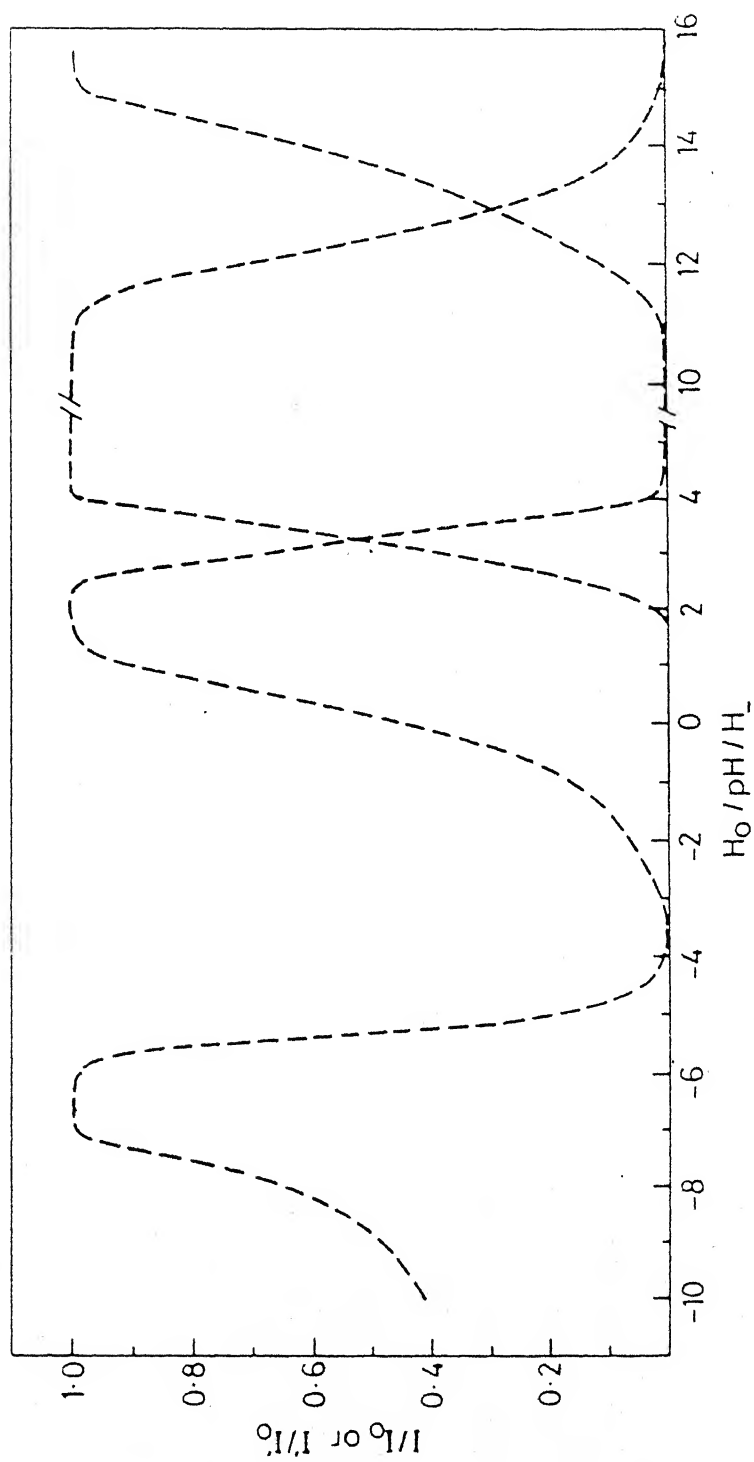


Fig.4.8 Fluorimetric titration curves for the different prototropic species of 2,3-diaminonaphthalene.



#### 4.2.4 Fluorescence Lifetimes

The fluorescence decay functions of the neutral and monocation species of DAN have been measured by a Picosecond Time Resolved Single Photon Counting method. The decay function of neutral at pH 8 follows single exponential with a lifetime of 5.7 ns (excited at 320 nm, monitored at 384 nm). Similarly the single exponential fluorescence decay function (excited at 320 nm monitored at 400 nm) measured for  $\text{DANH}^+$  at different pH (varying from 0.7 to 2) shows that the lifetime of 17.4 ns is independent of proton concentration (Table 4.6; a typical single exponential fluorescence decay of monocation is shown in Fig. 4.9). As pointed out by Schulman,<sup>88e</sup> the fluorimetric titration curves give the ground state  $\text{pK}_a$  value if the pseudo first order dissociation rate of an excited acid or protonation of an excited base is small ( $\sim 10\%$ ) in comparison with the reciprocal lifetimes of the excited acid or base and the rate of protonation of the excited conjugate base ( $k_{-2}[\text{H}^+]$ ) or the deprotonation of the excited conjugate acid is small ( $\sim 10\%$ ) in comparison with the reciprocal lifetime of the excited conjugate base or acid. As discussed earlier, since the prototropic equilibrium between  $\text{DANH}^+$  and DAN is not established during the lifetimes of the excited states of conjugate acid-base pairs, it suggests that  $k_2 < 5 \times 10^6 \text{ s}^{-1}$  and similarly  $k_{-2}[\text{H}^+] < 1 \times 10^6 \text{ s}^{-1}$ .

#### 4.2.5 Proton-Induced Fluorescence Quenching

Similar to DAF, the lack of correspondance between the increase of the fluorescence intensity of dication and decrease of fluorescence

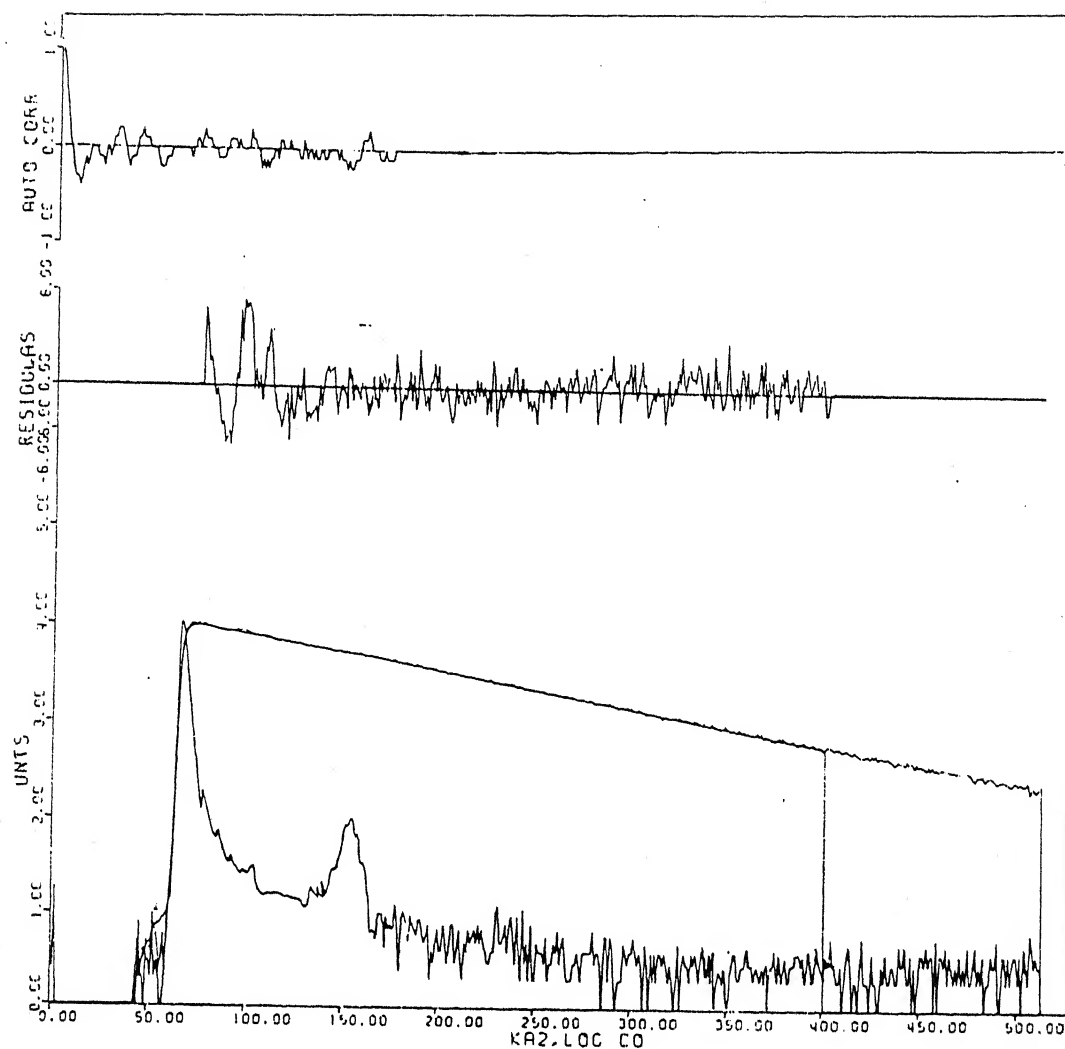
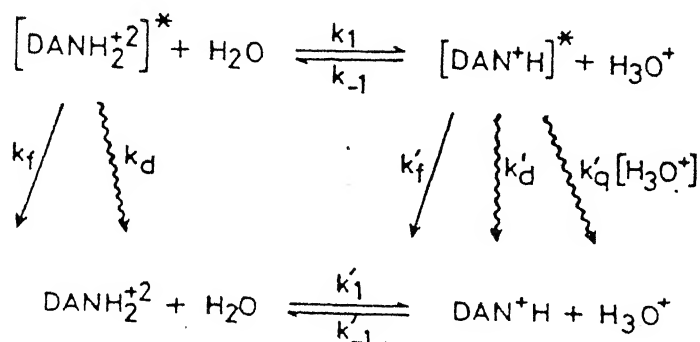


Fig.4.9 Fluorescence decay of the monocation of 2,3-diaminonaphthalene. The residuals and autocorrelation function were determined for a single exponential decay of 17.4 ns ( $\chi^2 = 0.14$ ).

intensity of monocation is attributed to proton-induced fluorescence quenching of the monocation. Model proposed (as shown below) by



Scheme 3

Shizuka et al.<sup>122d</sup> is also valid in this case and the complete equation can be reduced to the simple Stern-Volmer equation, under the conditions that lifetime of the monocation is small and the concentration of the proton is too small to have any backward reaction. The  $k'_q \tau$  value for the monocation was obtained from Stern-Volmer plot (Fig. 4.10). From the value of  $\tau (= 17.4 \text{ ns})$  and  $k'_q \tau (= 1.27 \text{ M}^{-1})$ ,  $k'_q$  is found to be  $7.2 \times 10^7 \text{ M}^{-1} \text{ s}^{-1}$ . This value is very small compared to that obtained for neutral amines and it is because of the presence of a positive charge on this species.

Table 4.6 lists the lifetimes of  $\text{DANH}^+$  at various acid concentration. It is clear from the data that lifetimes are unaffected by the change of acid concentration and thus indicates that proton-induced fluorescence quenching is of static in nature. This is

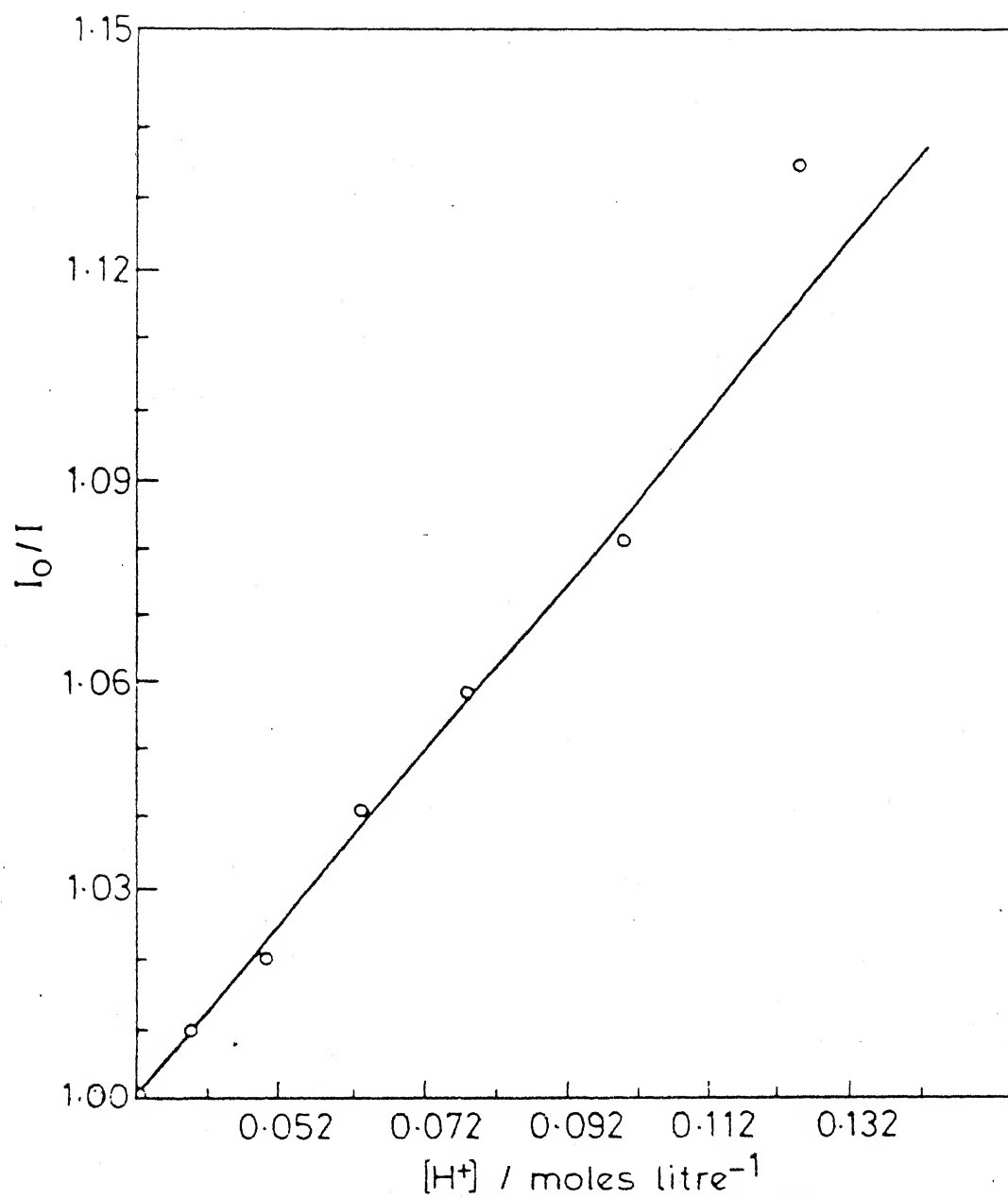


Fig.4.10 Stern-Volmer plot for proton-induced-fluorescence quenching of the monocation of 2,3-diaminonaphthalene.

further substantiated by the fact that the difference between  $K_{sv} (= k'_q \tau)$ , the Stern-Volmer constant and the association constant ( $K_{-1}$ ) of  $DANH^+$  with  $H^+$  is not very large. This may be explained as follows: The  $pK_a(1)$  for  $DANH_2^{+2} - DANH^+$  equilibrium is 0.7, thus the existence of both the species are possible in  $S_0$  state in the pH range 0.7-2.0. Since  $DANH_2^{+2}$  is a stronger acid in  $S_1$  state, it will dissociate into  $DANH^+$  and  $H^+$  upon excitation. But it seems that before the proton comes out of the encounter complex, it quenches the fluorescence of  $DANH^+$ , i.e. the proton with the solvated atmosphere does not have to diffuse to the fluorophore. This phenomenon may be related to local effects.

It can be concluded that, solvent and pH effects on the absorption and fluorescence spectra have clearly shown that both the amino groups are twisted with respect to the naphthalene moiety. The ground state  $pK_a$  value is observed from the fluorimetric titrations of the monocation and neutral species, indicating that the pseudo first order dissociation rate constant of the acid is  $< 1 \times 10^6 \text{ s}^{-1}$ . No proton-induced fluorescence quenching of DAN is observed prior to the formation of  $DANH^+$ . This is due to the fact that the decay rate of  $DAN^*$  ( $\sim 2 \times 10^8 \text{ s}^{-1}$ ) is faster than the proton quenching rate of  $k'_q[H_3O^+]$  at concentrations of acid around  $10^{-3} - 10^{-4} \text{ M}$ . On the other hand the proton-induced fluorescence quenching rate constant for  $DANH^{+*}$  is found to be  $7.2 \times 10^7 \text{ M}^{-1} \text{ s}^{-1}$ , which is quite small compared to that observed for other neutral aromatic amines. This is due to the presence of positive charge on the ring.

### 4.3 ISOMERIC PHENYLENEDIAMINES<sup>a</sup>

#### 4.3.1 Effect of Solvents

The absorption and fluorescence spectral data of o-phenylenediamine (oPA), m-phenylenediamine (mPA) and p-phenylenediamine (pPA) in different solvents are presented in Table 4.7 and the spectra are displayed in Fig. 4.11 to 4.13. The data indicate that the long wavelength absorption bands are intense, broad and largely red shifted as compared to the well known structured band systems of benzene.<sup>228</sup> The increase in the molecular extinction coefficients of phenylenediamines is due to the presence of amino groups. These groups reduce the symmetry of the benzene molecule and thereby allowing the transitions which are forbidden on symmetry considerations. The loss in structure in any one solvent is due to the strong interaction of the amino groups with the  $\pi$ -electron cloud of the benzene ring.

The trend in shifts of the absorption and fluorescence spectra of phenylenediamines in solvents are exactly similar to those observed for any aromatic amine<sup>223</sup> and those of DAF and DAN. The spectral shifts in different solvents can be rationalized on the same basis as has been done for DAF and DAN, i.e. these compounds act as proton donors in ether and acetonitrile whereas, as proton acceptors in methanol and water in  $S_0$  state but proton donors in all the solvents in  $S_1$  state. This is evident from the data of Table 4.7.

The Stokes shift (Table 4.8) observed for these amines is minimum for mPA ( $2630\text{ cm}^{-1}$ ) and nearly equal for oPA and pPA ( $4180\text{ cm}^{-1}$ ),

---

<sup>a</sup> R. Manoharan and S.K. Dogra, Bull. Chem. Soc. Jpn., in press.

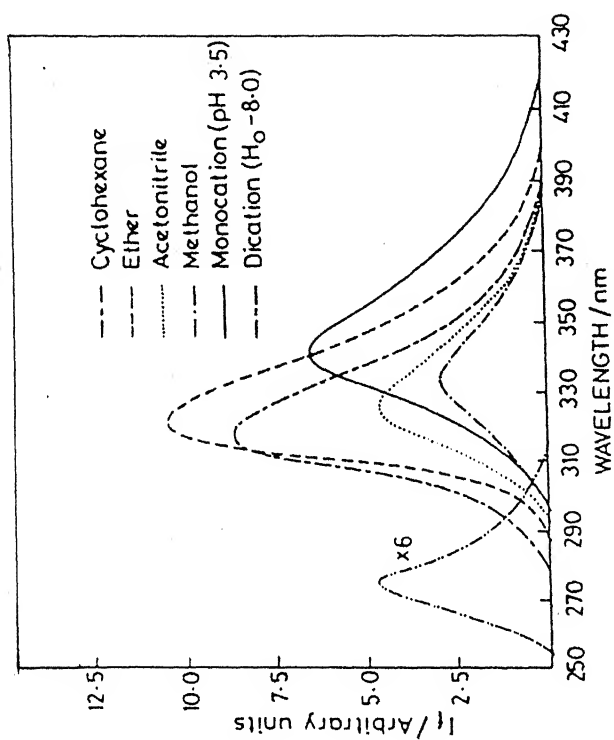


Fig.4.12 Fluorescence spectra of m-phenylenediamine in different solvents and at various acid concentration.

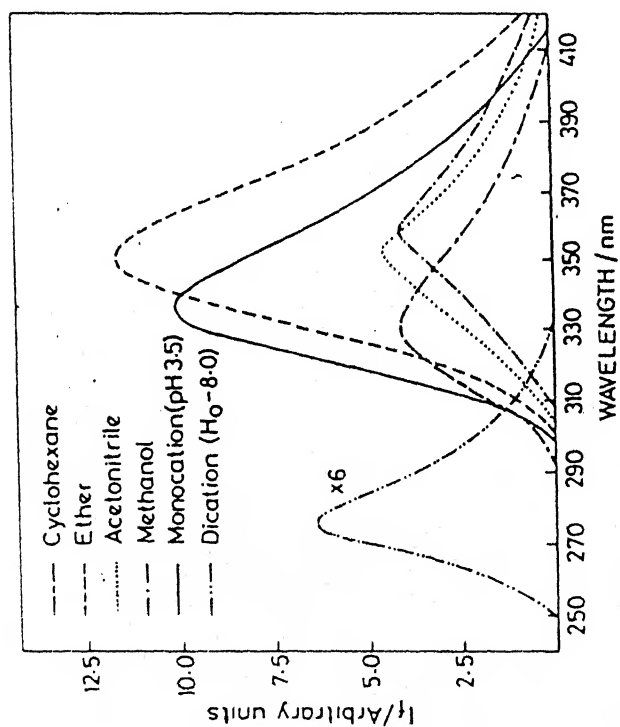


Fig.4.11 Fluorescence spectra of o-phenylenediamine in different solvents and at various acid concentration.

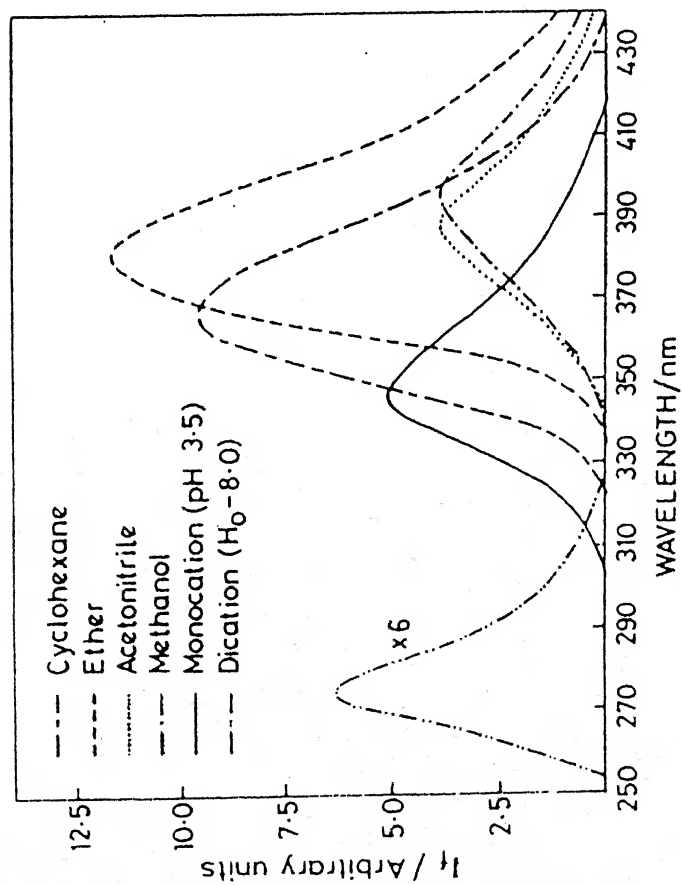


Fig.4.13 Fluorescence spectra of p-phenylenediamine in different solvents and at various acid concentration.

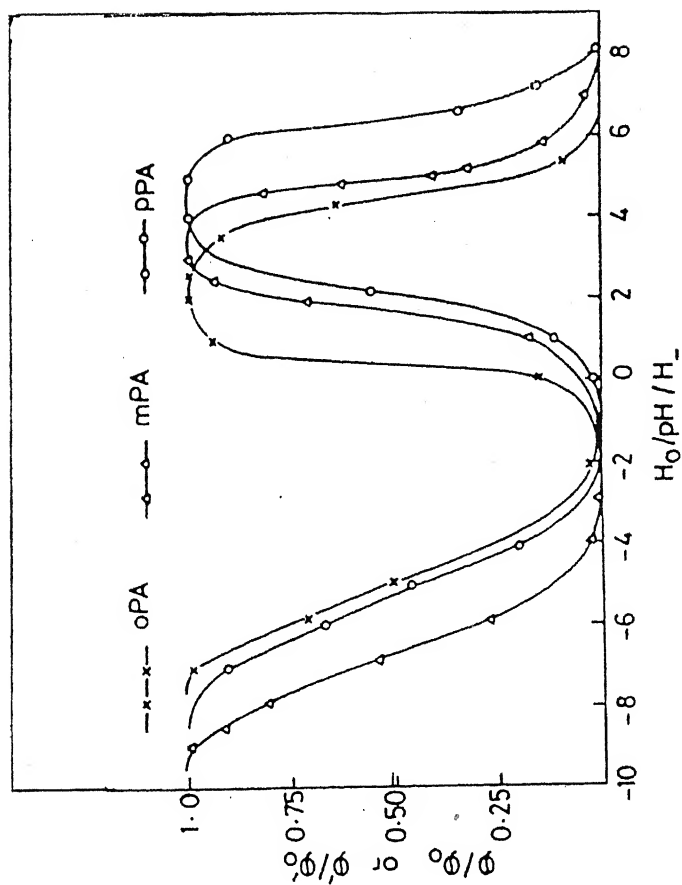


Fig.4.14 Fluorimetric titration curves for the different prototropic species of o-, m-, and p-phenylenediamines.



Table 4.7. Absorption and Fluorescence Spectral Data of Phenylenediamines in Different Solvents and at Various Acid Concentrations.

	oPA		mPA		pPA	
	$\lambda_a(\log \epsilon)$	$\lambda_f(\phi_f)$	$\lambda_a(\log \epsilon)$	$\lambda_f(\phi_f)$	$\lambda_a(\log \epsilon)$	$\lambda_f(\phi_f)$
1	2	3	4	5	6	7
Cyclohexane	290(3.59)		302(3.33)		317(3.23)	
	234(3.85)	330(0.02)	293(3.42)	318(0.10)	246(3.81)	365(0.13)
	210(4.45)		241(3.86)		208(3.69)	
Ether	294(3.55)		296(3.5)		320(3.37)	
	239(3.79)	350(0.06)	242(3.92)	322(0.09)	248(3.96)	381(0.17)
	212(4.35)		219(4.47)		208(3.79)	
Acetonitrile	295(3.66)		298(3.46)		321(3.25)	
	240(3.90)	352(0.02)	243(3.89)	326(0.02)	248(3.84)	388(0.07)
	208(4.55)		217(4.49)		200(4.20)	
Methanol	294(3.52)		293(3.36)		308(3.27)	
	239(3.79)	355(0.02)	243(3.85)	332(0.01)	243(3.96)	395(0.07)
	210(4.48)		214(4.48)		204(4.05)	

..contd.

Table 4.7 (contd.)

1	2	3	4	5	6	7
Water (pH 8)	288(3.53) 232(3.88) 205(4.57)	-	289(3.30) 238(3.86) 210(4.51)	-	303(3.28) 239(3.90) 198(4.33)	-
Monocation (pH 3.5)	280(3.24) 223(3.83) 194(4.16)	335(0.05)	283(3.24) 232(3.85) 205(4.08)	340(0.03)	284(3.08) 234(3.87) 201(4.01)	345(0.02)
Dication (H <sub>2</sub> O-8)	261(2.16) 257(2.32) 252(2.36) 247(2.31) 237(2.10) 207(2.98)	275	262(2.0 ) 258(2.19) 253(2.22) 248(2.15) 238(1.92) 208(2.99)	275	263(2.27) 258(2.4 ) 253(2.35) 244(2.26) 236(2.13) 206(3.0 )	275

Table 4.8. Stokes Shifts ( $\text{cm}^{-1}$ ) Observed for Phenylenediamines in Different Solvents at Various pH.

	oPA	mPA	pPA
Cyclohexane	4180	2625	4200
Ether	5440	2730	5000
Acetonitrile	5480	2940	5380
Methanol	5900	4070	7200
Water	—	—	—
Monocation	5860	5990	6290
Dication	1950	1800	1800

Table 4.9. Acidity Constants of Phenylenediamines in the Ground and First Excited Singlet State.

Equilibrium	$\text{pK}_a^a$	$\text{pK}_a^b$	$\text{pK}_a(S_1)^t$	$\text{pK}_a(S_1)^c$
oPA				
Dication - Monocation	1.86	1.2	-5.2	-5.2
Monocation - Neutral	4.65	4.5	4.3*	2.4
mPA				
Dication - Monocation	1.89	2.0	-6.9	-3.8
Monocation - Neutral	4.86	4.8	4.9*	3.1
pPA				
Dication - Monocation	2.54	2.4	-5.1	-5.9
Monocation - Neutral	6.11	6.1	6.2*	1.3

<sup>a</sup>from Ref. 232; <sup>b</sup>present study; <sup>t</sup>by fluorimetric titration;

<sup>c</sup>Förster cycle using absorption data; \* apparent value.

(from  $\sim 8$ , depending on particular diamine) the absorption spectra of all the diamines are blue shifted and on further increase of acid concentration, these bands are further blue shifted to give structured spectra. These two changes can be assigned to the formation of a monocation by protonating one of the amino groups and a dication by protonating both of the amino groups. This assignment of the spectral changes are based on their spectral similarities with those of aniline<sup>230</sup> and benzene<sup>228</sup> respectively. The absorption spectra of oPA and mPA start red shifting after  $H_{-15}$  and that of pPA after pH 13. This is in agreement with the deprotonation of the amino group at this basic condition.<sup>223</sup>

The neutral species of all the diamines are non-fluorescent in water. The fluorescence spectral behaviour of all the species are the same as those in the  $S_0$  state. That is, the species formed by protonating the lone pair of the amino groups are assigned to monocation and dication. These assignments have been made on the basis of their spectral resemblance with those of aniline<sup>230</sup> and benzene<sup>228</sup> respectively. The fluorescence spectra of the dication of all the diamines are not structured as observed for benzene molecule, and it might be due to stronger interaction with such a highly ionic medium. No fluorescence is observed from the monoanion even upto  $H_{-17}$ , which is consistent with the earlier results that monoanions formed by deprotonating the amino groups are generally non-fluorescent<sup>179</sup> with a few exceptions.<sup>231</sup>

#### 4.3.3 Dissociation Constants

Dissociation constants in  $S_0$  state of the dication-monocation and monocation-neutral equilibria have been calculated spectrophotometrically and are compiled in Table 4.9. The values are in good agreement with the literature values within the experimental errors.<sup>232</sup> The  $pK_a$  value of monocation neutral equilibria of mPA is almost the same and that of oPA is little smaller than that of aniline (4.66).<sup>233</sup> This can be rationalized as follows: Since the amino group is an electron donating group and it is o- and p- directing, it will not alter the electron densities at the other amino group in the case of mPA but the expected increase in charge densities of the  $-NH_2$  group of oPA may be counter balanced by the steric hindrance. The same behaviour has also been noticed in the case of 2,3-diaminonaphthalene as explained in the previous section. The high basicity of pPA as compared to aniline and other phenylenediamines is due to the presence of the two amino groups in the para position that favours the exchange of charge densities between the amino groups. This behaviour is similar to that noticed for the first protonation reaction of 2,7-diaminofluorene where both the amino groups are in para extended conjugated position. The monocations of the isomeric diamines are less basic, as expected, than aniline because of the presence of  $-NH_3^+$  group.

The  $pK_a^*$  values for the above mentioned equilibria have been calculated fluorimetrically and by employing Förster cycle method. The values are reported in Table 4.9. The values for the monocation and neutral equilibria have been calculated from the formation curve of the monocations, as the neutral species are non-fluorescent. The

fluorimetric titrations (shown in Fig. 4.14) have given the ground state  $pK_a$  values. This behaviour is anomalous and not commonly observed during the protonation of aromatic amines. In general, proton-induced fluorescence quenching of the neutral amine is observed prior to its protonation. The prime condition for this fluorescence quenching is that the emitting state should be of charge transfer in character. The effect of solvents on the fluorescence spectra of these amines show that emitting states are of charge transfer type and still no quenching is noticed. This can be further confirmed from the ground state  $pK_a$  value observed from the fluorimetric titration. If this quenching is observed, the calculated  $pK_a$  would be different from the ground state  $pK_a$  value. The similar results have also been observed for 4-(9-anthryl)-N,N'-dimethylaniline<sup>130</sup> and 2,3-diaminonaphthalene (section 4.2.4 and 4.2.5). In these cases it has been proved that the absence of excited state equilibrium between the monocation and neutral species is because of the short lifetimes of the conjugate acid-base pair. The similar explanation can also be given in case of the first protonation of the phenylenediamines. Because of this, fluorescence intensities of monocations reflect the ground state concentration of the species in this pH range. Förster cycle method using only the absorption data (as neutral is non-fluorescent) has indeed revealed that amino groups become stronger acids on excitation.

In the dication-monocation equilibrium, the fluorescence of monocation is quenched in the pH region where the dication is present in the  $S_0$  state and not in the  $S_1$  state. The dications start emitting

only below  $H_0 - 4$ . This decrease of monocation fluorescence without an appearance of the dication fluorescence is attributed to the proton-induced fluorescence quenching. The  $pK_a^*$  value, obtained from the formation curve of the dication indicate that  $-NH_3^+$  group is a stronger acid in  $S_1$  state than in  $S_0$  state, consistent with our earlier results. The  $pK_a^*$  values calculated from the Förster cycle method using absorption and fluorescence data do not agree with each other. This is because of, (i) difficulty in locating the O-O transition of two species and (ii) the solvent relaxation for the monocation in the  $S_1$  state is very large in comparison to that observed for the dication. This can be seen from the Stokes shift observed for the monocation ( $\approx 5900 \text{ cm}^{-1}$ ) and the dication ( $\approx 1900 \text{ cm}^{-1}$ ).

#### 4.3.4 Proton-Induced Fluorescence Quenching

Like in DAF and DAN, the lack of correspondance between the decrease and increase in the fluorescence intensities of the monocation and dication respectively is attributed to proton-induced fluorescence quenching of the monocations. The  $k_q \tau$  values have been obtained from Stern-Volmer plots (shown in Fig. 4.15). The natural lifetimes have been calculated from appropriate absorption bands and corrected fluorescence spectra of the monocations by employing Strickler-Berg relation.<sup>202</sup> To the first approximation, assuming that the monocations of diamines behave like aniline, the  $\tau_{FM}$  for the monocation of oPA, mPA and pPA (35 ns, 39 ns and 45 ns respectively) are comparable with the experimentally obtained  $\tau_{FM}$  of aniline

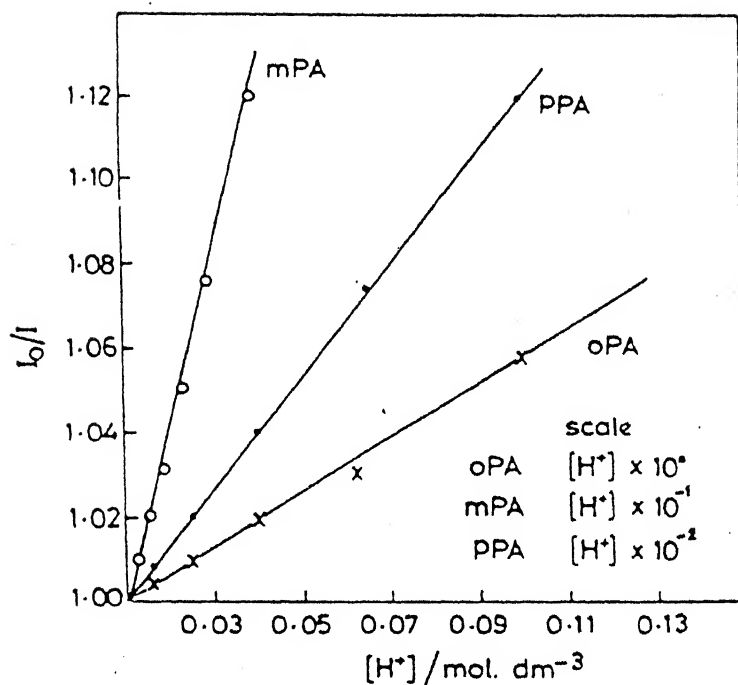


Fig.4.15 Stern-Volmer plots for proton-induced fluorescence quenching of the monocation species of o-, m-, and p-phenylenediamines.

Table 4.10. Proton Transfer Kinetic Data of Monocations of Phenylenediamines

Compound	$k_q \tau$	$\tau_{FM}$	$\phi_f$	$\tau$	$k_q$
oPA	0.63	35	0.05	1.7	$3 \times 10^8$
mPA	45	39	0.03	1.1	$4 \times 10^{10}$
pPA	128	45	0.02	0.9	$2 \times 10^{11}$



in ethanol.<sup>230</sup> The difference in  $\tau$  is due to the difference in their quantum yields. The smallest value of  $\tau (= \tau_{FM} \phi_f)$  for pPA is due to large interaction with the solvent molecules and it can be manifested by a large Stokes shift observed for this species. A large increase in  $k_q$  values (reported in Table 4.10) from oPA and pPA can not be rationalized from our data, however it may be speculated that steric factor may be playing a role in the proton-induced fluorescence process. Though the Stokes shift observed for the monocation of pPA is maximum but do not differ so much from other monocation if energy of the state has to do anything for this quenching.

This study has revealed that, (i) the amino groups of pPA and oPA are not coplanar with benzene ring, (ii) a large value of  $pK_a$  for the monocation-neutral equilibrium of pPA is due to the increased charge densities of the amino groups as they are in conjugated positions. But the low value for oPA shows the role of the steric factor. Fluorimetric titration curves have indicated that the lifetimes of the monocation-neutral pair are quite short to allow the establishment of acid-base equilibria in the excited singlet state.

#### 4.4 9,10-DIAMINOPHENANTHRENE<sup>a</sup>

##### 4.4.1 Solvent Effect

Fig. 4.16 illustrates the absorption and fluorescence spectra of 9,10-diaminophenanthrene (DAP) in different solvents. The absorption spectral data reported in Table 4.11 clearly indicate that the

---

<sup>a</sup>R. Manoharan and S.K. Dogra, communicated.

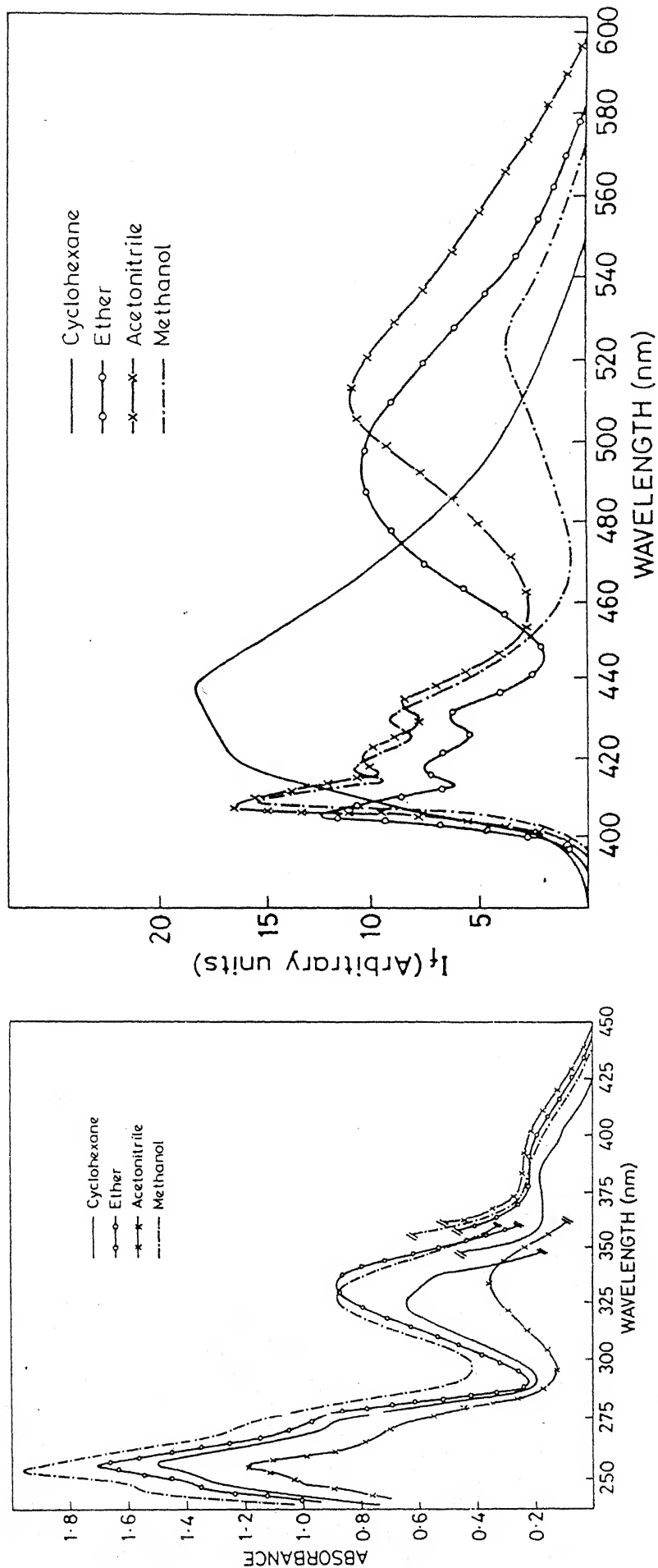


Fig.4.16 Absorption (left panel) and fluorescence (right panel) spectra of 9,10-diaminophenanthrene in different solvents.

Table 4.11. Absorption and Fluorescence Maxima (nm),  $\log \epsilon_{\max}$  and  $\phi_f$  of 9,10-Diaminophenanthrene in Different Solvents and at Various Proton Concentrations.

Solvent/ species	$\lambda_a (\log \epsilon_{\max})$			$\lambda_f (\phi_f)$	
	2	3	4	5	6
Cyclohexane	408 384	333 324	274 260 253	422, 438 (0.07)	—
Ether	— 395 (3.15)	333 (4.05)	277 (4.23) 270 (4.20) 259 (4.32)	431 418 405	— 492 (0.04) 485 <sup>a</sup>
Acetonitrile	400 (3.10)	332 (4.05)	274 (4.27) 270 (4.36) 258 (4.53)	434 420 408	— 511 (0.02) 490 <sup>a</sup>
Methanol	388 (2.9 )	328 (3.91)	275 (4.16) 270 (4.22) 256 (4.30)	430 416 406	— 522 (0.01) 475 <sup>a</sup>
Water pH 7 (Neutral)	383 (3.13)	323 (3.96)	275 (4.21) 260 (4.45)	— —	— 448 <sup>a</sup>

..contd.

Table 4.11(contd.)

1	2	3	4	5	6
Monocation	421	303	252		430(0.02)
pH 1	408	(3.35)	(4.36)	—	400,425 <sup>a</sup>
	396				410 <sup>b</sup>
	385				405 <sup>c</sup>
	374				
	360				
Dication	348	299	252	—	390
H <sub>o</sub> -6	(3.15)	(3.56)	(4.25)		368(0.31)
	337	288	246		354
	(3.22)	(3.53)	(4.19)		343,359,380,390 <sup>a</sup>
	332	278			
	(3.26)	(3.67)			
		265			
		(3.91)			
Monoanion	395	330	248	—	410
(H <sub>16</sub> )		304	227		

a = 77 K; b = cyclohexane + 0.5%(v/v) trifluoroacetic acid;

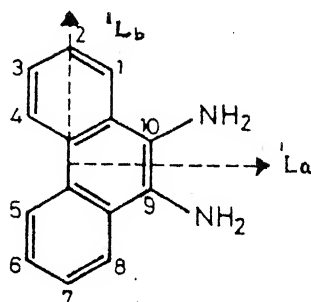
c = 0.75M H<sub>2</sub>SO<sub>4</sub> in methanol.

spectrum consists of three band systems. The long wavelength band centered at 400 nm is broad and less structured (with vibrational frequency of  $730 \pm 30 \text{ cm}^{-1}$  in cyclohexane) as compared to that of phenanthrene.<sup>234</sup> The short wavelength band which is centered at 275 nm is structured in all the solvents employed. The shifts observed in the absorption spectra, on increasing the polarity of the solvents are the same as noted for other diamines studied.

Fluorescence spectrum of DAP shows dual fluorescence in all the solvents except cyclohexane where only one band is observed. This dual fluorescence was verified by subjecting DAP into rigorous purification (vacuum sublimation and repeated recrystallization) and purging the solution with oxygen free nitrogen. The normal Stokes shifted band is nicely structured with the vibrational frequency of  $720 \pm 20 \text{ cm}^{-1}$  and the largely Stokes shifted fluorescence is a broad band. As one goes from cyclohexane to water, the abnormal Stokes shifted band gets red shifted whereas the normal Stokes shifted band remains unaffected. The decrease in fluorescence quantum yield of the abnormal Stokes shifted band is more than that observed for short wavelength fluorescence band. DAP is non-fluorescent in water.

The absorption spectrum of phenanthrene comprises of three band systems, that is, a long axis polarised, structured band ( $\alpha$  band, vibrational frequency  $705 \text{ cm}^{-1}$ ) at 340 nm, a moderately structured short axis polarised band (para, vibrational frequency  $1320 \text{ cm}^{-1}$ ) at 290 nm and a composite short wavelength band ( $\beta$ ) near 250 nm. The positions of amino groups in DAP (along short axis of the molecule as shown below) are such that, these groups will perturb the para

band more profoundly than  $\alpha$  and  $\beta$  bands. From the data of Table 4.11, it is concluded that the long wavelength absorption band is



Scheme 4

still the  $\alpha$  band for DAP. This is based on the following results (i) The molar extinction coefficient and the vibrational structure ( $1.2 \times 10^3 \text{ dm}^3 \text{ mol}^{-1} \text{ cm}^{-1}$ ,  $730 \pm 30 \text{ cm}^{-1}$  respectively) are close to those of phenanthrene ( $0.4 \times 10^3 \text{ dm}^3 \text{ mol}^{-1} \text{ cm}^{-1}$  and  $705 \text{ cm}^{-1}$  respectively). The increase in the molar extinction coefficient of  $\alpha$  band of phenanthrene in DAP is because of the presence of amino groups which increase the dipolar length of the transition moment integral of this transition. (ii) Though the difference between the  $\alpha$  band and para bands is  $\sim 56 \text{ nm}$  for phenanthrene spectrum, it is clear from the Fig. 4.16 that 400 nm band appear as shoulder to 335 nm band system. The loss in the vibrational structure of  $\alpha$  and para bands indicates the increased interaction of amino groups with phenanthrene moiety. Spectral shifts can be rationalized as has been done for other diamines.

From the data of Table 4.11, the normal Stokes shifted fluorescence band is assigned to a transition from <sup>1</sup>L<sub>b</sub> state. This is because the vibrational frequency observed for this emission ( $\sim 750 \text{ cm}^{-1}$ ) agrees with that noticed in the absorption spectra. This mirror image relationship between the long wavelength absorption band and

the short wavelength fluorescence band shows that the states involved in the absorption and fluorescence spectra are the same ( $^1L_b$ ). More evidences for this assignment will be discussed below. We assign the abnormally Stokes shifted long wavelength fluorescence band to an emission from  $^1L_a$  state. This assignment is based on the following facts: (i) The fluorescence excitation spectra have been recorded (shown in Fig. 4.17) in ether and acetonitrile as solvents. The fluorescence excitation spectra recorded at long wavelength possess a small peak at 400 nm, but the vibrational progression present in the absorption band is absent and the most intense band is near 350 nm, agreeing with  $^1L_a$  transition. On the other hand the fluorescence excitation spectrum recorded at short wavelength band is vibrationally resolved, with similar vibrational frequency as noticed in the long wavelength absorption spectrum. This spectrum does not contain the 350 nm band which arises out of  $^1L_a$  transition. The mixing of the small absorbance of 400 nm band in the former fluorescence excitation spectrum might be due to the mixing of these two transitions in the absorption spectrum of DAP. (ii) Electronically excited  $^1L_a$  state is generally more polar than the  $^1L_b$  state. The preferential red shift and the decrease in the fluorescence intensity of the long wavelength fluorescence band over the short wavelength one, on increasing the solvent polarity demonstrates that the former band originates from the  $^1L_a$  state. (iii) DAP in cyclohexane - TFA medium also reveals the more polar nature of the  $^1L_a$  state. The cyclohexane solution containing, TFA upto 0.02 % (v/v) produce a blue shift in the  $^1L_a$  band but  $^1L_b$  band gets red shifted as observed in the absorption

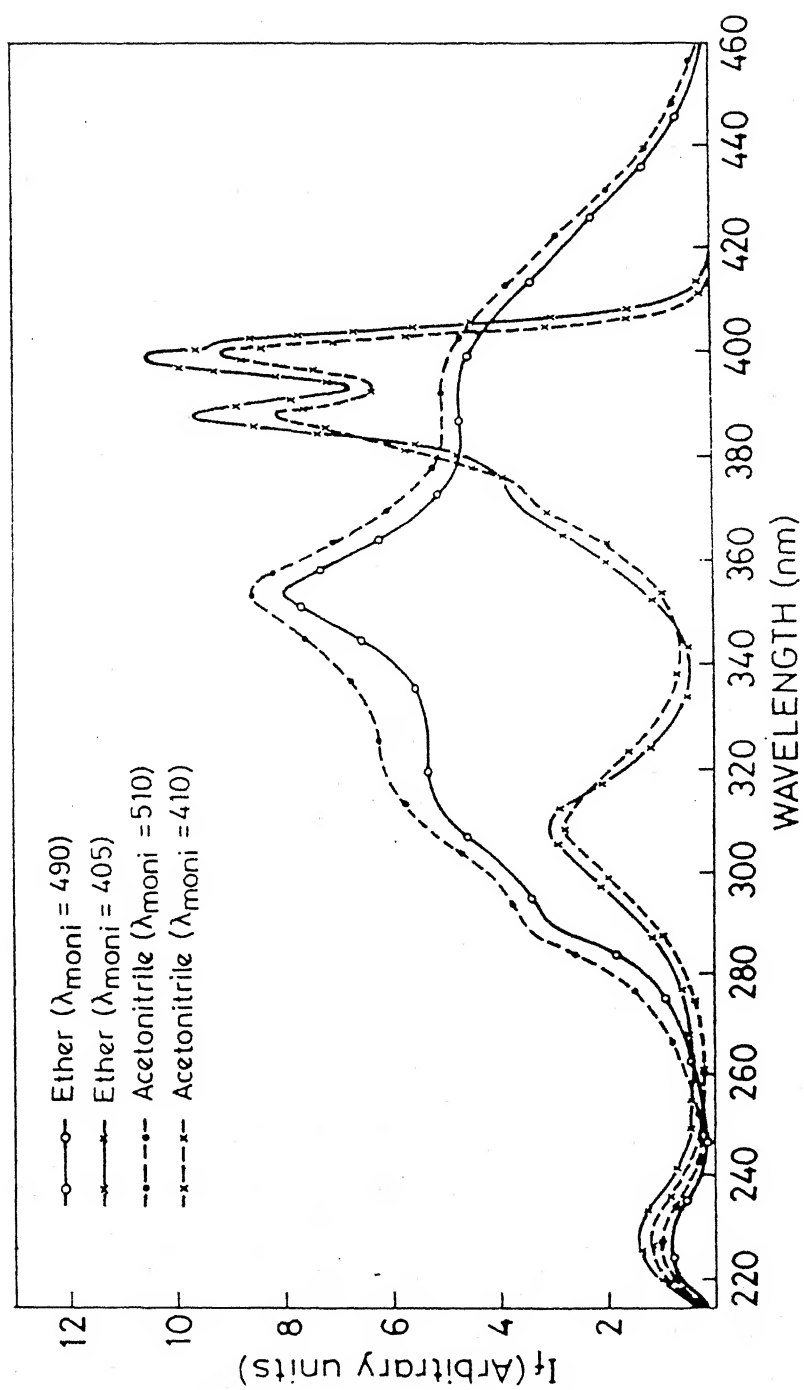


Fig.4.17 Excitation spectra of 9,10-diaminophenanthrene in ether and acetonitrile.



spectrum of DAP in aqueous  $\text{H}_2\text{SO}_4$  solution. But the fluorescence spectrum contains both the band systems and the red shift in the abnormal Stokes shifted fluorescence band increased with increase in TFA concentration upto 0.02% (v/v) (Table 4.12). This is because TFA makes cyclohexane more polar and stabilizes the  $^1\text{L}_a$  state more than  $^1\text{L}_b$  one. This is further manifested from the absence of fluorescence in cyclohexane + 0.2%TFA medium, which may have a similar polarity and hydrogen bond forming capacity as water.

#### 4.4.2 Effect of Acid Concentration

Fig. 4.18 represents the absorption and fluorescence spectra of the various prototropic species of DAP at different acid concentration and the relevant data are presented in Table 4.11. With the decrease of pH ( $\sim 2$ ), the long wavelength absorption band become structured and red shifted, whereas the middle bands (303 nm and 252 nm) follow blue shift to match with that of 9-phenanthrylamine.<sup>125a</sup> This change is due to the formation of monocation by protonating one of the amino groups. With further increase in acid concentration, absorption and fluorescence spectra are highly blue shifted and their profiles exactly resemble those of phenanthrene.<sup>223</sup> These changes in  $S_0$  and  $S_1$  are due to the formation of dication as a result of protonating both of the amino groups of DAP. In the high basic region above pH 14, a red shift in the absorption spectrum of DAP is observed and continued upto  $\text{H}_-17$ , indicating that the neutral-mono-anion equilibrium is not complete at this highly basic medium. A new fluorescence band ( $\sim 410$  nm) appeared at  $\text{H}_-15$ , attain maximum in intensity at  $\text{H}_-17$ .

Table 4.12. Absorption and Fluorescence Band Maxima of DAP in Cyclohexane + Different Amount of Trifluoroacetic Acid (TFA).

% TFA (v/v)	$\lambda_a$ (nm)			$\lambda_f$ (nm)	
0.00	408	333	274	438	—
	384	324	268	422	
			253		
0.001	408		287	442	
	396	309	277	430	494
	385			416	
	375			410	
	365				
	348				
0.002	408		288	442	
	396	312	277	430	502
	385			416	
	375			410	
	—				
	341				
0.02	408		286	430	502
	396	320		416	
	385	300		400	
	375				
	350				
	341				
0.2	357			Nonfluorescent	
	340	325			
		312			
1.0				410	

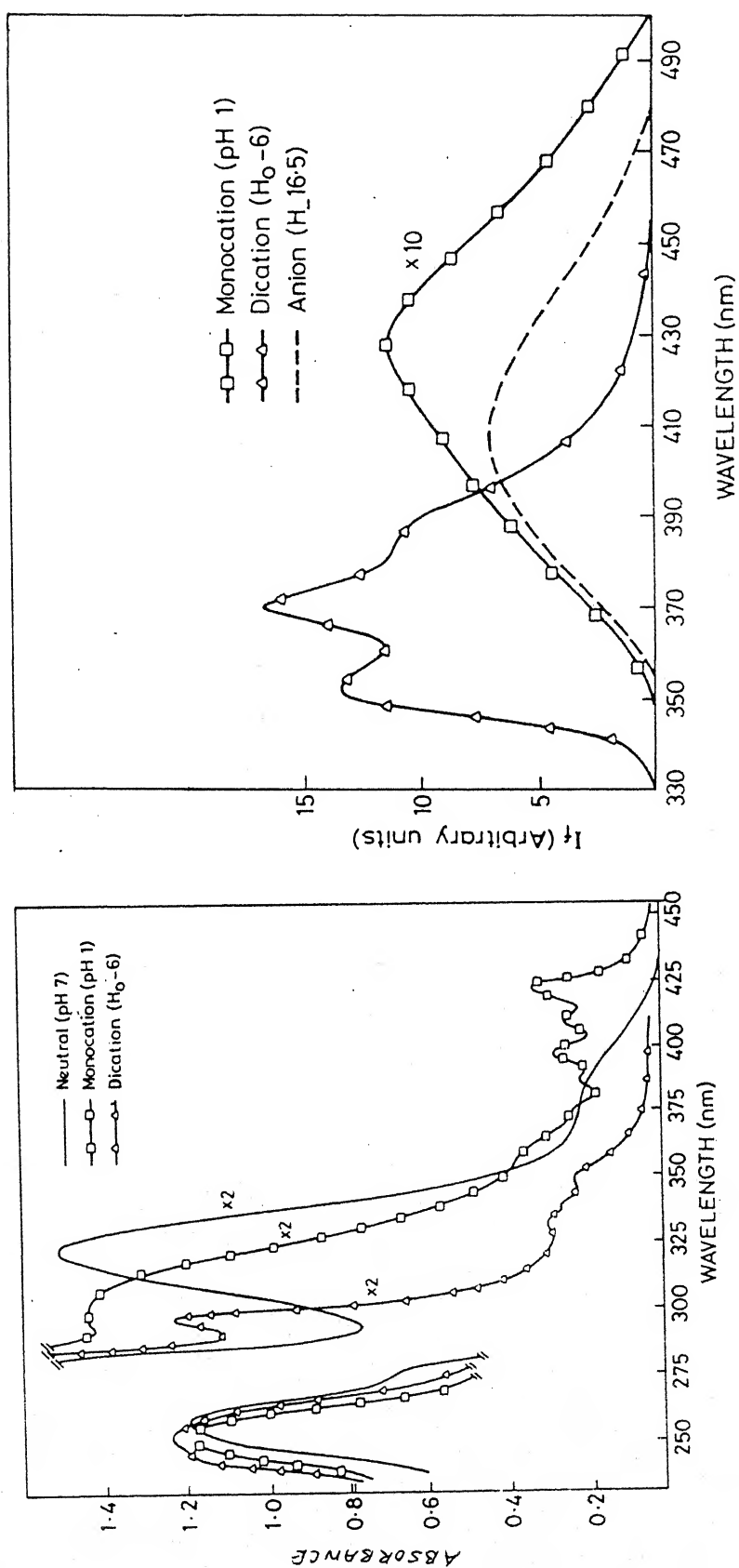


Fig.4.18 Absorption (left panel) and fluorescence (right panel) spectra of different prototropic species of 9,10-diaminophenanthrene.

Similar to earlier studies on the diamino compounds, the different prototropic species of DAP can be identified by the changes observed in the spectral features and comparing the spectral characteristics of these species with the prototype molecules. Though the formation of the monocation is confirmed in the  $S_0$  state for DAP, the appearance of a red shifted, structured long wavelength absorption band could not be attributed from our results. Further this absorption band system also does not resemble with that of 9-aminophenanthrene.<sup>235</sup> Since the neutral species as well as the monocation of DAF is non-fluorescent in aqueous medium, the fluorescence band observed at  $H_{15}$  is difficult to explain. The non-fluorescent nature of  $-NH^+$  species is a common feature with few exceptions.<sup>231</sup> However, the 410 nm fluorescence band can be assigned to dianion formed by deprotonating one of the amino groups and the ring hydrogen atom. This is based on following facts: (i) Amino group is stronger acid in  $S_1$  state as compared to an aromatic proton and the  $pK_a^*$  value generally observed is  $\sim 13$ . (ii) A similar fluorescence band is also observed for 9-phenanthrylamine,<sup>122d,125a</sup> 1-, 2-naphthylamines,<sup>227,235</sup> N,N'-dimethyl 1-,2-naphthylamines<sup>227</sup> and DAN and (iii)  $pK_a^*$  value for this reaction is 14.5, which closely resembles with that observed for 2-naphthylamine<sup>235</sup> and N,N'-dimethyl-2-naphthylamine.<sup>227</sup>

#### 4.4.3 Acidity Constants

The  $pK_a$  values of various prototropic reactions are listed in Table 4.13. The  $pK_a$  value (3.5) for the monocation-neutral equilibrium is much lower than that generally observed for aromatic amines.

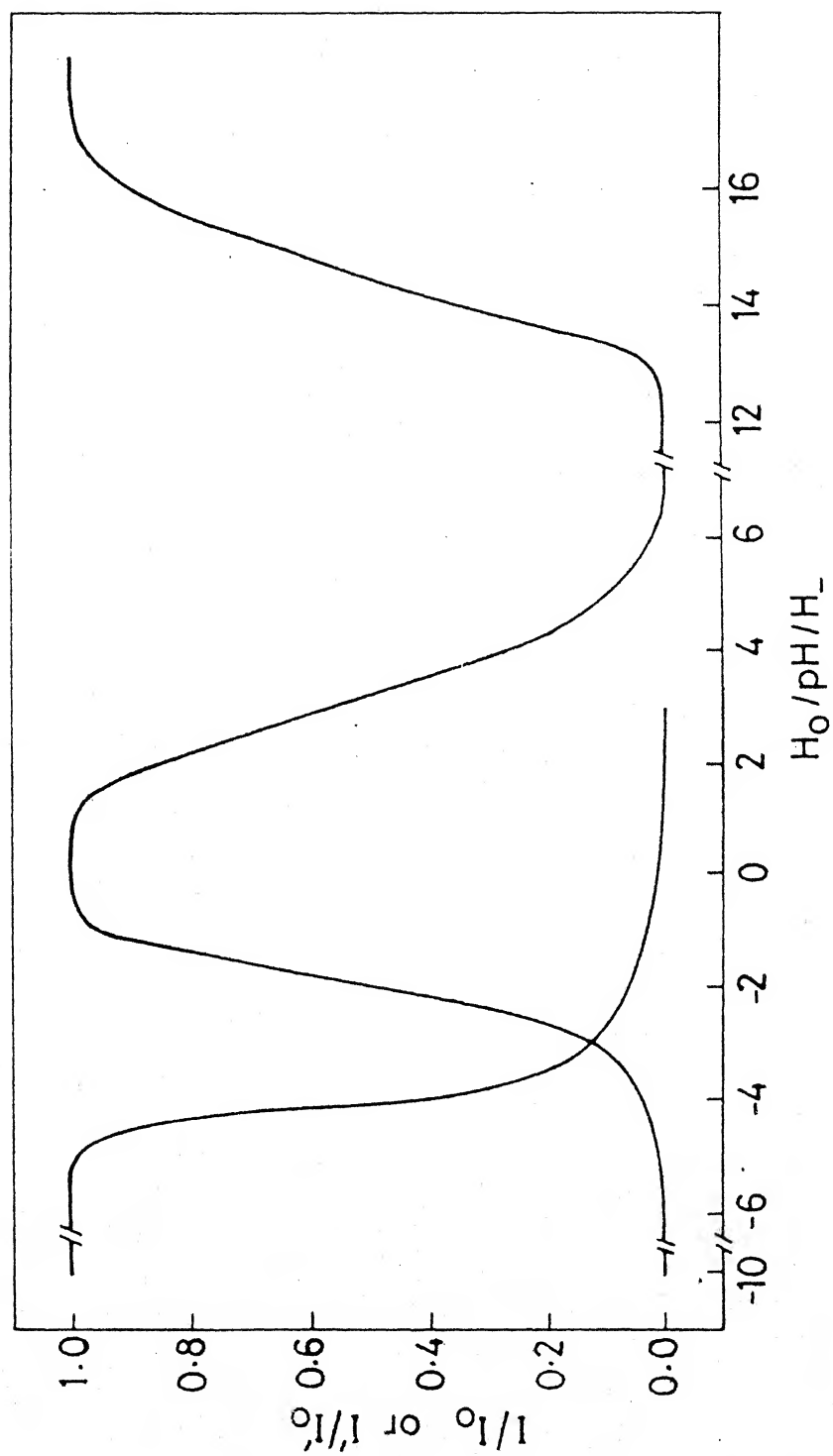


Fig.4.19 Fluorimetric titration curves for different prototropic species of 9,10-diaminophenanthrene.

Table 4.13.  $pK_a$  Values of Various Prototropic Reactions in  $S_0$  and  $S_1$  States.

Equilibrium	$pK_a$	$pK_a^*$		
		abs	flu	ft
Dication - Monocation	0.25	-10.2	-4.7	-4.2
Monocation- Neutral	3.5	8.4	-	3.3 <sup>a</sup>
Monoanion - Dianion	>16	-	-	14.5

$pK_a^*$  values using Förster cycle method and absorption and fluorescence data.

ft = fluorimetric titration.

a = apparent value.

But this value is equal to that of DAN (section 4.2.3) and oPA (section 4.3.3), indicating that steric factors might be playing a role in their protonation reactions. Similar is the case for dication-monocation equilibrium. The  $pK_a^*$  values have been determined with fluorimetric titrations (Fig. 4.19). The  $pK_a^*$  value for dication-monocation equilibrium shows that dication is more acidic in  $S_1$  state. The fluorimetric titration curves give the ground state  $pK_a$  value for the monocation-neutral equilibrium, indicating that prototropic equilibrium is not established within the short lifetimes of the acid-base pairs in the excited state. Nevertheless, the  $pK_a^*$  value calculated by Förster cycle method using low temperature (77 K) data has shown that ammonium ion becomes stronger acid on excitation in  $S_1$  state.

The lack of response between the decrease and increase in the fluorescence intensities of monocation and dication is attributed to the proton-induced fluorescence quenching. As it has been done for other diamines, the quenching rate constant,  $k_q$  was calculated from Stern-Volmer constant,  $K_{sv}$  (obtained from the plot 4.20) and the lifetime of the monocation. The natural lifetime was calculated by using an appropriate absorption envelope and the corrected fluorescence spectra. The quenching rate constant was found to be  $2 \times 10^7 \text{ dm}^3 \text{ mol}^{-1} \text{ s}^{-1}$ . This very low value as compared to that for the neutral amine is expected because of the presence of a positive charge on the monocation.

The following conclusion are made from the above study:

(i) Dual fluorescence is observed in polar solvents. Large Stokes

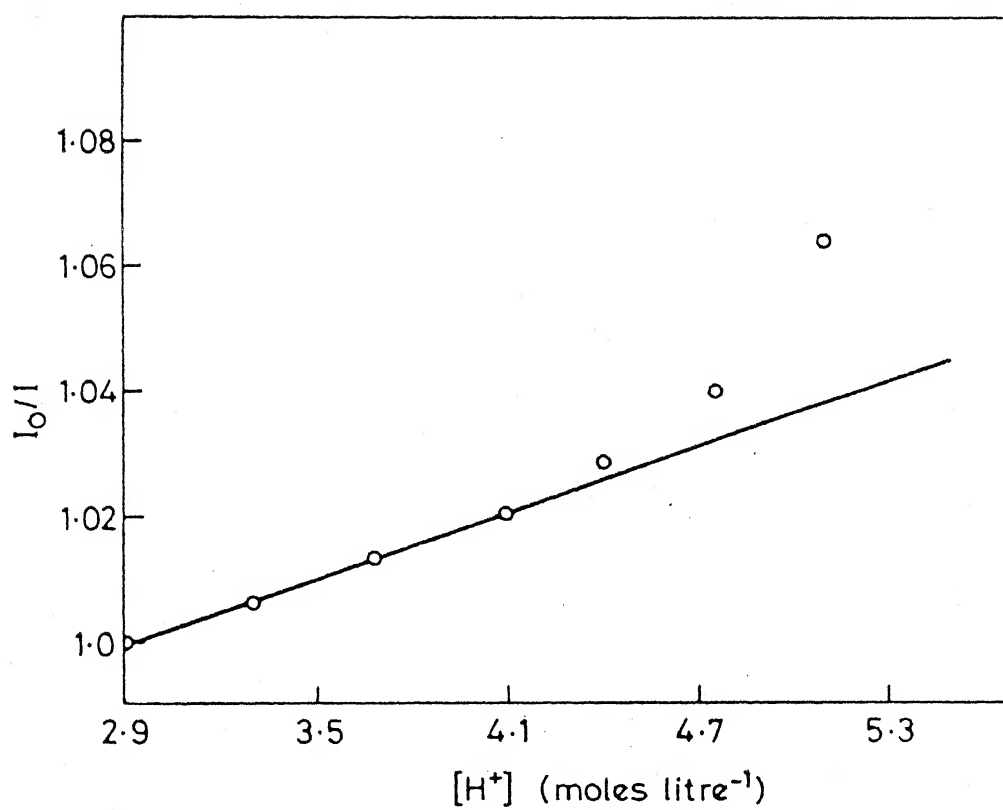


Fig.4.20 Stern-Volmer plot for proton-induced fluorescence quenching of monocation species of 9,10-diaminophenanthrene.



shifted band originates from  $^1L_a$  state and the normal Stokes shifted band from  $^1L_b$  state. (ii) Similar to other diamines the prototropic equilibrium is not established in  $S_1$  state might be due to the shorter lifetimes of the conjugate acid-base pair. (iii) Smaller value of  $k_q$  observed for the proton-induced fluorescence quenching of monocation is due to the presence of positive charge on the molecule.

## CONCLUSIONS

In the chapters III and IV, the effects of solvents and acid concentration on the absorption and fluorescence spectra of substituted fluorenes, 2,7-diaminofluorene and a few structurally related diamines have been discussed. Based on the above study, the following conclusions have been drawn.

- (i) There is no significant interaction of the methyl group at position-1 and  $-\text{CH}_2\text{OH}$  group at position-9 with the fluorene ring. These molecules undergo proton-induced fluorescence quenching similar to naphthalene analogues. Prototropic equilibrium between the monocation-neutral species is not established during the lifetimes of the conjugate acid-base pairs. This indicates that the rate of protonation is slower than the rate of fluorescence decay.
- (ii) Except 2-fluorenealdehyde, 2-acetylfluorene and 2-benzoylfluorene,  $\pi \rightarrow \pi^*$  is the lowest energy transitions in all the fluorene derivatives studied. In the former set of molecules,  $n \rightarrow \pi^*$  is the lowest energy transition in non-polar and polar but aprotic solvents. But in water,  $\pi \rightarrow \pi^*$  is the longest wavelength transition. Similar to earlier results the substitution of H atom of  $-\text{C} \begin{smallmatrix} \nearrow \text{O} \\ \searrow \text{H} \end{smallmatrix}$  group by  $-\text{OH}$ ,  $-\text{OCH}_3$  and  $-\text{NH}_2$  group shifts the  $n \rightarrow \pi^*$  transition to blue region.
- (iii) The substituents ( $-\text{C} \begin{smallmatrix} \nearrow \text{O} \\ \searrow \text{R} \end{smallmatrix}$ ,  $\text{R} = -\text{OH}$ ,  $-\text{OCH}_3$ ,  $-\text{NH}_2$ ) at 1- and 4-positions of fluorene are better conjugated in the  $\text{S}_1$  state

than in the  $S_0$  state i.e. the coplanarity of the  $-\overset{\text{O}}{\underset{\text{OR}}{\text{C}}}=\text{O}$  group with the fluorene ring increases upon excitation. The present study indicates that 1- substituents seem to be better conjugated than 4-substituents because of the possible intramolecular hydrogen bonding between the 1- substituent and hydrogen atom of the methylene group at position-9. The lowest energy transition is a mixture of long and short axes polarised transitions in these molecules.

The same substituents at position-2 of fluorene are non-planar in  $S_0$  and  $S_1$  states in non-polar solvents. But these groups attain coplanarity in polar and protic solvents. The lowest energy transition is long axis polarised one.

In the case of fluorene-9-carboxylic acid, the  $\pi$ -electronic interaction between the substituent and fluorene ring is negligibly small, so long 9-methylene group is not deprotonated.

- (iv) Amides follow  $H_A$  acidity scale, 2-fluorenealdehyde, 2-acetylfluorene and 2-benzoylfluorene follow benzophenone acidity scale, whereas all other molecules follow the Hammett's acidity scale for the prototropic reactions. The relation between the Hammett's  $H_0$  function and  $H_A$  has revealed that difference between the two acidity scales is because of the different hydration requirements of the prototropic reactions of the carboxamides relative to the hydration requirements of the dissociations of the primary amines used as indicators to establish the  $H_0$  scale.

- (v) The site of protonation in amides is the carbonyl oxygen and the medium effect is observed on the absorption spectrum of monocation.
- (vi) The dissociation constants, determined in  $S_0$  and  $S_1$  states demonstrate that  $-\text{C} \begin{smallmatrix} \nearrow \text{O} \\ \searrow \text{R} \end{smallmatrix}$  group becomes more basic on excitation.
- (vii) All the diamines in  $S_0$  state act as proton donors in polar and aprotic solvents but proton acceptors in the hydroxylic solvents, whereas in  $S_1$  state, diamines act as proton donors in all the solvents. These groups become more acidic upon excitation to  $S_1$ .
- (viii) Fluorimetric titration for monocation-neutral equilibrium of diamines give ground state  $\text{pK}_a$  values. Proton-induced fluorescence quenching is observed for monocation prior to the formation of dication.
- (ix) The monocation of 2,7-diaminofluorene experiences a greater solvent relaxation than the neutral species. In case of 2,3-diaminonaphthalene, both the amino groups are twisted with respect to the naphthalene moiety. Lifetime measurements for the neutral 2,3-Diaminonaphthalene have indicated that the rate of proton-induced fluorescence quenching of neutral species is less than that of its radiative decay. The similar study on its monocation indicates that the proton-induced fluorescence quenching is static in nature.
- (x) The  $-\text{NH}_2$  groups in o- and p-phenylenediamines are non-coplanar with respect to benzene ring, both in  $S_0$  and  $S_1$  states.

- (xi) Dual fluorescence is observed for 9,10-diaminophenanthrene. The abnormally large Stokes shifted fluorescence is from a more polar  $^1L_a$  state and the normal fluorescence is from a relatively less polar  $^1L_b$  state.
- (xii) The  $pK_a$  values for the diamines, where the two amino groups are close to each other, are less than that for the similar reaction of mono aromatic amines. This has been rationalized on the basis of steric factors.

### FUTURE PROSPECTS

In the present study, only a qualitative assignment of the coplanarity of functional groups with the parent ring has been made. But with the advent of jet cooled spectroscopy, actual geometry of these molecules can be explored both in  $S_0$  and  $S_1$  states. Except for 2,3-diaminonaphthalene, for other compounds, proton-induced fluorescence quenching rate constants have been determined with the knowledge of theoretical lifetimes. An accurate value of quenching rate constants can be obtained by employing time dependent fluorescence spectroscopic methods. Further, this study will also reveal whether the fluorescence quenching is static or dynamic.  $pK_a^*$  values for the various prototropic reactions have been determined either from fluorimetric titrations or using Förster cycle method. Better and more accurate values of  $pK_a^*$  can be calculated using time dependent fluorimeters. As mentioned earlier, fluorene derivatives have tremendous significance in biology. Some of these are also used as probes in the studies of chemical carcinogenesis in mammalian cell culture. In the light of this, the above prototropic studies can be extended into biomimetic systems. Infact, little study on the use of fluorene as a probe for organized media, like micelles has been pursued. Since fluorene is used as a phosphorescent probe for polymers, the phosphorescence spectral studies on fluorene derivatives would yield fruitful results.

## REFERENCES

1. A. Jablonski, Z. Physik., 94, 38 (1935).
2. P. Seybold and M. Gouterman, Chem. Rev., 65, 413 (1965).
3. S.K. Lower and M.A. El Sayed, Chem. Rev., 66, 199 (1966).
4. H.H. Jaffe and M. Orchin, In "'Theory and Application of Ultraviolet Spectroscopy''; John Wiley: New York, (1962).
5. H. Suzuki, In "'Electronic Absorption Spectra and the Geometry of Organic Molecules''; Academic Press: New York, (1967).
6. J.N. Murrill, In "'The Theory of Electronic Spectra of Organic Molecules''; Wiley: New York, (1983).
7. J.R. Platt, J. Chem. Phys., 17, 484 (1949).
8. G.N. Lewis and M. Calvin, Chem. Rev., 39, 273 (1939).
9. E.L. Wehry, In "'Practical Fluorescence: Theory, Methods and Techniques''; Ed. George G. Guilbault; Marcel Dekker Inc: New York, (1973); pp. 90.
10. P.J. Wheatly, In "'Determination of Molecular Structure''; Clarendon Press: Oxford, (1968); pp. 80.
11. R.M. Hochstrasser, Can. J. Phys., 39, 459 (1961).
12. A.W. Jackson, J. Org. Chem., 24, 833 (1959).
13. A. Weller, J. Chem. Phys., 40, 2839 (1964).
14. J. Almlöf, Chem. Phys., 6, 135 (1974).
15. A. Warsel and M. Karplus, J. Am. Chem. Soc., 94, 5612 (1972).
16. T.R. Evans and P. Leermakers, J. Am. Chem. Soc., 89, 4380 (1967).
17. A.S. Cherkasov and K.G. Voldaikina, Bull. Acad. Sci. USSR, Phys. Ser., 27, 630 (1963).
18. R.J.W. Lefebvre, L. Radom and G.L.D. Ritchie, J. Chem. Soc. B., 775 (1968).

19. M. Kasha, Radiat. Res. Suppl., 2, 243 (1960).
20. Silvia M. de B. Costa, Antonio L. Macanita and M.J. Prieto, J. Photochem., 11, 109 (1979).
21. T. Matsumoto, M. Sato and S. Hirayama, Chem. Phys. Lett., 47, 358 (1974).
22. S. Hirayama, J. Chem. Soc. Faraday Trans I., 78, 2411 (1982).
- 23.a. T.C. Werner, In "'Modern Fluorescence Spectroscopy'"; Ed. E.L. Wehry; Vol.2, Plenum, New York (1976); Chapter 7, pp. 277.  
b. T.C. Werner and R.M. Hoffman, J. Phys. Chem., 77, 1161 (1973).  
c. T.C. Werner, T. Mathews and B. Soller, J. Phys. Chem., 80, 533 (1976).  
d. T.C. Werner, W. Hawkins, J. Facci, R. Torrisi and T. Trembath, J. Phys. Chem., 82, 298 (1978).  
e. T.C. Werner and D.B. Lyon, J. Phys. Chem., 86, 933 (1982).  
f. T.C. Werner and J. Rodgers, J. Photochem., 32, 59 (1986).
- 24.a. K. Gustav, J. Sühnel and U.P. Wild, Helv. Chim. Acta., 61, 2100 (1978).  
b. K. Gustav, J. Sühnel and U.P. Wild, Chem. Phys., 31, 59 (1978).  
c. J. Sühnel, U. Kemka and K. Gustav, J. Prakt. Chem., 322, 649 (1980).  
d. J. Sühnel, U. Kemka and K. Gustav, J. Mol. Structure, 76, 213 (1981).
25. I.B. Berlman, J. Phys. Chem., 74, 3085 (1970).
- 26.a. J. Murakami, M. Itoh and K. Kaya, Chem. Phys. Lett., 80, 203 (1981).  
b. J. Murakami, M. Itoh and K. Kaya, J. Chem. Phys., 74, 6505 (1981).  
c. H.T. Jonkman and D.A. Weirsmas, J. Chem. Phys., 81, 1573 (1984).  
d. V. Swayambunathan and E.C. Lim, J. Phys. Chem., 89, 3960 (1985).



- e. D.W. Werst, W.R. Gentry and P.F. Barbara, J. Phy. Chem., 89, 729 (1985).
  - f. D.W. Werst, W.F. Londo, J.L. Smith and P.F. Barbara, Chem. Phys. Lett., 118, 367 (1985).
  - g. D.W. Werst, A.M. Brearley, W.R. Gentry and P.F. Barbara, J. Am. Chem. Soc., 109, 32 (1987).
  - h. V. Swayambunathan and E.C. Lim, J. Phys. Chem., 91, 6359 (1987).
27. W. Rettig, Angew. Chem. Int. Ed. English., 25, 971 (1986) and references cited therein.
- 28.a. A. Burawoy, J. Chem. Soc., 1177 (1939).
- b. A. Burawoy, J. Chem. Soc., 20 (1941).
29. N.S. Byliss and E.G. McRae, J. Phys. Chem., 58, 1002, 1006 (1954).
30. M. Kasha, Disc. Faraday Soc., 9, 14 (1950).
31. H. McConnel, J. Chem. Phys., 20, 700 (1952).
32. G.J. Brealey and M. Kasha, J. Am. Chem. Soc., 77, 4462 (1955).
33. V.G. Krishna and L. Goodman, J. Am. Chem. Soc., 83, 2042 (1961).
34. P. Pringsheim, In "'Fluorescence and Phosphorescence'"; Interscience Publication Inc : New York, (1949).
35. Th. Förster, In "'Fluoreszenz Organischer Verbindungen'"; Vandenhoeck and Ruprecht: Gottingen, (1951).
36. B.L. Van Duuren, Chem. Rev., 63, 325 (1963).
37. G.C. Pimental, J. Am. Chem. Soc., 79, 3323 (1957).
38. N. Mataga and Tsuno, Bull. Chem. Soc. Jpn., 30, 368 (1957).
39. N. Mataga and Y. Kaifu, Mol. Phys., 7, 137 (1964).
40. A. Weller, In "'Progress in Reaction Kinetics'", Vol I; Pergamon Press: London, (1961).
41. H. Inaue, M. Hida, N. Nakashima and K. Yoshihara, J. Phys. Chem., 86, 3184 (1982).

42. P.F. Barbara, L.E. Brus and P.M. Rentzepis, J. Am. Chem. Soc., 102, 2786 (1980).
43. S.R. Flom and P.F. Barbara, J. Phys. Chem., 89, 4489 (1985).
44. P.F. Barbara, S.D. Rand and P.M. Rentzepis, J. Am. Chem. Soc., 103, 2156 (1981).
45. S.P. Velsko and G.R. Flemming, J. Chem. Phys., 76, 3553 (1982).
46. S.Y. Hou, W.M. Hetherington, G.M. Kovenowski, and B.K. Eisinger, Chem. Phys. Lett., 68, 282 (1982).
47. P.F. Barbara, L.E. Brus and P.M. Rentzepis, Chem. Phys. Lett., 69, 447 (1980).
48. G.R. Seely and E.R. Shaw, J. Photochem., 28, 559 (1985).
49. L. Onsager, J. Am. Chem. Soc., 58, 1486 (1936).
50. P. Suppan and C.C. Tsiamis, Spectrochim. Acta., 36A, 971 (1950).
51. Y. Ooshika, J. Phys. Soc. Jpn., 9, 594 (1954).
- 52.a. E. Lippert, Z. Elektrochem., 61, 962 (1957).  
b. E. Lippert, Z. Naturforsch, A., 10A, 541 (1955).  
c. E. Lippert, Ber. Bunsenges, Phys. Chem., 61, 562 (1957).
- 53.a. E.G. Mcrae, J. Phys. Chem., 61, 562 (1957).  
b. E.G. McRae, Spectrochim. Acta., 12, 192 (1958).
- 54.a. N. Mataga, Y. Kaifu and K. Masao, Bull. Chem. Soc. Jpn., 28, 690 (1955).  
b. N. Mataga, Y. Kaifu and K. Masao, Bull. Chem. Soc. Jpn., 29, 465 (1956).  
c. N. Mataga, Bull. Chem. Soc. Jpn., 36, 654 (1963).  
d. N. Mataga and T. Kubota, In "Molecular Interactions and Electronic Spectra", Marcel Dekker: New York, (1970).
55. R. Cimiraglia, S. Miertus and J. Thomas, Chem. Phys. Lett., 80, 286 (1981).

56. B.S. Brunschwig, S. Ehrenson and N. Sutin, J. Phys. Chem., 91, 4714 (1987).
57. L. Bilot and A. Kowski, Z. Naturforsch., 18a, 621 (1962).
- 58.a. P. Suppan, Chem. Phys. Lett., 94, 272 (1983).  
b. P. Suppan, Spectro Chim. Acta., 41A, 1353 (1985).
59. M.J. Kamlet, Chem. Eng. News, 63, 20 (1985).
60. M.J. Kamlet, J.L.M. Abboud and R.W. Taft, Prog. Phys. Org. Chem., 13, 485 (1981).
61. M.J. Kamlet, J.L.M. Abboud, M.H. Abraham and R.W. Taft, J. Org. Chem., 48, 2877 (1983).
62. D. Saperstein and E. Levin, J. Chem. Phys., 62, 3560 (1975).
63. M.T. Encinas, M.A. Rubio and E.A. Lissi, J. Photochem., 18, 137 (1982).
64. H. Bulska, A. Grabowska, B. Pakula, J. Sepiol, J. Waluk and Urs P. Wild, J. Lumines., 29, 65 (1984).
65. J. Waluk, S.J. Komorowski and J. Herbich, J. Phys. Chem., 90, 3868 (1986).
66. A.C. Capomacchia, J. Casper and S.G. Schulman, J. Pharm. Sci., 63, 1272 (1974).
67. P.J. Kovi, C.L. Miller and S.G. Schulman, Anal. Chim. Acta, 61, 7 (1972).
68. S.G. Schulman and K. Abate, J. Pharm. Sci., 61, 1576 (1972).
69. R.J. Sturgeon and S.G. Schulman, J. Pharm. Sci., 65, 1833 (1976).
70. E.M. Kosower, R. Giniger, A. Radknowsky, D. Hebel and A. Schusterman, J. Phys. Chem., 90, 5552 (1986).
71. E.M. Kosower and D. Huppert, Ann. Rev. Phys. Chem., 37, 127 (1986).
72. D.W. Anthon and J.H. Clark, J. Phys. Chem., 91, 3530 (1987).
73. B. Bagchi, D.W. Oxtoby and G.R. Flemming, Chem. Phys., 86, 257 (1984).

74. I. Ganzalo and T. Montono, J. Phys. Chem., 89, 1608 (1985).
75. J.R. Lakowicz, In "'Principles of Fluorescence Spectroscopy'", Plenum Press: New York, (1986).
76. S.G. Schulman, In "'Fluorescence and Phosphorescence Spectroscopy: Physicochemical Principles and Practice'", Pergamon Press: Oxford, (1977).
77. K. Weber, Z. Phys. Chem., B15, 18 (1931).
78. Th. Förster, Naturwis, 36, 186 (1949).
79. Th. Förster, Z. Electrochem., 54, 42, 531 (1950).
- 80.a. A. Weller, Z. Physik. Chem. N.F., 3, 238 (1955).  
b. A. Weller, Z. Physik. Chem. N.F., 15, 438 (1958).  
c. A. Weller, Z. Elektrochem., 56, 662 (1952).
- 81.a. H.H. Jaffe and H.L. Jones, J. Org. Chem., 30, 964 (1964).  
b. H.H. Jaffe, D.L. Beveridge and H.L. Jones, J. Am. Chem. Soc., 86, 2962 (1964).
82. C.F. Mason, J. Phillip and B.F. Smith, J. Chem. Soc., 3051 (1968).
83. E.L. Wehry and L.B. Rogers, J. Am. Chem. Soc., 87, 4235 (1965).
84. C.M. Harris and B.K. Selinger, J. Phys. Chem., 84, 891 (1980).
85. H. Shizuka, K. Tsutsumi, K. Aoki and T. Morita, Bull. Chem. Soc. Jpn., 44, 3245 (1971).
86. E. Vander Donckt, In "'Progress in Reaction Kinetics'", Ed. G. Porter; Pergamon Press: New York, (1970); Vol.5, pp.273.
87. J. Jortner, R.P. Levine and S.A. Rice, In "'Advances in Chemical Physics'", John Wiley: New York, (1981); part 2.
- 88.a. S.G. Schulman, Rev. Anal. Chem., 1, 85 (1971).  
b. S.G. Schulman, P.T. Tidewell, J.J. Aaron and J.D. Winefordner, J. Am. Chem. Soc., 93, 3179 (1971).

- c. K. Abate, A.C. Capomacchia, D. Jacmar, P.J. Kovi and S.G. Schulman, *Anal. Acta.*, 65, 59 (1973).
  - d. S.G. Schulman, In ''Physical Methods in Heterocyclic Chemistry'', Ed. A.R. Katritzky; Academic Press: New York (1974); Vol.6, pp.147.
  - e. S.G. Schulman, Ref. 23a: Chapter: 6.
89. J.F. Ireland and P.A.H. Wyatt, In ''Advances in Physical Organic Chemistry''; Ed. V. Gold and D. Bethell; Academic Press: London, (1976); Vol: 12, pp. 132.
90. P.K. Sengupta and M. Kasha, *Chem. Phys. Lett.*, 68, 382 (1979).
- 91.a. M. Itoh, T. Adachi and K. Tokomura, *J. Am. Chem. Soc.*, 106, 850 (1984).
- b. M. Itoh and Y. Fujiwara, *J. Am. Chem. Soc.*, 107, 1561 (1985).
92. S. Nagaoka, N. Hirota, M. Sumitani, K. Yoshihara, E. Lipczynska-Kochany and H. Iwamura, *J. Am. Chem. Soc.*, 106, 6913 (1984).
93. D.J.-. Jang and D.F. Kelley, *J. Phys. Chem.*, 89, 209 (1985).
94. A.J.G. Stranjord and P.F. Barbara, *J. Phys. Chem.*, 89, 2355 (1985).
95. G. Woessner, G. Goeller, J. Rieker, H. Hoier, J.J. Strezowski, E. Daltrozzo, M. Neureiter and H.E.A. Kramer, *J. Phys. Chem.*, 89, 3629 (1985).
96. K.P. Ghiggino, A.D. Scully and I.M. Leaver, *J. Phys. Chem.*, 90, 5089 (1986).
97. R.S. Becker, C. Lenolbe and A. Zein, *J. Phys. Chem.*, 91, 3509, 3517 (1987).
- 98.a. M. Swaminathan and S.K. Dogra, *J. Am. Chem. Soc.*, 105, 6223 (1983).
- b. A.K. Mishra and S.K. Dogra, *Indian J. Chem.*, 24A, 285 (1985).
- c. H.K. Sinha and S.K. Dogra, *Chem. Phys.*, 102, 337 (1986).
99. C.A. Taylor, M.A. El-Bayoumi and M. Kasha, *Proc. Natl. Acad. Sci., USA*, 63, 253 (1969).
100. K. Tokomura, Y. Watanabe and M. Itoh, *Chem. Phys. Lett.*, 111, 379 (1984).

101. A. Fujimoto, J. Nakamura, I. Yamazaki, T. Murao and K. Inuzuka, Bull. Chem. Soc. Jpn., 58, 88 (1985).
102. M. Noda, N. Hirota, M. Sumitani and K. Yoshihara, J. Phys. Chem., 89, 399 (1985).
103. Work on Intramolecular Excited state double proton transfer is compiled (1986) by J. Waluk, Institute of Physical Chemistry Polish Academy of Sciences, Warsaw, Poland.
104. O. Chesnovsky and S. Leutwyler, Chem. Phys. Lett., 121, 1 (1985).
105. J. Lee, R.D. Griffin and G.W. Robinson, J. Chem. Phys., 82, 4920 (1985).
106. M.J. Politi and J.H. Fendler, J. Am. Chem. Soc., 106, 265 (1984).
107. E. Bonrdez, B.T. Goguilleon, E. Keh and B. Valeur, J. Phys. Chem., 88, 1909 (1984).
108. M. Gutman, E. Nachliel, E. Gershon and R. Giniger, Eur. J. Biochem., 134, 63 (1984).
- 109.a. H.Z. Cao, M. Allavena, O. Tapia and E.M. Evleth, J. Phys. Chem. 89, 1581 (1985).  
b. J. Waluk, H. Bulska, A. Grabowska and A. Mordziński, New J. Chem., 10, 414 (1986).
110. D.E. Magnoli and J.R. Murdoch, J. Am. Chem. Soc., 103, 7465 (1981).
111. S. Scheiner, Acc. Chem. Res., 18, 74 (1985).
112. H. Knibbe, D. Rehm and A. Weller, Ber. Bunsenges., 72, 257 (1968).
113. M. Kasha, J. Chem. Phys., 20, 71 (1952).
114. F.C. Collins and G.E. Kimball, J. Colloid. Sci., 4, 425 (1949).
115. M.H. Hui and W.R. Ware, J. Am. Chem. Soc., 98, 4172 (1976).
116. H. Boaz and G.K. Rollefson, J. Am. Chem. Soc., 72, 3425 (1950).
117. A. Weller, Z. Phys. Chem. (Frankfurt am main), 17, 224 (1958).

- 118.a. Th. Förster, Pure. Appl. Chem., 24, 443 (1970).  
b. Th. Förster, Pure Appl. Chem., 34, 225 (1973).
- 119.a. P.J. Kovi and S.G. Schulman, Spectros. Lett., 5, 443 (1972).  
b. P.J. Kovi, A.C. Capomacchia and S.G. Schulman, Spectros. Lett., 6, 7 (1973).
120. A.R. Watkins, Z. Phys. Chem. (Frankfurt Am Main), 75, 327 (1971).
121. C.M. Harris and B.K. Selinger, J. Phys. Chem., 84, 1366 (1980).
- 122.a. H. Shizuka and K. Tsutsumi, J. Photochem., 9, 334 (1978).  
b. K. Tsutsumi and H. Shizuka, Chem. Phys. Lett., 52, 485 (1979).  
c. S. Tobita and H. Shizuka, Chem. Phys. Lett., 75, 140 (1980).  
d. K. Tsutsumi, S. Sekiguchi and H. Shizuka, J. Chem. Soc. Faraday Trans I., 78, 1087 (1982).
123. H. Hofner, J. Worner, W. Steiner and M. Houser, Chem. Phys. Lett., 72, 139 (1980).
124. Z.R. Grabowski and A. Grabowska, Z. Phys. Chem. N.F., 101, 197 (1976).
- 125.a. M. Swaminathan and S.K. Dogra, Can. J. Chem., 61, 1064 (1983).  
b. A.K. Mishra and S.K. Dogra, J. Photochem., 23, 163 (1983).  
c. A.K. Mishra and S.K. Dogra, J. Chem. Soc. Perkins Trans II., 943 (1984).  
d. H.K. Sinha and S.K. Dogra, Indian J. Chem., 25A, 1092 (1986).
126. Th. Förster, Chem. Phys. Lett., 17, 309 (1972).
127. S.G. Schulman and R.J. Sturgeon, J. Am. Chem. Soc., 99, 7209 (1977).
- 128.a. H. Shizuka, Y. Ishii and T. Morita, Chem. Phys. Lett., 51, 40 (1977).  
b. H. Shizuka, Acc. Chem. Res., 18, 141 (1985).

- c. H. Shizuka and S. Tobita, J. Am. Chem. Soc., 104, 6919 (1982).
129. W. Brandon, A.L. Pincock, J.A. Pincock, P. Redden and C. Sehmbe, J. Am. Chem. Soc., 109, 2181 (1987).
130. H. Shizuka, T. Ogiwara and E. Kimura, J. Phys. Chem., 89, 4302 (1985).
- 131.a. P. Wan and K. Yates, J. Org. Chem., 48, 869 (1983).
- b. P. Wan, S. Culsaw and K. Yates, J. Am. Chem. Soc., 104, 2509 (1982).
132. N.J. Turro and P. Wan, J. Photochem., 28, 93 (1985).
133. P. Wan, J. Org. Chem., 50, 2583 (1985).
- 134.a. J.D. Winefordner, S.G. Schulman and T.C. O'Haver, In 'Luminescence Spectroscopy in Analytical Chemistry', Wiley Interscience: New York, (1972).
- b. Reference: 9, Chapter: 6 and 7.
- 135.a. C.D. Gutsche, B.A.M. Oude-Alink and A.W.K. Chan, J. Org. Chem., 38, 1993 (1973).
- b. G. Bartocci, P. Bortolus and U. Mazzucato, J. Phys. Chem., 77, 605 (1977).
- c. S. Inbar and S.G. Cohen, J. Am. Chem. Soc., 100, 4490 (1978).
- d. J.C. Scaiano, J. Am. Chem. Soc., 102, 7747 (1980).
136. A.G. Mac Diarmid, J.-C. Chiang, M. Halpern, W.-S. Huang, S.-L. Mu, N.L.D. Samasiri, W. Wu and S.I. Yaniger, Mol. Cryst. Liq. Cryst., 121, 173 (1985).
137. J.P. Travers, J. Chroboczek, F. Devreux, F. Genoud, M. Nechtschein, A. Syed, E.M. Genies and C. Tsintavis, Mol. Cryst. Liq. Cryst., 121, 195 (1985).



- 146.a. H. Inoue, J. Shiraishi and Y. Tanizaki, Bull. Chem. Soc. Jpn., 44, 1743 (1971).
- b. A. Bree and R. Zwarich, J. Chem. Phys., 51, 903 (1969).
- c. S. Siegal and H.S. Jude-kis, J. Phys. Chem., 70, 2205 (1966).
- d. R.L. Hummel and K. Rudenberg, J. Phys. Chem., 66, 2344 (1962).
- e. E.M. Layton, J. Mol. Spectros., 5, 181 (1960).
- f. C.A. Pickham and S.C. Wart, J. Mol. Spectros., 27, 326 (1968).
- g. J.H. Hofstratt, G. Ph. Hoornweg, C. Gooijer and N.H. Velthorst, Anal. Chim. Acta., 169, 225 (1985).
- h. K. Yoshihara and D.R. Kearns, J. Chem. Phys., 45, 1991 (1966).
147. I.B. Berlman, In "'Hand Book of Fluorescence Spectra of Aromatic Molecules'", Academic Press: New York, (1965); pp.119.
- 148.a. D.L. Horrocks and W.G. Brown, Chem. Phys. Lett., 5, 117 (1970).
- b. H. Saigusa and M. Itoh, J. Phys. Chem., 89, 5486 (1985).
149. F.L. Minn, J.P. Pinion and N. Filipescu, J. Phys. Chem., 75, 1794 (1971).
150. B.S. Vogt and S.G. Schulman, Chem. Phys. Lett., 89, 320 (1982).
- 151.a. F.L. Minn, G.W. Mushrush and N. Filipescu, J. Chem. Soc.(A), 63 (1971).
- b. G.W. Mushrush, F.L. Minn and N. Filipescu, J. Chem. Soc(B), 427 (1971).
152. H.H. Richtol and B.R. Fitch, Anal. Chem., 46, 1749 (1974).
153. J.G. Pavlopoulos, Spectrochim. Acta., 42A, 1307 (1986).
- 154.a. G.A. Olah and N.W. Meyer, In "'Fridel Crafts and Related Reactions'", Vol.I, Ed. G.A. Olah, Interscience: New York, (1963), 623.
- b. R.L. Flurry Jr. and P.G. Lukos, J. Am. Chem. Soc., 85, 1033 (1963).

- c. R.L. Flurry Jr., J. Am. Chem. Soc., 88, 5393 (1966).
- d. J.P. Colpa, C. Maclean and E.L. Mackor, Tetrahedron, 19, Suppl. 2, '65 (1963).
- 155.a. J.J. Aaron, A. Tine, M.E. Wojciechowska and C. Párkányi, J. Lumin., 33, 33 (1985).
- b. P.S. Song and W.E. Kurtin, J. Am. Chem. Soc., 91, 4982 (1969).
- c. M. Krishnamurthy, H.K. Sinha and S.K. Dogra, J. Lumin., 35, 343 (1986).
156. R. Stewart, In "The Proton: Application to Organic Chemistry", Vol. 46, Academic Press: New York, (1985), pp.185.
- 157.a. M. Liler, Adv. Phys. Org. Chem., 11, 267 (1975).
- b. M. Liler, J. Chem. Soc. Perkins Trans.II, 334 (1971).
- c. M. Liler, J. Chem. Soc. Perkins Trans.II, 71 (1974).
158. A. Berger, A. Loewenstein and S. Meiboom, J. Am. Chem. Soc., 81, 62 (1959).
159. I.M. Klotz and B. Frank, J. Am. Chem. Soc., 87, 2721 (1965).
160. F.A. Bovey and B.V.D. Tiers, J. Polym. Sci., A18, 849 (1963).
161. W.L. Paul and S.G. Schulman, Anal. Chem., 45, 415 (1973).
162. S.G. Schulman, P.J. Kovi and J.F. Young, J. Pharm. Science, 62, 1197 (1973).
163. A.R. Katritzky, A.J. Waring and K. Yates, Tetrahedron, 19, 465 (1963).
164. J.T. Edwards and I.C. Wang, Can. J. Chem., 40, 966 (1962).
165. K. Yates, J.B. Stevens and A.R. Katritzky, Can. J. Chem., 42, 1957 (1964).
- 166.a. K. Yates and J.B. Stevens, Can. J. Chem., 43, 529 (1965).
- b. R.A. Cox and K. Yates, J. Am. Chem. Soc., 100, 3861 (1978).

- c. R.A. Cox and K. Yates, Can. J. Chem., 59, 1560 (1981).
- d. R.A. Cox and K. Yates, Can. J. Chem., 59, 1568 (1981).
167. R.B. Homer and C.D. Johnson, In "'Chemistry of Amides'", Ed. J. Zabieky, Interscience: London (1970), Chapter 3.
168. C.R. Smith and K. Yates, Can. J. Chem., 50, 771 (1972).
- 169.a. C.L. Perrin, J. Am. Chem. Soc., 96, 5628 (1974).
- b. C.L. Perrin and E.R. Johnson, J. Am. Chem. Soc., 103, 4697 (1981).
- c. C.L. Perrin, E.R. Johnson, C.P. Lallo and P.A. Kobrin, J. Am. Chem. Soc., 103, 4691 (1981).
- d. C.L. Perrin, C.P. Lallo and E.R. Johnson, J. Am. Chem. Soc., 106, 2749 (1984).
- 170.a. R.J. Gillespie and T. Birchall, Can. J. Chem., 41, 148 (1963).
- b. T. Birchall and R.J. Gillespie, Can. J. Chem., 49, 2642 (1963).
171. A.R. Fersht, J. Am. Chem. Soc., 93, 3504 (1971).
172. J. Catalan and M. Yanej, Tetrahedron, 36, 665 (1980).
173. K. Brederick, Th. Forster and H.G. Oesterlin, In "'Luminiscence of Organic and Inorganic Materials'", Ed. H.P. Kallman and G.M. Spruch, Wiley: New York, (1962), pp.161.
174. R.S. Becker, In "'Theory and Interpretation of Fluorescence and Phosphorescence'", Wiley Interscience: New York (1969), Chapter 12.
175. W. Bartak, P.J. Lucchesi and N.S. Snider, J. Am. Chem. Soc., 84, 1842 (1962).
176. E.L. Wehry and L.B. Rogers, J. Am. Chem. Soc., 87, 4234, 4237 (1965).
177. J.D. Winefordner, S.G. Schulman and L.B. Sanders, Photochem. Photobiol., 13, 381 (1971).

178. E.L. Wehry, J. Am. Chem. Soc., 89, 41 (1967).
179. S.G. Schulman, P.T. Tidwell, J.J. Cetorelli and J.D. Widefordner, J. Am. Chem. Soc., 93, 3179 (1971).
180. R.W. Cowgill, Photochem. Photobiol., 13, 183 (1971).
181. J.W. Bridges and R.T. Williams, Biochem. J., 107, 225 (1968).
182. D.V.S. Jain, F.S. Nandel and Prem Lata, Indian J. Chem., 21A, 559 (1982).
183. R.S. Sarpal and S.K. Dogra, J. Photochem., 38, 263 (1987).
184. Reference: 98b and 130.
185. B.S. Furniss, A.J. Hannaford, V. Rogers, P.W.G. Smith and A.R. Tatchell, In ''Vogel's Text Book of Practical Organic Chemistry'', 4th Ed, ELBS: London (1986), pp.840.
186. F.A.L. Anet and P.W.G. Bavin, Can. J. Chem., 34, 991 (1956).
187. E.K. Weisburger and J.H. Weisburger, J. Org. Chem., 20, 1396 (1955).
188. Reference: 1, pp.792.
189. Reference: 1, pp.660.
190. J.A. Riddick and W.B. Bunger, In ''Techniques in Organic Chemistry - Organic Solvents'', Wiley Interscience: New York, (1970), pp.592, 798, 805.
191. A.K. Mishra, M. Swaminathan and S.K. Dogra, J. Photochem., 26, 49 (1984).
- 192.a. M.J. Jorgenson and D.R. Hartter, J. Am. Chem. Soc., 85, 878 (1963).  
b. G. Yagil, J. Phys. Chem., 71, 1034 (1967).
193. T.G. Bonner and J. Phillips, J. Chem. Soc.(B), 650 (1966).
194. K. Yates, J.B. Stevens and A.R. Katritzky, Can. J. Chem., 42, 1957 (1964).

195. D. Dolman and R. Stewart, *Can. J. Chem.*, 45, 903 (1967).
196. R.A. Cox, L.M. Druet, A.E. Klausner, T.A. Modro, P. Wan and K. Yates, *Can. J. Chem.*, 59, 1568 (1981).
197. R.A. Cox and K. Yates, *Can. J. Chem.*, 61, 2225 (1983).
198. A. Albert and E.P. Sarjeant, In "'The Determination of Ionization Constants'", 2nd Ed, Chapman and Hall: London (1971).
- 199.a. S.G. Schulman and Q. Fernando, *J. Phys. Chem.*, 71, 2668 (1967).  
b. N. Lasser and J. Feitelson, *J. Phys. Chem.*, 77, 1011 (1973).
200. M. Takkuja, *J. Phys. Chem.*, 83, 810 (1979).
201. Reference: 9, pp.12.
202. S.J. Strickler and R.A. Berg, *J. Chem. Phys.*, 37, 814 (1962).
203. R.A. Lampert, L.A. Chewta, D. Phillips, D.V. O'Conner, A.J. Roberts and S.R. Meech, *Anal. Chem.*, 55, 68 (1983).
204. Reference 75, pp.65.
205. R. Schuyler and I. Isenberg, *Rev. Sci. Instrum.*, 42, 813 (1971).
206. A. Grinvald and I.Z. Steinberg, *Anal. Biochem.*, 59, 583 (1974).
- 207.a. R. Argauer and C.E. White, In "'Fluorescence Analysis'", Marcel Dekker: New York (1970).  
b. C.E. White, M. Ho and E.Q. Weimer, *Anal. Chem.*, 32, 438 (1960).  
c. C.A. Parker and W.T. Rees, *Analyst*, 85, 587 (1960).  
d. W.H. Melhuish, *J. Opt. Soc. Amer.*, 52, 1256 (1960).  
e. R.F. Chen, *Anal. Biochem.*, 20, 339 (1967).  
f. C.A. Parker, In "'Photoluminescence of Solution'", Elsevier: Amsterdam (1968).
208. D.D. Perrin, In "'Dissociation Constants of Organic Bases in Aqueous Solutions'", Butterworth: London, (1965), pp.13.
209. E. Vander Donckt, J. Nosielski and P. Thiry, *J. Chem. Soc. Chem. Comm.*, 1249 (1969).

210. R.L. Flurry Jr. and R.K. Wilson, J. Phys. Chem., 71, 589 (1967).
211. S.F. Mason and B.E. Smith, J. Chem. Soc.(A), 325 (1969).
212. P.J. Kovi and S.G. Schulman, Anal. Chim. Acta, 63, 39 (1979) and references cited therein.
- 213.a. F.M. Klotz and B. Frank, J. Am. Chem. Soc., 87, 2721 (1965).  
b. F.A. Bovey and G.V.D. Tiers, J. Polym. Sci., A18, 849 (1963).
214. J. Trotter, Acta. Crystallogr., 13, 732 (1962).
215. M. Krishnamurthy and A.K. Mishra and S.K. Dogra, Photochem. Photobiology., 45, 359 (1987).
216. K. Yoshihara and D.R. Kearns, J. Chem. Phys., 45, 1991 (1966).
217. E.C. Lim and Jack M.H. Yu, J. Chem. Phys. 45, 4742 (1966) and references therein.
- 218.a. A.K. Mishra and S.K. Dogra, J. Photochem, 31, 333 (1985).  
b. M. Krishnamurthy and S.K. Dogra, Chem. Phys., 103, 325 (1986).
219. M.W. Lovell and S.G. Schulman, Anal. Chim. Acta., 127, 203 (1981).
220. W.F. Giaque, E.M. Hornung, J.F. Kuzler and T.R. Rubin, J. Am. Chem. Soc., 82, 62 (1960).
221. R. Stewart and K. Yates, J. Am. Chem. Soc., 80, 6355 (1958).
222. J.F. Ireland and P.A.H. Wyatt, J. Chem. Soc. Faraday Trans.1, 69, 161 (1973).
223. Reference: 98a, 125a and 125b.
- 224.a. M. Swaminathan and S.K. Dogra, J. Chem. Soc. Perkin Trans II, 947 (1984).  
b. M. Krishnamurthy and S.K. Dogra, Spectrochim. Acta., 42A, 793 (1986).  
c. H.K. Sinha and S.K. Dogra, J. Photochem, 36, 149 (1987).

225. R.S. Sarpal and S.K. Dogra, unpublished results.
226. Reference: 147, pp.104.
227. N. Chattopadhyay and M. Choudhury, J. Photochem, in press.
228. Reference: 147, pp.42 and 43.
229. C.P. Smyth, In "'Dielectric Behaviours and Structure'", McGraw Hill: New York (1955).
230. Reference: 147, pp. 59 and 60.
231. U. Pande, N.B. Joshi and D.D. Pant, Chem. Lett., 72, 209 (1980).
232. Dictionary of Organic Compounds, Ed. J. Buckingham, 5th Ed., Chapman and Hall: London (1982), pp. 1529, 1530.
233. Reference: 208, pp. 58.
234. Reference: 4, pp. 12, 193 and 357.
235. A.K. Mishra and S.K. Dogra, J. Photochem, 28, 87 (1985).

VITAE

Born on April 19, 1962 at Viralippatti, Anna district (Tamilnadu), the author had his early education at Viralippatti and Seepalacottai, Anna district. He obtained his pre-university and B.Sc., degrees from Arul Anandar College, Karumathur, Madurai Kamaraj University in 1979 and 1982 respectively. He received his M.Sc. degree in 1984 from V.O.C. College, Tuticorin, Madurai Kamaraj University.



### LIST OF PUBLICATIONS

1. R. Manoharan and S.K. Dogra,  
Electronic spectra of fluorene-1- and -9-carboxylic acids.  
Spectrochim. Acta., 43A, 91 (1987).
2. R. Manoharan and S.K. Dogra,  
Unusual spectral shifts in the prototropic reactions of  
2,7-diaminofluorene.  
Can. J. Chem., 65, 2013 (1987).
3. R. Manoharan and S.K. Dogra,  
Spectral characteristics of phenylenediamines and their  
various protonated species.  
Bull. Chem. Soc.<sup>Jpn</sup>, 60, (1987).
4. R. Manoharan and S.K. Dogra,  
Acidity constants in the excited states: Absence of excited  
state prototropic equilibrium for monocation-neutral pair  
of 2,3-diaminonaphthalene.  
J. Phys. Chem. (communicated).
5. R. Manoharan and S.K. Dogra,  
Prototropic equilibria of electronically excited molecules:  
Fluorene and its derivatives.  
J. Photochem. Photobiol., A: Chem. in press.
6. R. Manoharan and S.K. Dogra,  
The absorption and fluorescence spectra of 2- and 4-fluorene-  
carboxylic acids.  
J. Photochem. Photobiol., A: Chem. in press.
7. Ramasamy Manoharan and S.K. Dogra,  
Prototropic reactions for 1-, 2- and 4-fluorenamides in the  
ground and excited singlet states.  
Can. J. Chem. (communicated).

8. R. Manoharan and S.K. Dogra,  
Electronic spectra of 9,10-diaminophenanthrene: Evidence  
for dual fluorescence.  
J. Photochem. Photobiol., A: Chem. (communicated).
9. R. Manoharan and S.K. Dogra,  
Prototropic reactions of 2-fluorenaldehyde, 2-acetylfluorene  
and 2-benzoylfluorene in the ground and first excited singlet  
states. (Manuscript under preparation).
- <sup>φ</sup>10. S. Mazumdar, R. Manoharan and S.K. Dogra,  
Solvatochromism and excited state dipolemoment of structurally  
related diamines. (Manuscript under preparation).

---

<sup>φ</sup>not included in the thesis.